Bangor University

MASTER OF PHILOSOPHY

Keratin from Human hair and Sheep wool: Characterisation and its uses in the Fabrication of Hydrogels

Mondragon De La Cruz, David

Award date:
2020

Awarding institution:
Bangor University

Link to publication

Keratin from Human hair and Sheep wool: Characterisation and its uses in the Fabrication of Hydrogels

_____

Thesis submitted to the school of Natural Sciences, Bangor University

In partial fulfilment of the requirements for a

Masters of Philosophy (MPhil) Degree

By

David Andres Mondragon De la cruz, BSc

MPhil supervisor: **Dr Hongyun Tai**

_____

PRIFYSGOL

BANGOR

UNIVERSITY

Abstract

The focus of this MPhil project is the isolation of keratin from hair and wool by using two different methods in order to obtain keratin in sufficient quantity and quality to synthesise hydrogels using the reactivity of thiol groups in keratin (Michael addition reactions), as well as some preliminary works for gel casting by photo-crosslinking reactions and 3D printing. This thesis includes four chapters briefly introduced below.

Chapter 1 introduces the main topics covered in this thesis by providing a quick definition of the concepts concerning polymer chemistry, natural polymers and hydrogels. In addition, a review of the literature follows this section by referring to the most relevant works published with regards to the natural occurrence, properties and isolation methods of keratin. Finally, the chapter presents the applications of keratin in the biomedical sector, describing some of the derived materials that can be obtain from keratin.

Chapter 2 reports the methodology implemented in this thesis. The methods include two isolation procedures by using reducing agents (Na_2S method) and denaturing agents (Shindai). The experimental procedures for the synthesis of hydrogels by Michael addition reactions, photo-crosslinking reactions and early work on gel casting by 3D-prining are described in this chapter. Furthermore, the analytical techniques used to characterise the obtained products are also covered.

Chapter 3 details the results obtained from the experimental work along with a discussion explaining the observations made on the data obtained with regards to the keratin isolated from wool and hair from reduction with Na_2S and Shindai method. The implications of these isolation methods are discussed along with the determination of the solubility of the keratins, their molecular weight by GPCGPC and thiol content by Ellman's assay. Fundamental characterisation of the extracted keratins by NMR, FTIR and UV-vis spectroscopy are also discussed in this chapter. Similarly, for the

synthesis of the keratin-based hydrogels by Michael addition reactions the morphology observed by SEM as well as some visual observations made on the obtained gels are explained in terms of the properties imparted by the acrylates/methacrylates keratin was combined with (PEG-DA, Soybean oil epoxidised acrylate and methacrylated alginate). Subsequently, the discussion moves on the photo-crosslinking experiments on methacrylated alginate in an attempt to physically combined this system with keratin. The photo-crosslinked gels were also tested for water retention by swelling studies and as drug delivery system of antioxidant glutathione.

Chapter 4 condenses the main ideas and information gathered throughout the research work by providing conclusions as well as projecting further work that should be carried out in future studies.

Acknowledgement

The research reported in this thesis would not have been possible without the support of the School of Natural Sciences formerly named School of Chemistry of Bangor University in Wales, United Kingdom.

I would like to start by giving sincere thanks to Dr Hongyun Tai, my supervisor in this MPhil project for her valuable guidance, constructive suggestions and mentoring throughout two years of laboratory work and the final months of writing up of this thesis. She welcomed me in her research group and provided me with the resources necessary to carry out my research, her mentoring inspired me and her direction motivated me to do things better every day and to grow not only as a chemist but also as a person and for that, I'm deeply grateful.

Secondly, I would like to thank the other members of the research groups, they were not only my colleagues but also my friends and they made me feel like at home and kindly introduced me into the school's practices and security regulations. In the same way, I want to thank the my fellow post graduate students from the school who along with my research group colleagues showed me the surrounding area and the culture which was crucial for my adaption into the British society as an overseas student. I'm immensely grateful for their friendship and companionship and I wish them the best in their future careers.

Special thanks to my personal tutor Dr Leigh Jones from the School of Chemistry for his co-mentoring, guidance and bringing the light in those moments of hesitation and uncertainty that comes along in the life of every researcher.

Similarly, I would like to express sincere thanks to the members of staff of the School of chemistry and the School of Computer Science and Electronic

Engineering for keeping good maintenance and assistance in the usage of the equipment in their facilities.

There would be countless thanks to give to every person who made a contribution in this project and for all of them, whom I did not mention by name or by department, I say thanks for being there for me and caring for me, understanding the person behind the laboratory coat I am and how meaningful this research project is in my life.

Finally I would like to thank all the members of my family, specially my mother Rosario De la cruz, for their unconditional support and love, without them I would not be the person I am and the education I received throughout these years has been the result of their great efforts to sponsor and cultivate my talents. More importantly, my education started at home and the environment in which I grew up with my family brought me to become the masters in chemistry I'm aspiring to be with this work and also the 28-year old man I am at present.

For everything, thank you

David Andres Mondragon De la cruz

List of abbreviations

2D	Two dimensional
3D	Three dimensional
ATR	Attenuated Total Reflectance
A.U.	Absorbance Units
B.S.	Bulk Solution
BSA	Bovine Serum Albumin
CAD	Computer Aid Design
c.c.1	Calibration curve 1
c.c.2	Calibration curve 2
cm	centimetre
Conc.	concentration
DNA	Deoxyribonucleic Acid
DTNB	5,5'-Dithiobis(2-nitrobenzoic acid)
FDM	Fused Deposition Modelling
GMA	Glycidyl Methacrylate
HA	Hydroxy Apatite
GPC	High Performance Liquid Chromatography
Inject.	Injection
2-Mc.Ethanol	2-mercaptoethanol
MND	Multi Nozzle Deposition
MPEG	Poly(ethylene glycol) methyl ether
MW	Molecular weight
PBS	Phosphate Buffer Solution
PEG	Poly(ethylene glycol)
PEGDA	Poly(ethylene glycol) Diacrylate
PLA	Poly(Lactic Acid)
PLLA	Poly(L-lactic acid)
PVC	Poly Vinyl Chloride
rpm	Revolution per minute
R.time	Retention time
RNA	Ribonucleic Acid
SEM	Scanning Electron Microscopy
SFF	Solid Freeform Fabrication
SL	Stereo Litography
SLS	Selective Laser Sintering

S.S.	Stock solution
TEA	Triethylamine
Tris HCL	2-Amino-2-(hydroxymethyl)-1,3-propanediol hydrochloride
Trizma base	2-Amino-2-(hydroxymethyl)-1,3-propanediol
TNB	5-Thio(2-nitrobenzoic acid)
T.vol	Total volume
UV-vis	Ultraviolet-visible
Vol	Volume

Table of Contents

List of Figures:

List of tables:

List of schemes:

Chapter 1: Introduction

The focus of this MPhil project is on keratin as a bio-material that can be isolated from readily available natural sources, e.g. wool and hair, for the fabrication of hydrogels. This chapter introduces some general concepts about polymer chemistry in particular related to keratin and continues with a review on the latest research studies published concerning isolation methods and designing of bio-devices and derived materials where keratin is a key component.

1.1. Fundamentals about polymers and hydrogels

This sections will briefly explain some fundamental facts about polymers and hydrogels focussing on concepts of relevance for the present work. This section is a short literature review from secondary sources mainly extracted from polymer chemistry textbooks and some examples of the latest works published in journals.

1.1.1. Polymer

Polymers are macro molecules composed of repeated units joined together, these repeated units are referred to as monomers and they constitute the bricks that build the skeleton or backbones of the polymers. Polymers are classified as linear (Figure1.1 A) or branched (Figure 1.1 B) depending on the architectures they exhibit. Another way to distinct sub classes of polymers relies on their origin, some of them can be synthesised under

laboratory conditions while others are found in nature, the former are known as synthetic and the latter are natural polymers. Both natural and synthetic polymers have significant relevance in industrial processes and current research in the development of new materials take into account both classes in the formulation of novel materials [1-3].
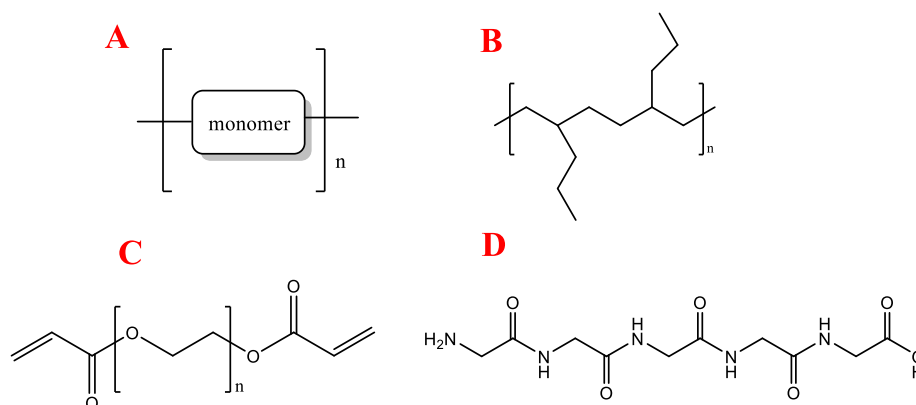
Figure 1.1. *General structural of a linear polymer **(A)** and a branched polymer **(B)**, indicating the monomer is repeated in the structure n timesStructure of the linear,synthetic polymer polyethylene glycol terminated with acrylates groups at each end **PEG-DA (C)**. Structure of a simple polypeptide composed of 5 glycine residues **(D)** joint together as a typical example of the peptide bond displayed in proteins.*

1.1.2. Natural Polymers

Natural polymers are naturally occurring macromolecules often referred to as bio-polymers due to their biological function in living organisms. These substances are widely spread in nature, and the main sub categories comprises polysaccharides (carbohydrates), proteins (polypeptides), nucleic acids and lipids, all considered essential biomolecules for living organisms. Natural polymers unlike synthetic polymers are almost exclusively obtained by enzyme chemical reactions and still a synthesis challenge for synthetic chemistry. Therefore the acquisition of these natural substances is almost limited to their natural sources.

Polysaccharides are made of mono saccharides joint by glycosidic bonds, these large structures arealso known as "carbohydrates", carbohydrates are important biomolecules and play roles ranging from energy strorage

e.g. glycogen as the energy resource in animals to structural functions e.g. chitin as a main component of exoskeleton of arthropods and fungi. Proteins are made monomeric units of amino acids joint by a peptide bond that forms polypeptides (Figure 1.1 D, Proteins and their functions vary from structural e.g. fibrous proteins constituting tissues in living species to regulation e.g. hormones that serve as regulators for the activity of organs. Nucleic acids are easily exemplified by DNA and RNA, and their function is to store and transmit genetic information contained as a sequence of monomeric units of nucleotides comprising the genetic material of living organisms. Lipids are another form of energy storage for many animal and plant species. Their biological importance is varied but well-xxx to their structural role as main component of the cell membranes. Some of the most common examples of lipids include waxes, steroids, and phospholipids and fats. Each class having a distinctive molecular structure that is not defined in terms of a single monomeric unit due to the fact that lipids are not strictly found in polymeric arrangement in nature, but they are often present as small-to-medium-size biomolecules . Natural polymers due to their stunning bio properties have been extensively studied throughout the years.They have served and remain serving as inspiration to most of modern procedures involving acute and chronical diseases This project is concerned about the chemistry of naturally occurring protein keratin as well as polysaccharide alginate which will be involved in the development of some of the materials based on keratin [4-7].

1.1.3. Synthetic Organic Polymers

Synthetic organic polymers are produced by organic synthesis in accordance with the reactivity of the monomers. The process or chemical reaction by which a polymer is obtained as the final product is known as polymerisation and there exist two main methods defined as addition and condensation polymerisation. Polymerisation by addition happens when the

monomer molecules bond to each other without the loss of any of the original atoms in the reactants. Polymerisation by condensation, on the other hand, implies the loss of a small molecule (usually water) during the bonding process of monomers. Polymers can be synthesised by a number of methodologies and approaches, used in both research and industrial processes, however, all of these procedures and sub classifications fall into the most general classification, the addition polymerisation or condensation polymerisation.

Some common examples include Polyethylene which is used in plastic bags, film wraps, bottles, electrical insulation, toys, etc, Polyvinyl Chloride (PVC) is used in siding, pipes and flooring purposes. Polystyrene is used in cabinets and in packaging. Polyvinyl acetate is used in adhesives and latex paints. For the present work, the synthetic polymer Poly(ethyleneGlycol) Diacrylate (PEG-DA) was utilized in combination w keratin for the fabrication and bio-materials [8,9] (Figure 1.1 C).

1.1.4. Functionalisation of polymers.

The functionalisation of polymers is the process by which the molecular structure of a polymer is chemically modified following synthetic procedures. The main purpose of this procedure is to introduce functional groups into the backbone of the polymers in a way to enhance the reactivity and molecular properties of the macro molecule. This modification is especially useful for natural polymers that are not active for a specific task in their native state. Current biomedical applications take advantage of the bio-compatibility and low toxicity of natural polymers for the treatment of chronic diseases by functionalising these polymers in order to make them deliver a specific biological function.

Some examples of active functional groups that can be introduced include acrylate groups, methacrylate groups, thiol groups, amine groups and carboxylic groups. Methacrylates and acrylates groups are particularly

useful in natural polymers that require water retention, e.g. as reservoir or as an active fluid-deliver system. The functionalisation of polysaccharides using glycidyl methacrylate is used for the fabrication of hydrogels. The process by which the functionalisation takes place can occur via a transesterification or by opening an epoxide (figure 1.2 [10]).
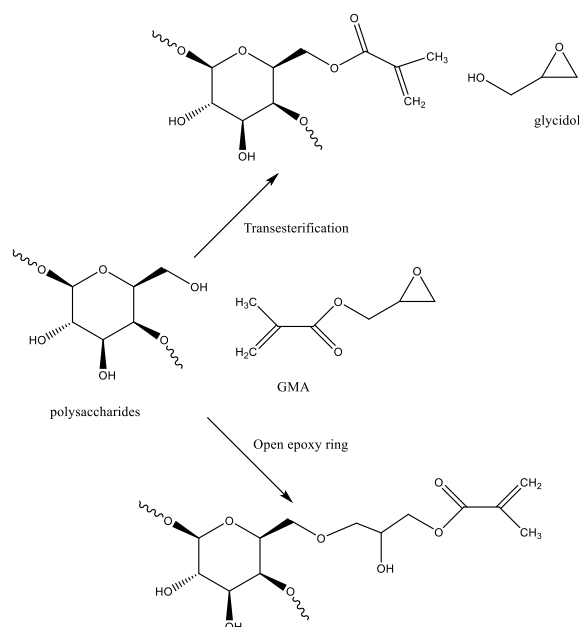
Figure 1.2. *Schematic representation of the methacrylation of polysaccharides with GMA: transesterification (a) and epoxide opening (b). Original illustration taken from reference 10*

1.1.5. Hydrogels

Hydrogels are 3D arrangements that consist of a network made of crosslinked polymers characterised by their gel-like properties capable of retain considerable amounts of water in their structure. This behaviour is evident by the instantaneous swelling that takes place after the material is in contact with water as a consequence of the hydrophilic nature of the cross-linker and/or polymer that causes the absorption of water (Figure 1.3). On account of this ability to store water, hydrogels represent an important bio device in regenerative medicine for the treatment of open wounds since they keep wounds hydrate and promote autolytic debridement [11-13].
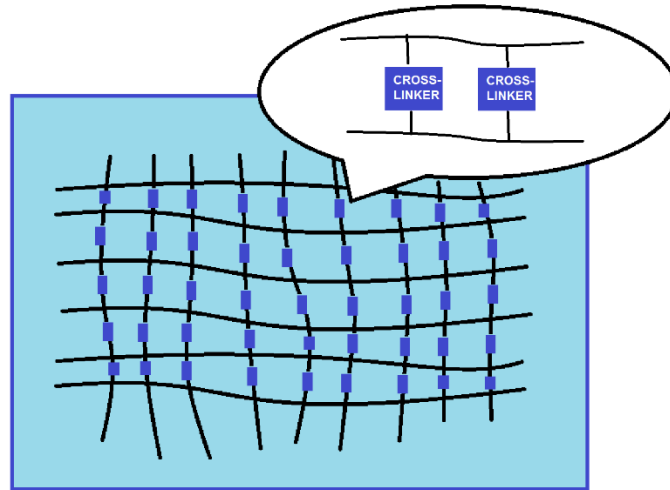
Figure 1.3. *Hydrogel structure: 2D scheme of the alignment of the cross-linked polymers chains in a hydrogel arrangement.*

Hydrogels are synthesised by a cross-linking process that consists of the union of several polymeric strands resulting in a network arrangement. Figure 1.3 displays a schematic representation of the network observed in a hydrogel where the spacing between polymer chains corresponds to the dimensions of the cross linker that brings them together. On the basis of the polymer-crosslinker interactions, the cross-linking process can be physical or chemical. Physical interactions can lead to crosslinking based on ionic interactions or supramolecular interactions (intermolecular forces) as exemplified in the ionic-crosslinking of the polysaccharide sodium alginate by Ca^{2+} Ions (Figure 1.4 A). Other physical types of crosslinking can be achieved via intermolecular forces such as van der Waals forces and hydrogen bonding. Chemical interactions result in crosslinking by generation of covalent bonds. These covalent bonds are diverse and they take place according to the reactivity of the functional groups involved in the reaction and some of them can occur quickly, e.g. the Michael addition click reaction (Figure 1.4 B) where thiol groups react with α,β unsaturated carbonyls right at the double bond position as described in a Michael addition reaction [14].
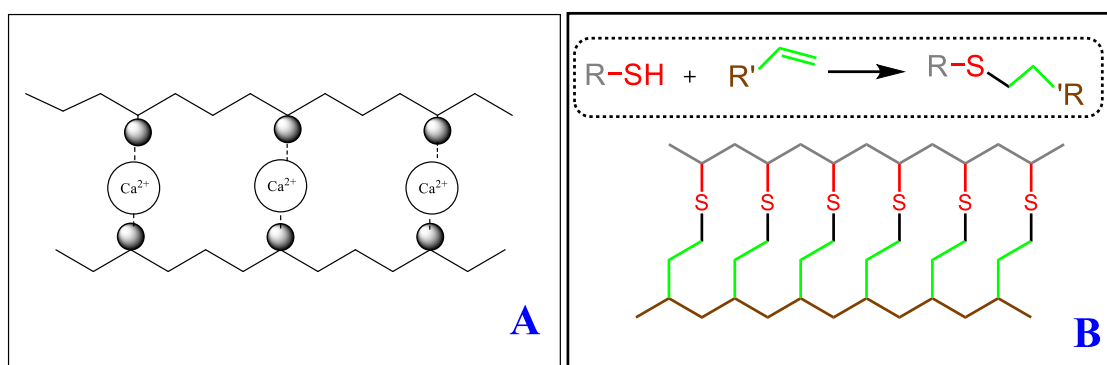
Figure 1.4. Schematic representations of: *Ionic crosss linking of alginate polymer chains with Ca^{2+} cations. The ionic interactions between carboxylic acid groups in their anionic form (gray circles) with Ca^{2+} is strong enough to crosslink the sugars chains resulting in a hydrogel structure* **(A)**. *Covalent cross-linking by Michael addition click cross-linking reaction. General equation (dashed box) and structural illustration of the crosslinked polymer obtained by this method* **(B)**.

1.2. Keratin: natural occurrence, obtention and bio-inspired materials

This section contains a literature review addressing specific approaches and current research related to keratin, as well as the relevance of keratin as biopolymer for living organisms. Unlike the previous section aimed to define basics of the chemistry utilised in this work, the present section will rather introduce some of the previous works and novel methodologies reported in scientific journals regarding the properties of keratin as a biopolymer and its potential as a key component for the development of new devices in the biomedical sector.

1.2.1 Natural sources of Keratin

The demand for primal matters to satisfy the industry needs is constant growth and it doesn't seem to be fully met by synthetic procedures making worth it to look for assistance of primal matters from natural origin that can be modified and purified by synthetic chemistry. Given the fact that these natural-occurring raw materials are readily available and that they can

possess properties not reproducible in synthetic products, justifies the inclusion of these natural products in industrial procedures.

From an academic point of view, nature provides a wide range of compounds that are subject of current research for the role they play in many bio medical studies, where many synthetic compounds cannot satisfy the compatibility and non-toxicity often required in such applications. Proteins and polysaccharides are especially suitable for this purpose not only because of their bio-properties but also their abundance in nature. Polysaccharides are also vital raw materials in industrial processes as it occurs to cellulose the most abundant polymer in nature, present in wood and many vegetal structures that constitute the primary source of paper and wooden materials. Similarly, fibrous proteins play important roles in the production of textile products made of wool, where fibrous protein keratin is the main component. In addition to wool, keratin is also present in other type of structure in nature and its occurrence in living organisms is evident by its structural function as major component in animal tissue due to its structural function, making of Keratin not only the most abundant structural protein in epithelial cells but also as vital as collagen is for animal cells[15-17]. This association with collagen is mainly observed in the skin where the combination of keratin and collagen results in a very elastic and tough material that constitutes the barrier that protects internal organs and veins in the body from external attacks. Similarly, keratin is part of the bulk of epidermal appendages in the form of hair, nails, , horns, claws, turtle scutes, whale baleen, feathers and beaks, where keratin has been blended with some other materials and moulded to harden in response to a greater level of protection, defence, predation and fishing[18]. These three aspects are key topics for the occurrence of keratin in different families of species in the animal kingdom. Protection is satisfactorily exemplified in fur, feathers and scales, three types of hard structures, where the first two were designed to protect from the external conditions and maintain body heat in physiological temperature and the latter has evolved as a shield to

protect softer tissue from external attacks from predators or environmental conditions. Fur and feathers are exclusive and typical features found in mammals and birds respectively, whereas scales are found in the three families where the frequency of occurrence prevails in all species of reptiles and birds and one species of mammals e.g. pangolin truly possess this feature[15]. Many reptilian species have developed a greater level of protection in structures like turtle and tortoise scutes where the armour is designed to protect the individual from predator attacks by providing a mechanically strong shield not easily broken by claws or teeth[19].

Defence is easily observed in the form of horns and antlers in a number of mammalian species e.g. bovine species where the armour is designed to fight rivals over territory and mating rights, as well as defence against predator attacks. Reptilian species e.g. horned chameleon seems to be a suitable example of the develop of horns for defence purposes in the same way as explained for mammals, however the vast majority of horn-like structures found in most reptilians e.g. Horned lizards are spiny scales that serves as adaptation to their arid environment where the armour serves as camouflage and protection from predators making the lizard difficult to swallow[20]. In contrast with the two families already mentioned, bird species have developed horns in few species and it provides sex appealing in mating rituals where the males boast their virility by the looks of the horn as evident in species like guinea birds and cassowary where a prominent single horn-like helmet raises above their heads often referred to as casque[21].

Predation is probably one of the most remarkable behaviours where the presence of keratin as a structural protein can be observed at its maximum expression. Nails and claws represent the most well know expression of keratin in this category, since they are vital tool for the success of predators in catching prey. Their function is to tightly grasp prey and prevent it from scape and some cases as it occurs in birds of prey, claws are also killing tools that pierce flesh, but for many mammals and reptiles claws are fundamentally holding tools with long and sharp characteristics. In addition

to claws and nails, beaks are another well-known keratin-based structure typical of birds and some reptiles where predation is also well exemplified as the equivalent version of the jaw, making them essential for the survival of those species. Beaks are also long and sharp structures, designed to cut flesh and small bones and unlike claws that are considered dead tissues, solid in consistency and with little contact with living tissues, the connection between beaks and living tissues is superior due to the fact the beaks supply the carcass of the mouth so the architecture is intended to contain and product soft tissues inside, making beaks less solid in consistency than their fellow predatory tool.

Given the wide spread and natural abundance of keratin and the versatility of structures it can form ranging from soft materials e.g. hair, fur, feathers to hard materials e.g. horns, claws, scales, the importance of this material is not only a natural concerned but also an economical need too for some industrial process nowadays, where the soft structures have been found particularly useful for textile production and cushion fillings. For these purposes mammalian wools and skins and bird feathers are especially important representing primer matters that result into commercial grade wool, fabrics, clothes, cushion fillings amongst many derived products. As a result of other economic activities keratin-rich materials e.g. furs, skins and birds feathers are also a waste by-product from poultry and cattle slaughtering processes and from this perspective, this waste product have become an environmental concern on account of the high demand of meat nowadays that produces enormous amounts of wastes annually that are directly disposed into landfills. The estimated annual keratin waste exceeds 5 million tons per year of which a great deal are contributed by the textile industry and slaughterhouses[22-24] in the form of Chicken feathers, cattle fur and sheep wool. These waste products have a low rate of bio-degradability despite of their organic composition, which places them in a position similar to plastics that are long lasting materials that account for accumulated inert solid material that pollute the ecosystem by their enduring nature. Current

research in the development of new materials consider keratin as a potential and relevant starting material due its remarkable mechanical properties and because of its content in sulphur which makes keratin useful for some biological applications and considering the environmental impact keratin waste products are causing new technologies for isolation and purification of keratin from sources like chicken feather, wool keratin and even human hair have been proposed for research purposes as an alternative to disposed of the great amount of keratin waste products produced every year.

1.2.2. Properties of keratinous materials

In addition to the abundance and availability in nature, keratin is important in industrial processes for its mechanical properties that allows to build mechanically-resistant products such as textiles and fabrics. These mechanical properties are explained at a great extent by the sulphur content from cysteine residues (7-20% in total amino acid content)[25-27]that form intra and inter-molecular disulphide bonds that results into a highly stable arrangement suitable for structural functions[28-30]due to the its poor solubility in water and organic solvents that protects the integrity of the protein. Keratin on account of its structural function in many living organism it is often considered a dead tissue due to its low reactivity but this doesn't refrain keratin from reacting with surrounding substances, since the reactivity will vary and depend on the amino acid composition, where every individual amino acid residue undergoes the chemical reactivity typical of the functional groups they contain. Some examples of the amino acids found in wool keratin and hair keratin are reported in tables 1.1 and 1.2 [31-35] respectively, including individual amino acid content.

Table 1.1. *Amino acid composition of keratin extracted from wool (taken from references 31-35)*

Amino acid	Keratin (wt%)
Aspartic acid	5.88
Threonine	5.07
Serine	8.99
Glutamic acid	8.74
Proline	9.51
Glycine	3.03
Alanine	3.54
Cystine	5.07
Valine	4.33
Methionine	0.19
Isoleucine	2.73
Leucine	6.47
Tyrosine	2.98
Phenylalanine	2.04
Lysine	1.2
Histidine	Undetected
Arginine	7.49
Tryptophane	0.34

Table 1.2. *Amino acid composition of hair keratin (taken from references 31-35)*

Amino acid side-chain type[a]	Approximate micromoles per gram hair
1. *Hydrocarbon* (except phenylalanine)	2,800
Glycine, alanine, valine, leucine, isoleucine, and proline	
2. *Hydroxyl*	1,750
Serine and threonine	
3. *Primary amide + carboxylic acid*	1,450
Primary amide (ammonia estimation)	1,125
Carboxylic acid (by difference)	325
4. *Basic amino acids*	800
Arginine, lysine, and histidine	
5. *Disulfide*	750
Cystine	
6. *Phenolic*	180
Tyrosine	

Similarly, as occurred in the mechanical properties, the sulphur coming from cysteine residues seem to be the dominant functional group responsible for the majority of the reactivity of keratin due to being susceptible to oxidation-reduction processes by atmospheric oxygen on the outside and reducing agents from inside in morphological conditions. The

former is more frequently observed for natural occurring materials and the latter although less frequent observed for these materials remains likely to happen but it usually occurs under physiological conditions where reducing agents are commonly present. The explanation for the oxidation-reduction reactions keratin undergoes is primarily evident by the easiness by which cysteine residues can form disulphide bonds which constitute an oxidative state and can also remain as free thiol groups which are the product of breaking a disulphide bond by the action of reducing agent leaving two thiol groups which are the reduced molecules[36]. These two reactions are part of the cycle many proteins with cysteine residues undergo as part of biochemical reactions in living organisms, but for keratin oxidation is more important and frequent since most of cysteine residues are in the form of disulphide bonds that confer mechanical strength and resistance to the structures they form on account of the covalent bonds that are strong-linking bonds only susceptible to reducing agents that are usually absent in the surroundings of keratin structures.
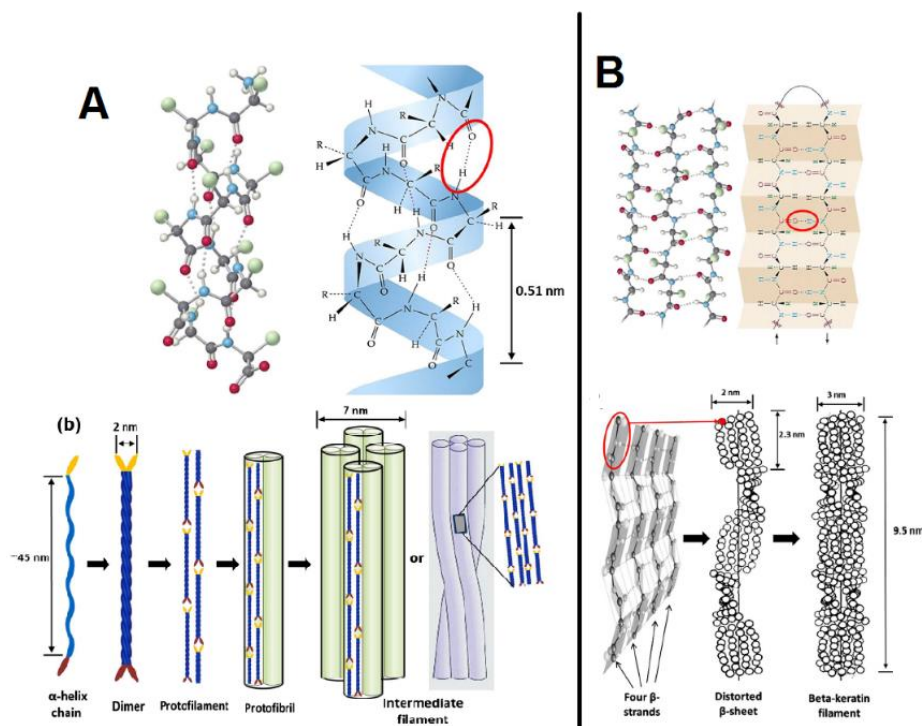
Figure 1.5. Stuctural representation of α keratins (A) displaying an α helix arrangement and β keratins (B) displaying β sheets conformation (taken from reference 15).

The outstanding mechanical properties of keratin are largely understood by the chemical composition but another structural aspect plays an important role in the explanation of the mechanical properties of keratins and this aspect refers to the secondary structure in which keratin could be assembled in. As occurs in many proteins, keratin might show two types of arrangements or conformations known as α-helix or β-sheet (Figure 1.5). Depending on the orientation the polypeptide chains are they can adopt the α-helix conformation where the chains coil into a spring-like structure resembling a helical rod held by hydrogen bonds or they can form β pleated sheets that are formed by beta strands bonded laterally with each other by hydrogen bonds, where each beta strand could contain 510 residues widely distributed in an expanded conformation[37]. These types of conformations allow the distinction between keratins not only by the way they are spatially assembled but also by the molecular weight each type of keratin displays, being 40-70 kDa for alfa keratins[38-40]commonly found in greater abundance in mammalian keratin and in lower abundance in bird and reptilian keratins. Beta keratins on the other hand are common and abundant in reptilian and bird keratin and in a lower concentration in mammalian keratins displaying molecular weights from 11 to 28 kDa[39,41-43].

Reptilian keratin has not been thoroughly studied and all the known evidence suggest a similarity with feather keratins. On the other hand, there is enough information about the chemical properties of these keratins that points at a lack many of the integrin binding sites or motifs in feather keratins and mammalian keratins on the contrary, are abundant in this sites, especially the hair types. This binding sites are patterns in the amino acid sequence that have specific binding functions for a range of substrates which makes mammalian keratins potentially useful for biomedical applications where such functions are desirable and sometimes fully required[44-46].

Keratin is a material that consist of intercellular proteins filaments packed up tightly together surrounded by a protein matrix that glue them together.

Mammalian are said to be formed faithfully by this composition, while feather and reptilian keratins are unbalanced formed predominantly by the protein matrix that is associated with β keratins. The co-existence of both α and β keratins in mammalian keratins in spite of the domain of the former over the latter is justified by the fact that the α-filaments cannot be held together without the β-matrix, notwithstanding the greater presence of the filaments over the matrix in this recipe and this is why mammalian keratin are regarded as a heterogeneous mixture of α and β keratins whereas feather and reptilian keratins are rather considered mainly a heterogeneous matrix of β-keratins[18].

Another general classification of keratin, divide the family of sub species into two groups according to their pH-properties that might be acidic for those keratins likely to display acidic properties on account of the functional groups from their amino acids in their protein back bone. Other keratins on the contrary might be display no pH fluctuations or slight basic properties and they are considered to belong to a common group known as neutral-basic keratins. Both groups are also referred to as type I and II for acidic and basic-neutral keratins respectively. Molecular weights are also a characteristic of every group ranging from 46-55 kDa for type I keratins and 54-57 kDa for type II[47].

1.2.3. Isolation of Keratins

Keratin unlike many other natural polymers is not extensively commercialised so the extraction from natural sources is a common practice in current research. Various attempts have targeted to extract keratin from wool or hair and most of them employ strong acid and alkali hydrolysis as a way to promote chemical cleavage of the disulphide bonds to extract keratins [22,48,49]. Other approaches involve physicochemical methods, such as high-density steam flash explosion, requiring high pressure equipment [50]. Among the small number of processes undergone

at industrial scale for isolation of keratin Ionic fluids and enzymatic hydrolysis stand as distinctive methods with little diffusion within the industrial sector due to their higher cost and longer production cycle [51-53]. On account of the number of process of methods for the isolation of keratin, there has been a prevalence of some methodologies over others normally based on the substrate or natural source used as raw material. This is evidenced in the isolation of the protein from animal hair which is commonly carried out under alkaline conditions to allow the hydrolysis. In addition, oxidative and reductive conditions are also currently included in the isolation of keratin yielding keratose and keratein as the final product for the oxidative and reductive methods respectively [54-56]. Some typical reducing agents in recent studies e.g. thioglycolic acid, thiourea and 2-mercaptoethanol facilitate the cleavage of disulphide bonds formed between cysteine residues by reducing them into thiol groups [57-59,49].

Some other methods rely on stronger reducing agents like Na_2S in an attempt to improve yields and some other methods are conducted via 1-pot methodology by combining the milder reducing action of 2-mercaptoethanol aided by denaturing agents such as urea and thiourea which altogether preserves the integrity of keratin and also produces a product with better solubility. The combination of 2-mercaptoethanol with denaturing chemicals is commonly known as Shindai method (Figure 1.6), since this method is currently used for the extraction of keratin from natural sources and has proved to be reliable for the isolation of the protein under mild conditions.

Shindai method

Hair samples were immersed in 300 μL of buffer containing 20 mM tris-hydrochloric acid (tris-HCl) (pH 8.5), 2.6 M thiourea, 5 M urea and 5% (w/v) 2-mercaptoethanol

50 °C

24 h   48 h

protein extracts

Undissolved hair fractions were separated from supernatant using QIAquick spin column by centrifugation

Acetone precipitation

pellets were resuspended in a suitable sample buffer

Figure 2.6. Shindai method applied for the isolation of keratin from hair (taken from reference130)

1.2.4. Keratin based materials and bio-composite systems

Biomedical sciences are science-related disciplines dealing with the understanding of physiological systems in order to provide solutions to the treatment of human diseases. Current research on this subject is focussed on innovative alternatives that can replace standard protocols by conducting processes that resemble biological reactions in the body. The development of biological devices often includes natural substances that exhibit enough structural resemblance as to induce a positive response when introduce in the body.

The water-solubility, biocompatibility, biodegradability and non-toxicity properties of proteins makes them superior over many synthetic polymers in biomedical applications. Keratin is one natural occurring protein of great interest in research nowadays, due to their inexpensiveness and relatively simple extraction from natural sources that are often waste products of industrial or manufacturing processes such chicken feather and wool-based textiles. Regenerated keratins from these resources can be transformed in

17

to membranes, powders, sponges, films, hydrogels and foams for a wide range of applications that includes water absorption, air purification and scaffolds for tissue engineering [60,61].

Keratin obtained from chicken feather or other animal sources extracted using chemical methods, is used as additive in commercial cosmetic products for healthcare where the intact protein has significant relevance in restoring the mechanical strength of the damaged hair fibers [62-67]. The presence of keratin K31, the major protein lost in the damaged hair [68-73], seems to integrate into the damaged hair filling the gaps smoothing its texture and enhancing their elasticity and mechanical strength.

Keratin derived material e.g. keratin-based hydrogels and keratin nanoparticles are considered suitable as delivery systems for anti-inflammatory, anti-tumor or antibiotics drugs [60,74-76]. Electro spinning of keratin blended with synthetic polymers allowed the fabrication of wool keratin/polyamide nanofiber mats in formic acid, displaying a randomly orientated pattern potentially useful for the adsorption pf heavy metal ions and dyes [77,78]. Following the same principle, Wool keratin has been blended with poly(L-lactic acid) (PLLA) in an attempt to improve the cell affinity the results suggest the presence of keratin has enhanced the interactions between osteoblast cells and the polymeric membranes [79].

Hydroxyapatite is a widely used inorganic material used in tissue engineering that is blended with keratin to obtain the (HA)-keratin nanocomposite via in situ biomimetic synthesis approach. As a result of in vitro cell culture studies performed on this composites, significant bone formation was observed, demonstrating the relevant contribution of keratin in promoting cell growth [80].

Similar results have been achieved in tissue engineering aiming to treat cartilage conditions, wound healing and skin regeneration by combining

keratin with other bio-polymers such as chitosan, collagen and alginate moulded into 2D and 3D nano fibrous scaffold materials [81-86]. The anti-fungal and antibacterial properties of chitosan combined with the bio-compatibility and wound healing ability of keratin yields an enhanced material suitable for the fabrication of wound dressings [87-90]. Similarly, alginate has been included in the treatment of chronic wounds where the gelation properties of the bio-polymer serve as filling material in deeper wounds. Collagen imparts elasticity and allows moulding into fine materials as evidenced in chicken-feather keratin-collagen composite films which also proved fast wound healing properties [91-96].

Keratin extracted from hard dead tissues have been widely used in the fabrication of scaffolds and drug delivery carriers for skin, muscle, and nerve tissue engineering [56,97-100] showing positive response on animal models and clinical patients [83,101-105]. Other types of keratin regardless of their origin have particular features useful for a number of bio-medical procedures and that is why current research in the development of new bio devices still counts on keratin as an important component for fabrication of these devices.

Thiol groups lead the reactivity in keratin and many applications of keratin are based on this. Michael addition reactions are increasingly used for the synthesis of keratin-based hydrogels, used to functionalise or cross-linked the protein (Figure 1.6). Michael addition
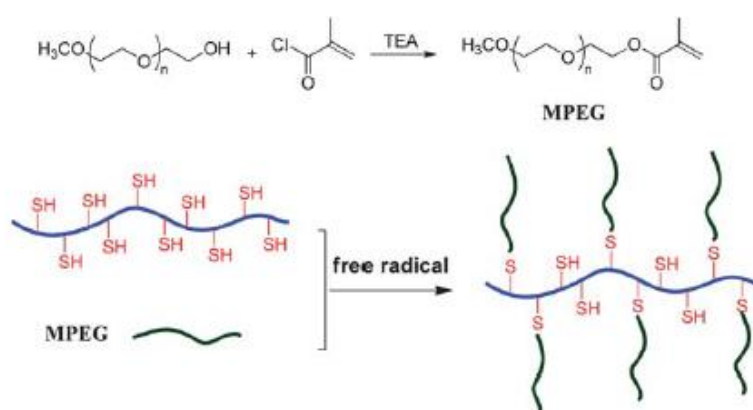
Figure 1.7. *Synthesis of keratin-g-PEG copolymers through thiol–ene (reference 106).*

1.2.5. 3D printing and photo crosslinked materials

Hydrogels are interesting bio-devices that can be built using keratin in the bio-medical sector some casting techniques have emerged in order to personalise the architecture of the gels according to their purpose, hence improving their efficiency in health treatments. 3D printing and photo-crosslinking are two novel gel-casting methods that can facilitate the fabrication of keratin-based hydrogels in combination with the formulations previously reported.

Recent research works have used a wide range of biomaterials to fabricate hydrogel scaffolds, including synthetic PEG and PLA based polymers as well as natural polymers such as proteins, alginate and chitosan [107]because of their biocompatibility and degradability properties. The manufacturing of such scaffolds is often carried out by well-known techniques such as molding, gas foaming, solvent casting with particulate leaching and electro-spinning [108-113]. Those casting techniques represent different approaches to obtain gels in laboratory conditions that share common limitations regarding shape control and consistency. Recently, a novel technique named 3D printing has emerged to meet the requirements for tissue engineering by providing a manufacturing process of 3D objects constructed from digital models designed by CAD software (Computer Aided Design) that simplifies the prototyping of the objects [114,115]. The software designs a virtual model that can be constructed layer by layer, allowing the creation of novel inner structures with defined pore size or complex geometries [116].

3D printing processes can be classified into different types according to the materials and the deposition method used for the construction of the layers. Some of them use melt or soften rigid/powdery materials to generate the layers, such as Fused Deposition Modeling (FDM) [114,115], while some others

form a solid material from a powdery starting material by using a laser, e.g. Selective Laser Sintering (SLS) [114-116]. Similar approaches use lasers to solidify and cure liquids (resins) sensitive to light by forming polymers after exposing the resins to UV light. This technique is usually referred to as Stereo lithography (SL or SLA) [114-116]. These two techniques are suitable for polymer systems due to the instrument arrangement that allows to include molecules sensitive to temperature or light (Figure 1.8) (SL is regarded as a Solid Freeform Fabrication (SFF) technique that exclusively produce objects by curing liquids usually with UV light. SFF is a versatile photo-casting process that offers various casting systems ranging from direct curing of resins contained in an open reservoir to extruding viscous liquids from an enclosed reservoir in order to produce filaments that instantaneously solidify after subsequent exposure to UV light [117]. The latter is a variation of SFF known as nozzle deposition and is aided by photo-initiators that trigger a photo-polymerization reaction by free radicals between the monomers in the resin [118].

Modern SFF devices are adapted to perform Multi Nozzle Deposition (MND) in which an extruder constructs a filament by combining the depositions from several nozzles, each one containing different concentrations of monomer and photoinitiator. This approach enables the transition from hydrogel systems to rigid scaffolds, constructed by layer-by-layer deposition producing well-defined three-dimensional networks. Moreover, MND has demonstrated to have influence in the pore size of the scaffolds for polymer systems constituted of Alginate and $CaCl_2$ (cross linker) where, it is possible to obtain pore cross-sectional areas of 13731 μm^2 [118].

In the same way, a four-micro-nozzle array with sizes from 30 to 500 μm can be incorporated to the same polymer system, using different types of nozzles such as pneumatic microvalve, piezoelectric nozzle, solenoid micro-valve and spray nozzle. As a general observation, the former displays the best performance at depositing a wide range of viscosities of Sodium Alginate solutions, confirming not only the ability to extrude viscous

solutions of sodium alginate but also the construction of scaffolds layer-by-layer using this polymer, which exhibits desirable properties for tissue engineering.
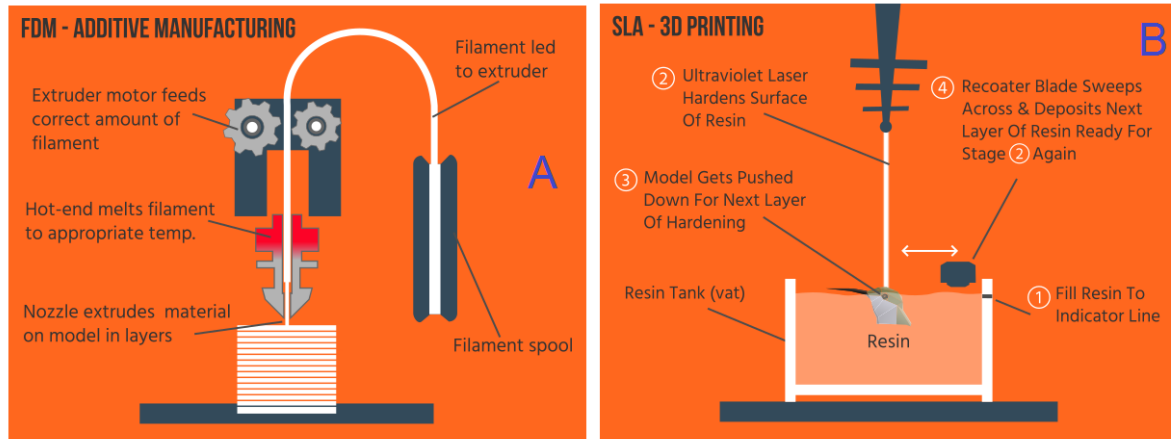
Figure 1.8. General representation of 3D printing systems, FDM (A) and SLA (B). source: (taken from reference 119)

1.3. Aim of the project

The present work is part of an MPhil project aimed to conduct research on the isolation of keratin from natural sources such as sheep wool and human hair, recognising the easy accessibility of these natural sources as well as their intrinsic properties as a biopolymer. The first stage of the project involves the isolation and characterisation of keratin from both sources. Two methodologies for the extraction of extraction of keratin are included as part of the first stage. The second stage of the project aims to produce keratin-based hydrogels by using Michael addition click crosslinking due to the relative abundance of thiol groups in keratin. Finally, some preliminary work on gel casting by photo-crosslinking reactions is planned to improve the mechanical properties of keratin gels and possibly bring this approach to a higher level of prototyping as it is 3D printing. Functionalised polysaccharides are part of this process as a potential paste for 3D printing.

2.0. Experimental procedures and methodology.

2.1. Introduction

This section describes the experimental procedures and methodology used for the extraction of keratin from natural sources via two isolation methods known as reducing with Na_2S (section 2.3.2) and the Shindai (section 2.3.3) method, further, the gelation studies with keratin via Michael addition reactions in which keratin reacted with a series of acrylates and methacrylates synthesised for this purpose, are described. In addition, this section also describes the procedures used for photo-crosslinking of the synthesised methacrylated compounds under UV-light as an alternative gelation procedure potentially useful for a higher level of gel casting.

2.2. Materials and chemicals

Most chemicals and solvents used in this work were purchased from Sigma-Aldrich. These include reducing agents Na_2S (nonhydrate 98%, Sigma-Aldrich) and 2-mercaptoethanol (98%, Alfa Aesar), denaturing agents such as urea (99.5%, Acros) and thiourea (99.0%, Acros), pH adjusting agent 2-amino-2-(hydroxymethyl)-1,3-propanediol also known as Trizma base (99.9%, Sigma-Aldrich). Washing and delipidising solvents as chloroform (reagent grade, Fisher Chemical), methylated Spirit Industrial: ethanol (99%, Fisher Chemical), methanol (GPC grade, Fisher Chemical) were used for the pre-treatment of raw materials in both isolation methods.

Three different human hair samples from Asian (female), British Caucasian (male) and South American (male) origin and one wool fibre sample from

the sheep breed *Badger Face Welsh Mountain sheep* were selected and used as the raw materials for the extraction of keratin (Table 2.1).

Table 2.1. *Raw materials for the extraction of keratin from natural sources*

No.	Type	Origin	Detail	
1	Hair	Female Asian	Black straight hair strands. Approximately 10 cm long	
2	Hair	Male South American	Black straight hair pieces. Approximately 3 cm long	
3	Hair	Male British Caucasian	Light Brown straight hair pieces. Approximately 5 cm long	
4		Wool	Welsh Sheep: Yellow long strands (entangled). Approximately 30 cm long	

Some other chemicals used in this work include HCl (37.0%, Fisher Chemical), phosphate buffer powder (reagent grade, Sigma-Aldrich) and deuterium oxide D_2O (99.6%, VWR Chemicals). DNTB 5,5'-dithio-bis-(2-nitrobenzoic acid) (98%, Sigma-Aldrich). H_2O (GPC grade, Fisher Chemical), KH_2PO4 (99%, Sigma-Aldrich), K_2HPO4 (99%, Sigma-Aldrich) and NaCl (reagent grade, Fisher chemical), Egg lysozyme and Bovine (crystalline/white powder extracted from hen egg white, Fluka analytical) Serum Albumin BSA (Lyophilized bovine plasma powder Poly(ethylene-glycol) diacrylate PEG-DA (reagent grade, Mn: 575 Da, Sigma-Aldrich), Soybean oil epoxidised acrylate (reagent grade, Sigma-Aldrich), Glycidyl methacrylate (97%, Acros) sodium hydroxide Methylated Spirit Industrial Ethanol (99%, Fisher Chemical). Acetonitrile (GPC grade, Fisher chemical), 2-Hydroxy-4'-(2-hydroxyethoxy)-2-methylpropiophenone   commonly referred to as Irgacure 2959 (98%, Sigma-Aldrich).

2.3. Isolations of Keratin from Hair and Wool samples

Reducing and denaturing chemicals played an important role in the two procedures carried out to obtain keratin, namely as reducing with Na_2S and Shindai methods. Detailed information is provided with regards to the experimental conditions for each method in successive sections, quoting some of the chemicals and materials mentioned previously.

2.3.1. Pre-treatment

This pre-treatment protocol was applied to all hair and wool samples used in this work before extraction procedures were taken place either by Na_2S or by Shindai methods. Welsh-sheep wool and the three types of hair samples were initially washed with approximately 500 mL of soapy water

(5 mL detergent liquid in 495 mL of tap water) and 1.5 L of tap water, giving a final wash with approximately 200 mL of ethanol solution (70 % v/v) and then air-dried. Following air-drying, delipidation of the material was achieved by leaving the material soaking in a Chloroform-Methanol mixture (66.6% v/v Chloroform, 33.4% v/v Methanol) for 24 hours. Upon delipidation, the wool or hair was air-dried and finally cut into smaller pieces (approximately 1-3 cm long) in order to undertake the keratin-extraction process (regardless of the type) more effectively.

2.3.2. Isolation of keratin by Reduction with Na$_2$S

Extraction by this method was conducted based on previous works previously reported[120,121]. Firstly, 200 mL of sodium sulphide solution 10 M were prepared by placing 156 g of anhydrous Na$_2$S into a conical flask with approximately 100 mL of deionised water, leaving this mixture under stirring at 200 rpm for 30 minutes. Gentle heating up to 30 °C was applied to the mixture, because the endothermic nature of the solubilisation of the anhydrous Na$_2$S in water can decrease the temperature in solution which reduces solubility. Further, 50 mL of deionised water was added to the solution and upon the mixture had turned into a solution (approximately 30 minutes), another 50 mL of deionised water were added to the solution in order to make a total volume of 200 mL of solution. The chemical equation (Scheme 2.1) describes the chemistry involved in the solubilisation of Na$_2$S in water producing sodium hydroxide and sodium sulfhydryl in solution.

$$Na_2S + H_2O \rightleftharpoons NaOH + NaSH$$
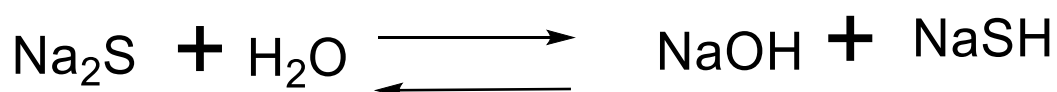
Scheme 2.1. *Chemical reaction for the dissolution of sodium Sulphide in water*

Following the preparation of Na_2S solution, Wool/hair samples (5 g) were placed in a round-bottomed flask containing 200 mL of Na_2S solution (10 M), at 40 °C (oil bath) and the mixture stirred at 250 rpm for 4 hours. The reaction solution was filtered in vacuum to remove insoluble material, keeping the filtered solution for dialysis against water in cellulose membrane tubes (molecular weight cut-off 2 kDa). The total volume of filtered solution (approximately 200 mL) was split in two cellulose tubes (25 cm long according to the tube capacity 4.6 mL/cm plus additional length to be occupied by dialysis clips).The dialysis process involved submerging the cellulose tubes in a 5-L glass beaker filled with deionised water up to the 5-L mark applying magnetic stirring to facilitate fluency of impurities from inside the tube to the outer media on account of the concentration gradient formed. Every 24 hours, the volume of water was replace by clean and fresh deionised water, making a total of 6 water changes. After purification by dialysis, the solution containing keratin was freeze dried for 72 hours to finally obtain keratin. All of the keratins extracted (batch 1 and batch 2 in Table 3.1 by this method were exclusively purified by dialysis and freeze dried and the raw material used for the extraction of both batches was raw material 1 (Table 1.1).

2.3.3. Shindai Method

Extraction by this method was conducted based on similar works previously reported by Nakamura Et al[122].A solution containing 200 Ml of urea (5 M), thiourea (2.6 M), trizma base (25 mM) and 2-mercaptoethanol (5 % v/v) fully dissolved prior to start the chemical reaction once the raw material was deposited inside. The total volume of reaction solution for this method was 200 mL, starting with 150 mL of deionised water to dissolve the denaturing agents: 60.0600 g of Urea and 39.5824 g of Thiourea both weighed in analytical balance. These denaturing agents due to be present

in high concentration required three quarters of the total volume to be dissolved plus gentle heating up to 45 °C and magnetic stirring at 250 rpm for 1 hour. Once the agents were fully dissolved, 50 mL of deionised water were added to make a total of 200 mL of solution. Subsequently, 0.6055 g (analytically weighed) of the pH-adjusting agent Trizma base was added to the solution, setting the pH value in 8.89 (keeping the same stirring speed, no heating was required for this step). The reducing agent 2-mercaptoethanol was the last reactant to be added into this solution, 10 mL of the reactant measured in glass-syringe for GPC sample injection were dropwise added to the solution under stirring at room temperature. After this step was completed and all the reactants were fully dissolved, 5.0308 g of Wool/hair were immersed in this solution. The reaction mixture contained in a 500-mL round-bottomed flask was attached to a reflux column circulating cold water through the column, setting the temperature at 50 °C (oil bath), under magnetic stirring (300 rpm) for 72 hours. Post-reaction treatment of keratins was identically performed by dialysis and freeze drying as described in section 2.3.2 for the reduction with Na_2S (Bacthes: 3,5,7 ,8 and partially 6 in sample W2, see table 3.3). Keratins obtained from Isolation batches 7 and 8 were extracted from raw materials 3 & 4 in table 1 respectively and Isolation batches 3 and 4 produced keratins exclusively extracted from raw material 1 in table 2.1.

In addition, purification by pH precipitation was another post-reaction treatment conducted on some hair keratins (Batch 4). This precipitation was carried out on the solution obtained from vacuum-filtration originally displaying a pH value of 6.56. This pH value was gradually lowered until precipitation was achieved by adding HCl 10% (v/v) solution dropwise. The reported pH threshold (final pH) for reaching precipitation was 4.8, no HCl solution was added after this value and sedimentation of keratins at the bottom of the beaker took place after the solution was left to settle for about 20 minutes. Supernatant transparent solution on the top was decanted and the concentrated bottom part was filtered in vacuum using a

Buchner funnel (qualitative filter paper) collecting the wet solid keratin which was subsequently washed with ethanol (99%) and finally vacuum-dried in Buchner funnel.

In a similar way, precipitation in cold acetone was the separation and purification step for some wool keratins (half of the total volume of batch 6). The post reaction treatment of the total volume of batch 6 was completed until the dialysis step the same as the procedure described for both Na_2S and Shindai methods. Upon completion of the dialysis step, the total volume was equally divided into two portions (approximately 100 mL each portion). The first portion was subsequently freeze dried under identical conditions as in reduction with Na_2S and the second portion underwent an additional step: precipitation in cold acetone. This precipitation was achieved by adding the portion dropwise into 100 mL of magnetically-stirred cold acetone (acetone was cooled down overnight in a conventional freezer), after which entangled strands were formed as soon as keratin solution entered into contact with cold acetone. Precipitated keratin in acetone was under stirring at 250 rpm for 30 minutes to allow full precipitation and subsequently the solution was decanted, vacuum filtered in Buchner funnel (qualitative filter paper) and finally freeze dried for 24 hours. Wool keratins obtained from isolation batches 5 and 6 were both extracted from raw material 4.

2.4. Characterisation

^{1}H-NMR Spectra were recorded in a Bruker Ultrashield TM Plus 400 Equipment, using D_2O as solvent at 20 °C and Phosphate Buffer powder (1 mg/mL) to increase solubility of keratin in D_2O. Fourier Transform Infrared spectra were measured in FTIR spectrometer ALPHA in solid state using ATR accessory, at a resolution of 2 cm^{-1}.

Thiol groups in keratins were quantified by Ellman´s method[123-125]. The general procedure involves the stoichiometric reaction between DTNB and thiol groups from sulfhydryl molecules (Scheme 2.2), followed by the release of TNB anion which was measured at 412 nm in a Perkin Elmer, Lambda 35 spectrometer, using quartz cells (1 cm light path).

In addition, UV-VIS spectra of keratins were recorded operating the same spectrometer at a resolution of 1 nm. For the obtention of the UV-VIS spectra, every keratin sample was prepared by dissolving 2-3 mg of Keratin in 2 mL of Phosphate buffer solution at pH 7.4, followed by stirring in a vial-vortex mixer at 1000 rpm for 5 minutes at room temperature.

Thiol content of keratins by Ellman's method involved in the construction of two calibration curves using 5 different concentrations of a sulfhydryl standard compound 2-mercaptoethanol. Phosphate Buffer solution pH 7.4 was used as the solvent for preparing all the solutions while DTNB (Ellman's reagent) was the reactant by which UV quantification was achieved at 412 nm upon release of TNB. Detailed experimental data about the solution preparation for constructing the calibration curves as well as the keratin solutions (analyte) are confined in tables 2.2 and 2.3. Figure 2.1 shows the flow chart of the experimental steps for the construction of the calibration curves. Bulk solutions were the starting solutions to prepare the stock solutions. DTNB Bulk solution is identical to the DTNB Stock solution 1, since the target concentration for S.S.1 was easily achieved from the solid reagent without further dilution, unlike 2-mercaptoethanol solutions that required a step-by-step preparation. DTNB dilutions were made with Phosphate buffer solution pH 7.4 whereas 2-Mc.Ethanol solutions were diluted in deionised water. 2-Mercaptoethanol bulk solution was prepared by dissolving 1 mL 2-Mc.Ethanol in 99 mL of deionised water to reach a final concentration of 0.142 M. DTNB bulk solution was prepared by dissolving 0.001 g DTNB dissolved in 1 mL Phosphate buffer solution pH 7.4 to reach a final concentration of 2.52×10^{-3} M. Stock solutions were prepared according to table 2.2. Calibration curve (Figure 2.2) was

prepared following the stoichiometry of the equation in scheme 2.2, in which identical equivalents of reactants produce the disulphide interchange reaction. The curve was constructed according to the data presented in table 2.3 that describes a series of 5 chemical reactions that were read in the UV-Vis instrument at 412 nm after reaching the yellow appearance of TNB anion that indicates the reaction has occurred.
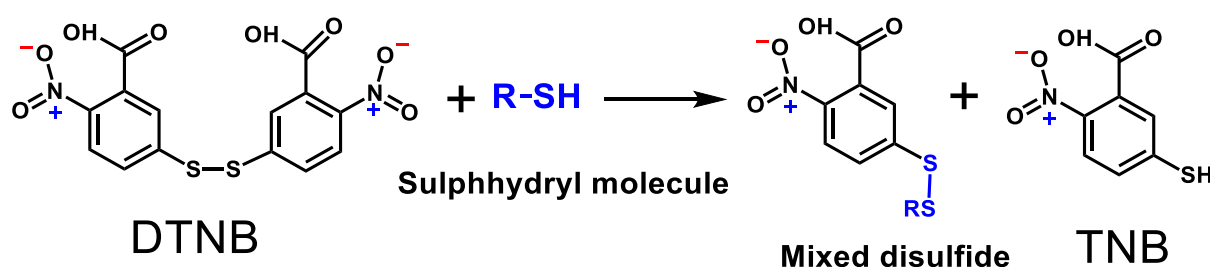
Scheme 2.2. *Chemical reaction for thiol content determination by Ellmans' assay.*

GPC was performed in a Prominence GPC System equipped with a LC-20AD pump and UV detector SPD-20AV and the separation was carried out using a Biosep SEC-S2000 protein column (300x7.80 mm) under isocratic elution with Phosphate Buffer Solution pH 7.5 as the mobile phase. The eluent was prepared by dissolving 0.544 g of KH_2PO_4, 0.913 g of K_2HPO_4 and 11.69 g of NaCl in two litres of GPC water and the pH was adjusted to 7.5 by dropwise addition of 2 mL of aqueous solution of NaOH (40% w/v). Prior running Keratin samples on the system, a calibration curve was obtained using standards: egg Lysozyme and bovine serum albumin BSA to create a range of molecular weights between 14.4 and 66.5 kDa with respect to the molecular weight of the standards. Figure 2.3 describes the experimental conditions under which GPC calibration curve was obtained and keratin samples were run. Keratin samples were all prepared by dissolving 1 mg of keratin in 1 mL of eluent, following by stirring in vortex mixer for 3 minutes. Standards egg Lysozyme and BSA solutions were prepared as follows: approximately 3 mg of solid egg lysozyme were dissolved in 1 mL of eluent and BSA pure liquid reagent (1.52 mg/mL) was used (0.5 mL) without further dilutions.
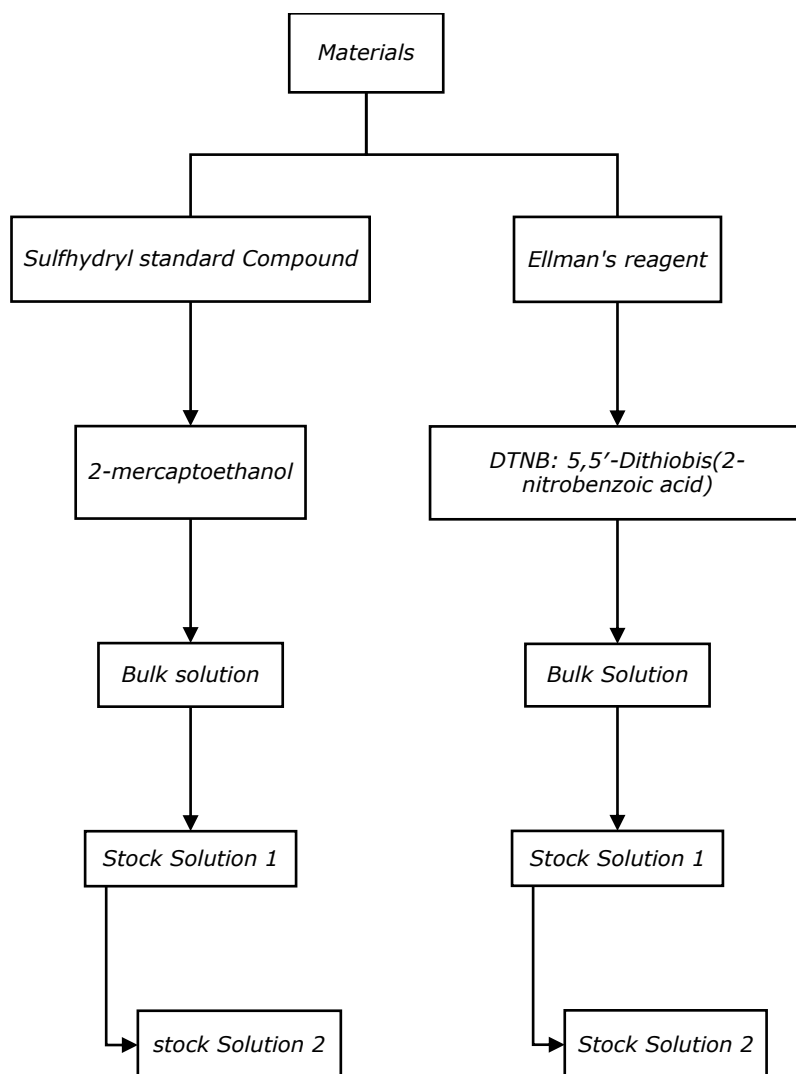
Figure 2.1. *Flow chart of experimental steps for preparing stock solutions in Ellman's assay.*

Table 2.2. *Preparation of stock solutions for Ellman's assay following flow chart in figure 2.1. Each stock solution was prepared to make a total volume of 1000 µL.*

	Stock solutions (S.S)			
Solution	**aliquot (µL)**	**Solvent vol. (µL)**	**Conc.(M)**	**Type**
Stock solution 1	1000 from B.S	0	2.52E-3	DTNB
	18 from B.S	982	2.56E-3	2-Mc.Ethanol
Stock solution 2	10 from SS1	990	2.52E-5	DTNB
	10 from SS1	990	2.56E-5	2-Mc.Ethanol

Scanning Electron Microscopy SEM images were obtained using a 1984 Hitachi S-520 scanning electron microscope equipped with a secondary electron detector and a PC based image capture system. The instrument can operate with a variable accelerating voltage ranging from 1-30 kV adjustable in 1 kV steps, and a magnification range of 20x-200,000x. For the sample preparation, hydrogel samples were freeze dried for 24 hours first in order to remove all the water content that could interfere with the microscope. Hair samples on the other hand, only required washing with detergent followed by air drying. After drying, the samples were mounted on a 0.5" aluminium specimen stub (12.5mm diameter), using a double sided adhesive carbon tab, then they were gold coated in a thermal evaporator Edwards E306A equipped with a single evaporation source and PC based crystal thickness monitor, under a high vacuum of 8×10^{-6} mbar. After 10 nm of gold was deposited onto every sample, they were introduced into the microscope and images were obtain at x60, x250, x700 and x1000 zoom-in.
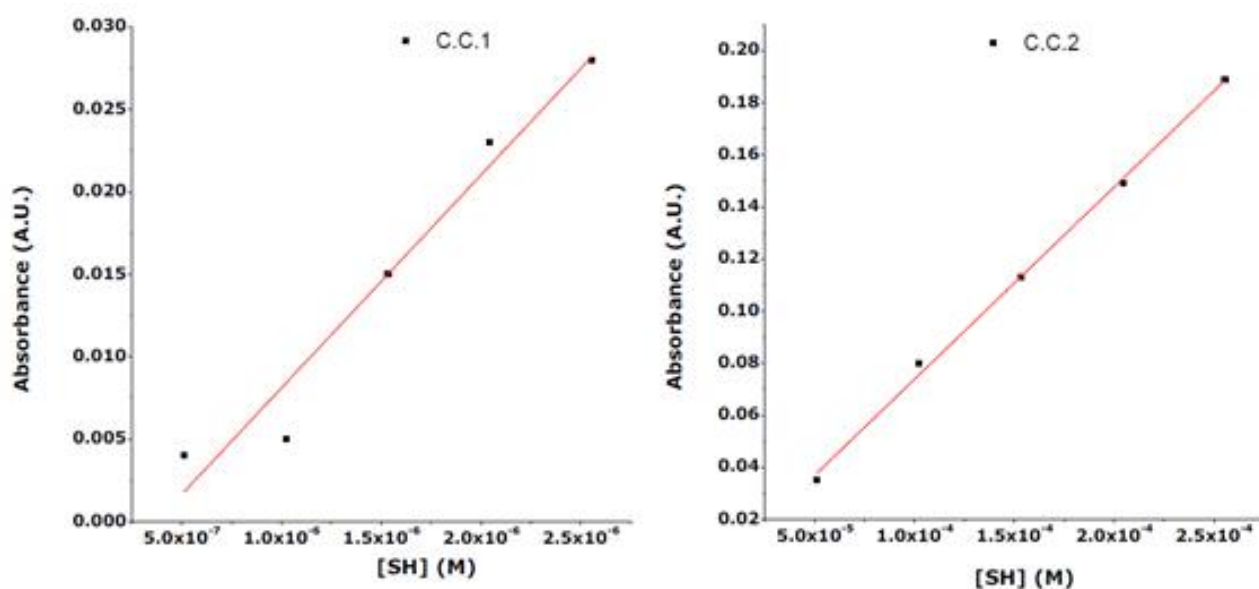
Figure 2.2. *Calibration curves (cc1 & cc2) for Ellman's Assay.*

Table 2.3. *Calibration curves and linear regression for Ellman's assay.*

Sln	Preparation		Thiol Concentration (M)		Absorbance (A.U.)	
	Calibration Curve 1	Calibration Curve 2	C.C.1	C.C. 2	C.C.1	C.C.2
1	20 µL of each type of S.S.2 + 960 µL PBS pH 7.4	20 µL of each type of S.S.1 + 960 µL PBS pH 7.4	5.11E-07	5.11E-05	0.004	0.035
2	40 µL of each type of S.S.2 + 920 µL PBS pH 7.4	40 µL of each type of S.S.1 + 920 µL PBS pH 7.4	1.02E-06	1.02E-04	0.005	0.08
3	60 µL of each type of S.S.2 + 880 µL PBS pH 7.4	60 µL of each type of S.S.1 + 880 µL PBS pH 7.4	1.53E-06	1.53E-04	0.015	0.113
4	80 µL of each type of S.S.2 + 840 µL PBS pH 7.4	80 µL of each type of S.S.1 + 840 µL PBS pH 7.4	2.04E-06	2.04E-04	0.023	0.149
5	100 µL of each type of S.S.2 + 800 µL PBS pH 7.4	100 µL of each type of S.S.1 + 800 µL PBS pH 7.4	2.56E-06	2.56E-04	0.028	0.189

Linear regression and beer-lambert law						

$Y = mX$ *Straight line equation* $Y = A \; ; \quad X = C \; ; \quad m = \varepsilon l$

$A = \varepsilon l C$ $Beer - Lambert\ law$

C.C	Slope "m" (M^{-1})	Path length "l" (cm)	ε (M^{-1}cm^{-1})	r^2
1	12911	1	12911	0.9595
2	737.48	1	737.48	0.9978
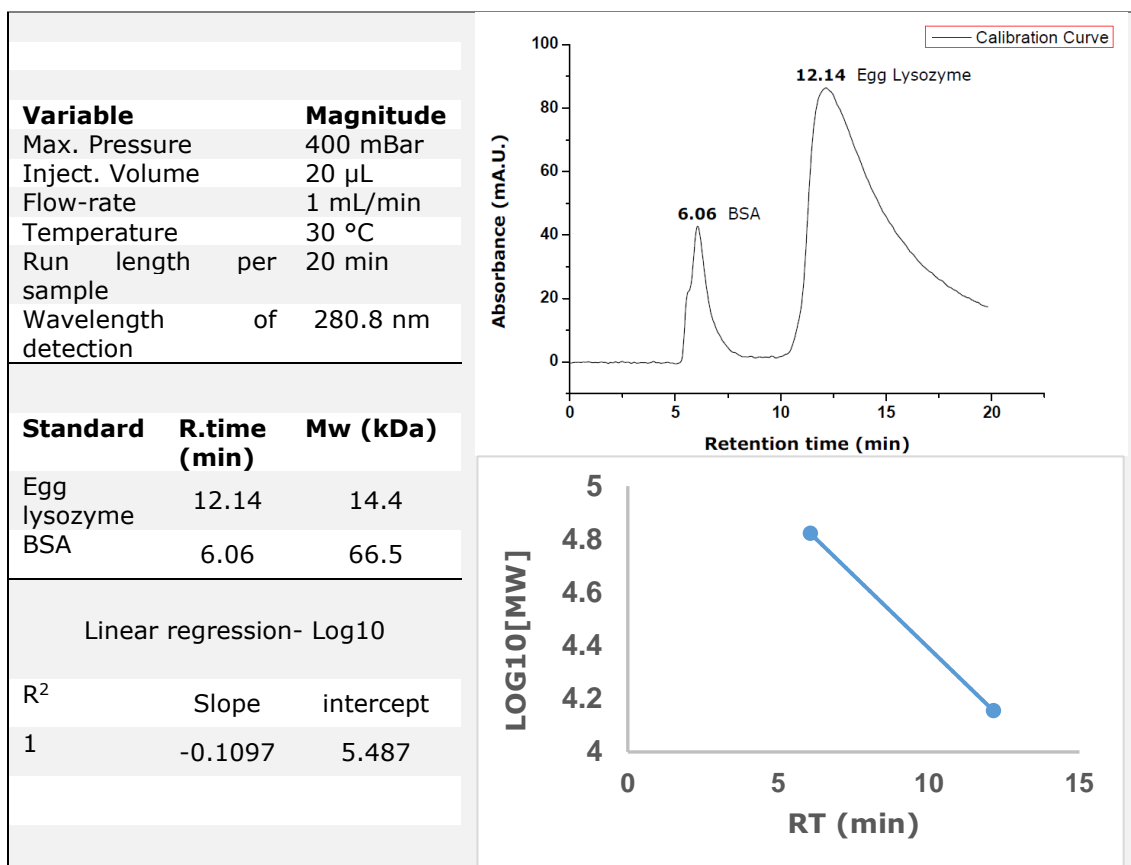
Figure 2.3. *Experimental conditions for GPC calibration curve displaying standards: Bovine Serum Albumin (BSA) and egg Lysozyme eluting at 6.06 and 12.14 minutes respectively.*

2.5. Methacrylation of Sodium alginate and Chitosan

Polysaccharides-derived compounds were initially synthesised as the precursors (monomers) for the UV-light assisted reactions described in section 2.7. Sodium Alginate and Chitosan underwent functionalisation by introducing methacrylate groups in their sugar backbones. Methacrylation of Sodium alginate was achieved via synthetic general procedure reported in literature[126,127], however modifications were made to the reactant ratio (double amount of each reagent). The synthesis was conducted as follows: 3.9971 g of Sodium Alginate were dissolved in 100 mL of water followed by pH adjustment by dropwise addition of NaOH solution (10% w/v) until pH value was 10. This solution was then purged with N_2 in order to maintain an inert

atmosphere prior of addition of the air-sensitive reagent glycidyl methacrylate (GMA). 11.3603 g of GMA in liquid state were analytically weighed out and introduce into the basic alginate solution by dropwise insertion using a hypodermic needle attached to a plastic syringe. Original amounts of reagents from previously reported work[126,127]were doubled in order to promote functionalisation)

The reaction (Scheme 2.3) was then started by setting temperature for 60°C and magnetic stirring at 250 rpm overnight (approximately 11 hours). After this time, the solution which was originally clear turned cloudy, indicating the formation of the derived compound. This solution was then dropwise added to 200 mL Ethanol (95%) under magnetic stirring (250 rpm) to allow precipitation of Methacrylated alginate. The solid product obtained was filtered in vacuum (Buchner funnel), washed with ethanol 95% and left in the freezer overnight for subsequent freeze-drying for 48 hours.

In a similar way Methacrylated Chitosan was synthesised following protocols from the literature[128,129]and introducing variations as follows: 1.0025 g of Chitosan were dissolved in aqueous acetic acid solution pH 3.0 and left under magnetic stirring (250 rpm) until fully dissolved for 30 minutes, subsequently pH was increased to 3.8 by adding dropwise KOH aqueous solution (10% w/v). Once Chitosan was fully dissolved and pH was adjusted for 3.8, the reaction mixture was purged with N_2 and left under this inert atmosphere before the addition of the methacrylating agent. 4.0092 g of GMA in liquid state were analytically weighed and introduced into the acidic Chitosan solution by dropwise insertion using a hypodermic needle attached to a plastic syringe. Upon addition of GMA into the solution, the reaction (Scheme 2.4) was set at 58°C, magnetic stirring (250 rpm) and N_2 atmosphere for 18 hours. After this time no changes in colour were observed but some increase in the viscosity was evident when the solution was dropwise added to 800 mL of acetonitrile under magnetic stirring (250 rpm).

Methacrylated chitosan precipitated out in acetonitrile forming a white solid strand that were collected by filtration in vacuum using a Buchner funnel. The solid collected was frozen in a conventional freezer, followed by freeze-drying for 48 hours.
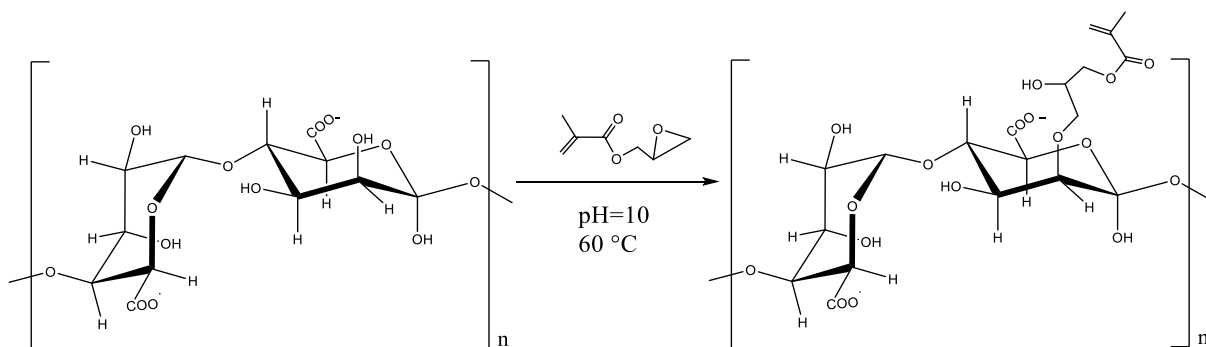
Scheme 2.3. *Chemical equation for the methacrylation of sodium alginate under basic conditions.*
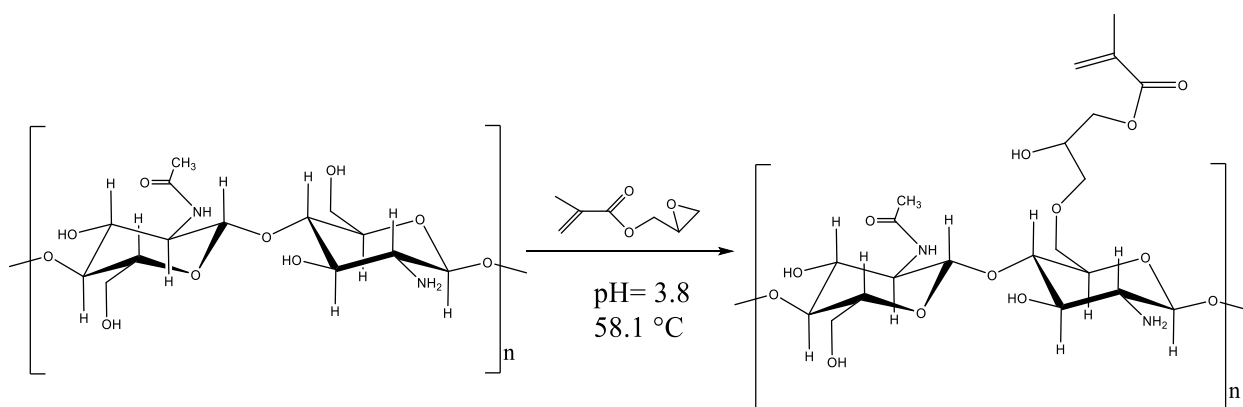
Scheme 2.4. *Chemical equation for the methacrylation of Chitosan under acidic conditions.*

2.6. Gelation studies with keratins by Michael addition reactions

Fully characterised keratins were used to prepare gels with a series of cross-linkers following a Michael addition reaction approach (Scheme 2.5). Keratin were mixed with a series of acrylates and methacrylates in basic solutions under similar conditions, but different reaction time. The reactants kerating, acrylates and metacrylates in basic solutions were incubated in a water bath at 38.5 °C until reaching gelation. The

ratio of Keratin/acrylates as well as the conditions under which each reaction was carried out are displayed in table 2.4. Every reaction was contained in an Eppendorf tube (1.5 mL, translucent plastic tube) which was secured using poly urethane foam on the top part to maintain a vertical floating orientation during reaction (Figure 2.4).

$$R-SH + R' \diagup\!\!= \longrightarrow R-S\diagup\!\!\diagdown_{'R}$$
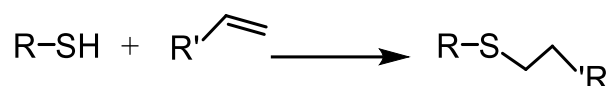
Scheme 2.5. *Michael addition chemical reaction between a thiol group and double bond producing a new single covalent bond linking the two molecules.*

Table 2.4. *Experimental conditions for Michael addition reactions.*

R.No	Materials	Detail	% w/w	T.Vol (µL)	Solvent	Temp (°C)	Time (h)
1	Keratin	Wool keratin (batch 5)	15	200	PBS pH 7.4	38.5	27
	PEG-DA	575 Dalton	15				
2	Keratin	Wool keratin (batch 5)	7.5	400	DMSO	38.5	21
	SoyBean oil. E.A	Reagent grade	7.5				
3	Keratin	Wool keratin (batch 5)	7.5	400	PBS pH 7.4	38.5	29.5
	Ma. Alginate	Batch 1	7.5				

Notes 1. Conditions specifying chemicals (materials), type (detail), composition (%w/w), total volume of reaction solution (T.Vol), solvent system, temperature and reaction time.
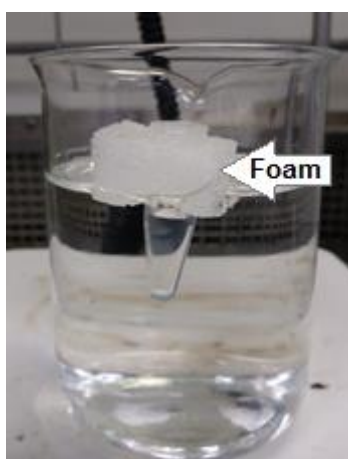
Figure 2.4. *Water bath used for Michael addition reaction where an eppendorf tube containing the reaction solution is kept floating in vertical position by using a poly urethane foam*

2.7. Photo crosslinking using methacrylated alginate and methacyralted chitosan

After successful methacrylation of Chitosan and sodium alginate, a UV-Vis-light curing system was developed and used for the crosslinking reactions of methacrylated alginate and methacyralted chitosan via free-radical reactions. The system configuration developed for the photo-crosslinking experiments (Figure 2.5), included a BlueWave® 200 version 3.0 light-curing Spot Lamp equipped with a rod lens mounted on a clamp stand and confined on a black-cardboard exposure box. The BlueWave® 200 version 3.0 light-curing Spot Lamp delivers a light beam with a range of wavelengths from 280-450 nm with a total intensity of 40 W/cm^2, capable of manual intensity adjustment from 1-100% output. The spot lamp can be operated by a manual, timer or PLC mode of which the former was the selected mode for these experiments, activating the shutter by a foot pedal and working at full intensity (100%) for all reactions. The general procedure for the photo-crosslinking reactions (Figure 2.6) involved mixing 250 µL of monomer solution with 15 µL of photo initiator inside a 5-mL plastic syringe, clamping the syringe at 4.5 cm of distance from the light source (rod lens). The clamp stand attaching the syringe and rod lens was then covered with the black-cardboard exposure box prior to irradiation, subsequently the foot pedal was stepped on opening the shutter and releasing the light beam inside the box, irradiating the sample for 6 minutes (shutter closes once the pedal is stepped off).

1. BlueWave 200 version 3.0 light-curing spot lamp. 2. Lightguide. 3. Black-cardboard exposure box. 4. Rod lens. 5. Clamp stand. 6. Sample container (plastic syringe). 7. Pedal.
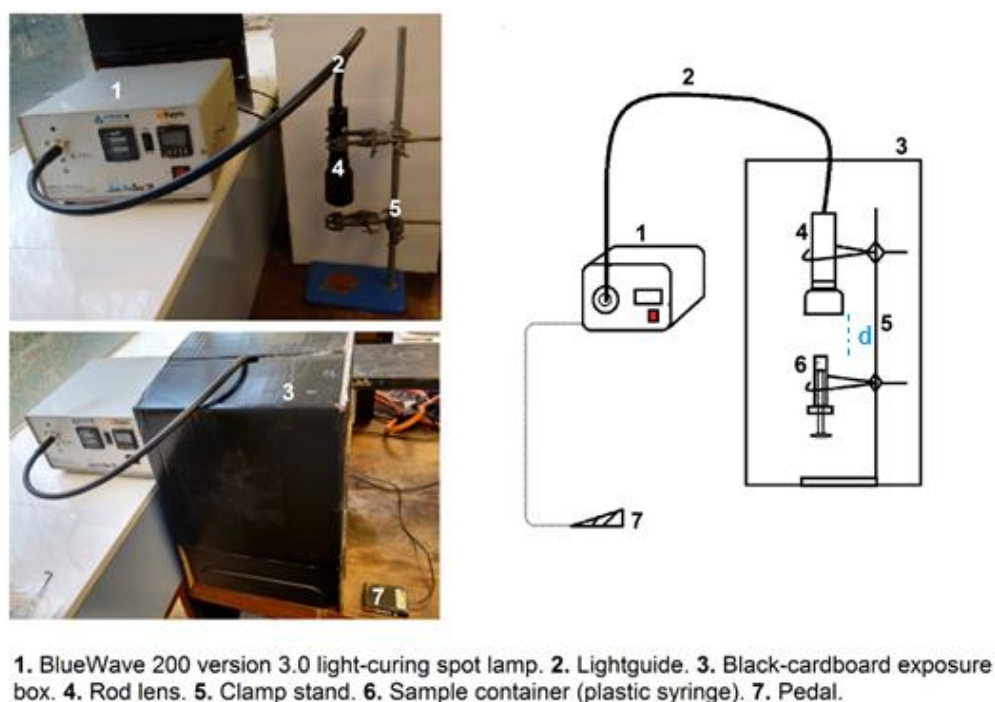
Figure 2.5. *Schematic representation of the Photo-crosslinking apparatus for photo-crosslinking experiments with methacrylated polysaccharides.*

Monomer samples consisted of methacrylated alginate and methacrylated chitosan alone and a mixture of both for some experiments. Every monomer solution was prepared by dissolving an amount of the monomer in in deionised water to reach a concentration of 5% w/v solution. The Photo initiator selected for all the photo crosslinking reactions was Irgacure D-2959 which was dissolved in a mixture of water-ethanol mixture (9:1) to reach a concentration of 1% w/v.
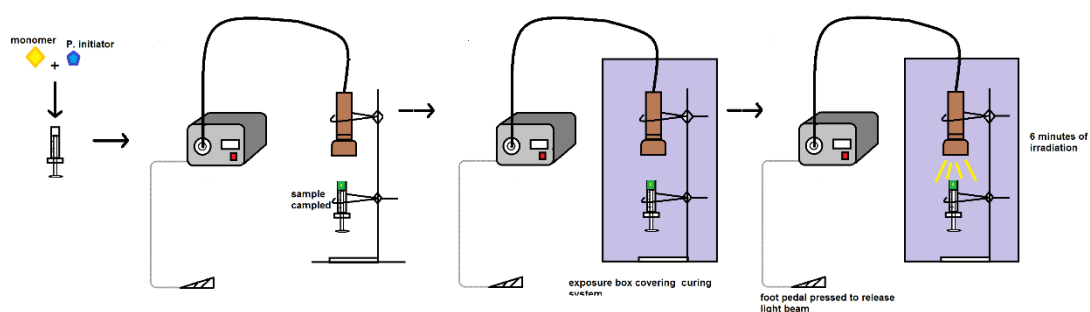
Figure 2.6. Representation step by step of the photo crosslinking procedure with methacrylated alginate and methacrylated chitosan

2.8. Two-step casting method

200 µL aqueous Methacrylated Alginate solution (5% w/v) and 50 µL Keratin aqueous solution (15% w/v) were mixed in an eppendorf tube. Initially, Michael addition reaction between thiol groups from keratin and double bonds from Methacrylated alginate was conducted under identical conditions described in section 2.5. (Incubation in water bath for 4 h at 38.5 °C). Once incubation time reached completion, the second step involved adding 15 µL irgacure (1% w/v) and curing for 6 minutes, using the UV-light curing system described in section 2.7.

2.9. 3D Printing experiments with sodium alginate

Sodium alginate was incorporated as the polymer system for the experiments and the design of a 3D for methacrylated polysaccharides was developed. The gel casting instrument (Figure 2.7) was constructed by assembling a Velleman K8200 3D printer kit, including a replacement to the original head extruder designed to operate with PLA or ABS filament for a K8205 Paste Extruder Modification Kit adapted to highly viscous liquid or soft solid raw materials that matches the consistency of Methacrylated alginate and unmodified sodium alginate aqueous solutions. Plastic and glass syringes containing Sodium alginate or Methacrylated alginate aqueous solutions were mounted on the K8205 Paste extruder accessory for the experiments, working without heating under the print bed. The printer was entirely operated and controlled from Repetier-Host V2.0.5 software installed on a portable computer connected to the printer via USB cable.
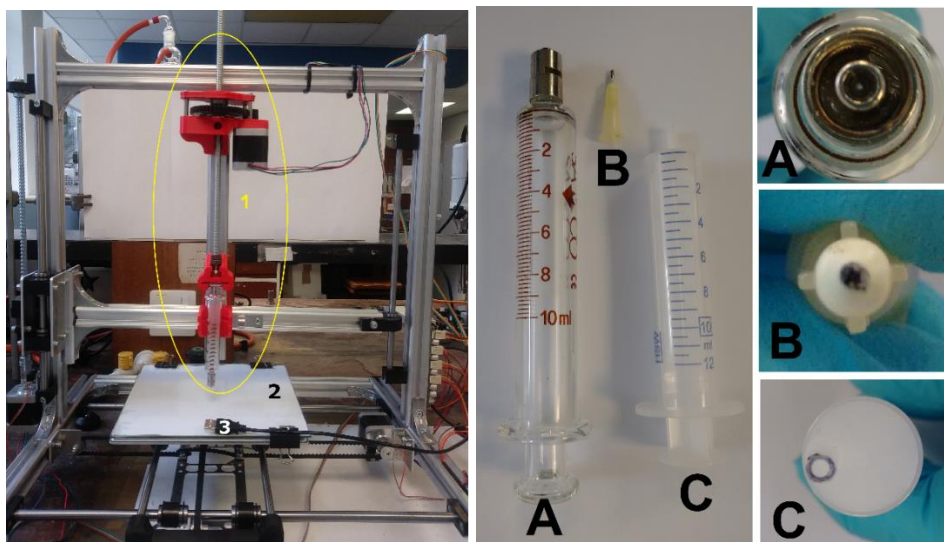
Figure 2.7. 3D Printing instrument: 1. K8205 paste extruder, 2. Print bed, 3. USB cable connection to pc. Syringes and nozzles used for printing experiments: A. 10-mL glass syringe and its original nozzle, B. 1 mm needle nozzle C. 12-mL Plastic syringe and its original nozzle.

2.10. Swelling studies on methacrylated alginate and methacrylated chitosan gels

Swelling studies were entirely performed in deionised water by triplicate using methacrylated alginate and chitosan gels identically shaped. Both Methacrylated alginate and Methacrylated chitosan gels were synthesised as described in section 2.7. (disc-shaped gels, 13 mm diameter and 4 mm height). Every swelling test was carried out by triplicate, starting by weighing out every gel prior to submersion in water in order to determine their dry masses. Once the dry mass was calculated by weighting directly on to the analytical balance, immersion in deionised water occurred, monitoring their wet weight every 5, 10, 15, 30, 60 and 120 minutes (Figure 2.8). Monitoring of the wet weight was carried out by using plastic tweezers to remove the gels from the media without damaging the integrity of the gel and keeping the overall swollen shape from first to last weight measurement.

Figure 2.8. *Swollen gels in deionised water*

3.0. Results and Discussion

3.1. Introduction

Results on isolation experiments using reduction methods named as Shindai and Na$_2$S are discussed (section 3.2.1), focusing on finding the optimum isolation conditions to obtain the better yields. Considering the results obtained from isolation and characterisations, Shidai method was choosen as the most appropriate extraction method for further studies in which successive keratin isolation batches were conducted using natural sources from different origin (section 3.2.2). Moreover, the results from using keratin obtained to prepare hydrogels are also discussed in detail (section 3.5) within this section.

3.2. Isolation methods for extraction of keratin from hair and wool samples

3.2.1. Introduction

Current research in the extraction process of keratin from natural sources often involves basic hydrolysis, enzymatic, oxidation and reduction reactions[26] to unfold keratin strands from their natural sources and release them in solution to facilitate the purification and isolation of the protein. The selection-making of the extraction method is a consensus among factors such as the type of raw material, yields and applications or purposes to which the keratin will be implemented in. Isolation of keratin can be carried out either oxidation or reducing methods (ref.) Reduction procedures are usually recommended when the protein is required to maintain free thiol groups and higher molecular weights leaving only traces of harmless chemicals in the final product. This type of applications could be biomedical interventions in

which keratin could provide a clean material for physiological environments and the reactivity of the free thiol groups in its structure allows it to participate in some biochemical reactions as well as being functionalised for targeted functions. Shindai and Na_2S are both reduction methods that satisfy the needs of many biological materials by supplying a protein almost at its whole dimension with traces of chemicals with low toxicity that would cause side effects on health. Shindai and Na_2S extractions were performed on hair samples to evaluate their influence in yields in the first place and further characterisation was conducted to compare their properties, as well.

3.2.2. Factors affecting yields and solubility of keratins extracted by reduction with Na_2S Method

The first batch of keratin extraction by reduction with Na_2S was conducted on human hair (female, Asian origin) following the protocol described in previous sections. The volume obtained after dialysis was split in three portions and freeze dried in identical conditions for 72 hours, obtaining three keratins with slight differences in physical appearance suggesting each sample has assembled differently leading to variations in their properties, therefore every sample was stored separately for further characterisation.

The three samples obtained after extraction for this first batch using Na_2S were named as H1, H2, H3. The first sample H1 displayed a significant difference in appearance from the other two, showing compact and shiny-dark flakes (Figure 3.1) plus a high solubility in Phosphate Buffer Solution pH 7.4 (Figure 3.2). In contrast, H2 and H3 solidified differently as a fluffy material with soft texture (Figure 3.1), slightly more pronounced on H3 than H2 which has some powder-like consistency. Solubility test in Phosphate Buffer Solution pH 7.4 for

these samples revealed a greater solubility in H2 than H3 where a great portion of the material remained insoluble (Figure 3.2). A second extraction reaction (2nd batch) was carried out using identical conditions and hair sample as in the first batch, however the final product was stored altogether without segregating partials portions as occurred during the first batch. The keratin obtained in this second batch named as H4 was similar in appearance to H2 and H3 with fluffy and soft texture. The solubility test of H4 in Phosphate Buffer Solution pH 7.4 resulted in a fairly visually-confirmed solubility at room temperature.
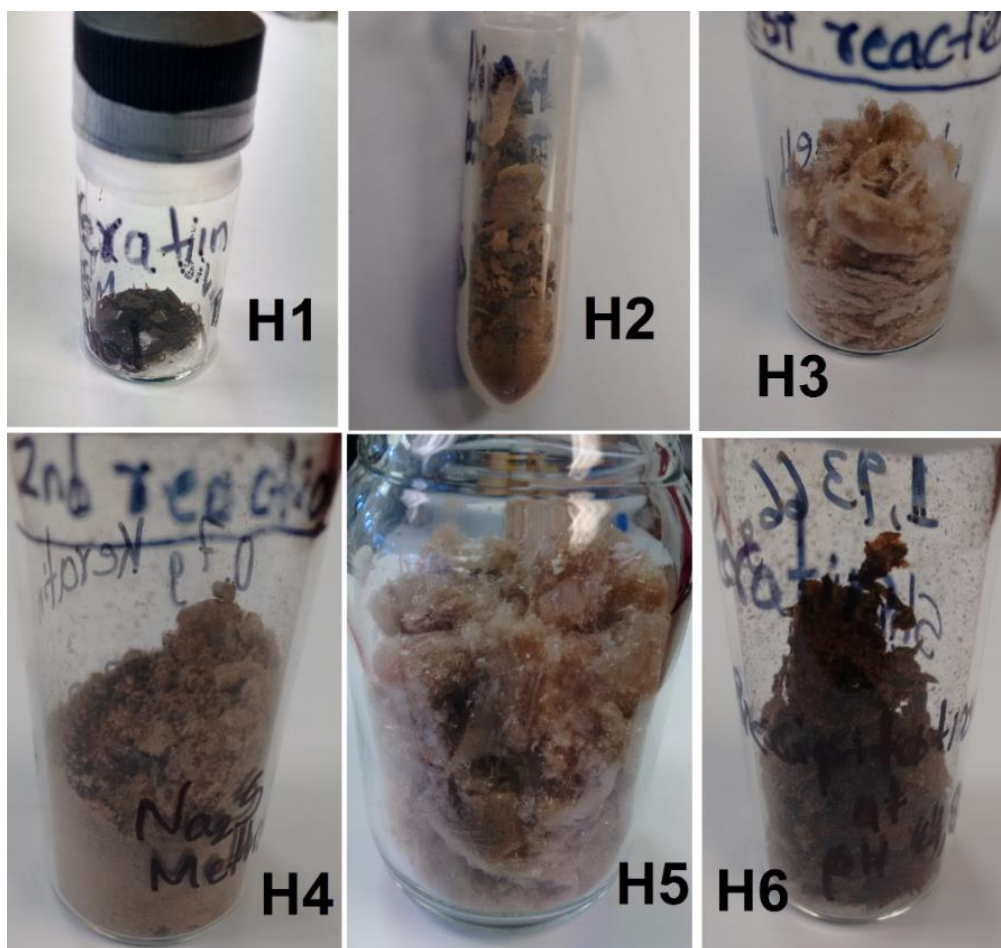
Figure 3.1. Hair keratins obtained from the same source by following Na_2S extraction (H1-H4) and Shindai extraction (H5 and H6).
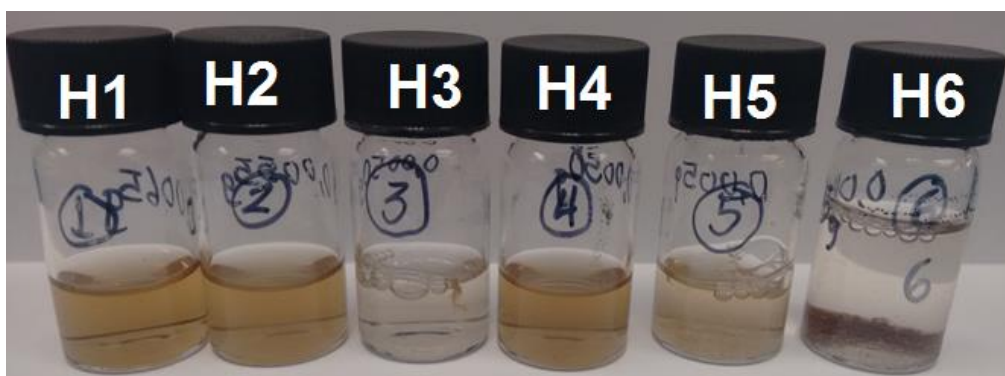
Figure 3.2. *Keratins in Phosphate Buffer Solution pH 7.4: H1 (3.2 mg/mL), H2 (2.7 mg/mL), H3 (2.5 mg/mL), H4 (2.5 mg/mL), H5 (3 mg/mL), H6 (2.5 mg/mL). Solubility test for all the samples was conducted at room temperature.*

The isolation of keratin by reduction with Na_2S conducted over two batches demonstrated yields ranging from 10% (1st batch) to 14% (2nd batch) producing soft-fluffy keratins with solubility in Phosphate Buffer Solution pH 7.4 ranging from 2.5 to 3.2 mg/mL. These results are a first approach to a qualitative characterisation of these keratins extracted using Na_2S the strongest reducing agent among the chemicals used for the extraction procedures implemented in this work and none of these preliminary results are conclusive with regards of the quality of the keratin resulting from this procedure. However, only two batches were performed in total by following this method due to the high risk of protein damage that can result from using a strong reducing agent like Na_2S which also releases NaOH in aqueous solution. Further characterisation was carried out on these keratin samples and the results are be presented in subsequent sections.

3.2.3. Factors affecting yields and solubility of keratins extracted by Shindai Method

This is an extraction method originally proposed by Nakamura ET Al [122]aiming to extract keratin from natural sources in mild conditions, without compromising efficiency. The method combines the action of 2-mercaptoethanol as reducing agent with denaturing agents such as Urea and Thiourea. These denaturing agents make sure the keratin is accessible to the reducing agent by unfolding and releasing the protein from its highly packed natural, usually protein's tertiary structure. The assistance of the denaturing agents improves the efficiency of the reducing extraction; however, it requires longer exposure due to 2-mercaptoethanol which is a mild reducing agent.

Two batches were carried out following this method both extracting the keratin from the same raw material (No. 1). These two batches produced two keratins named as H5 (3rd isolation batch) and H6 (4th isolation batch) and each one was stored without partial-fraction segregation. Samples H5 and H6 (Figure 3.1) differed in physical appearance, being the former a fluffy material similar to the keratins obtained in Na_2S extraction and the latter a highly-dense flaky material which possibly has self-assembled different due to the purification process that underwent. Unlike samples H1-H5 that were purified in identical conditions under freeze-drying conditions, H6 was purified differently by pH precipitation and dried under vacuum on Buchner funnel, instead of freeze-drying. In this approach the pH in the dialysed solution was lowered until observing precipitation. The pH in the original dialysed solution was taken from 6.56 to 4.8 by adding HCl 10% (v/v). Keratin seems to be pH sensitive due the acidic properties in thiol groups from cysteine residues in keratin. Thiols groups in general have acidic properties that allows them to release a proton in solution and the pH value at which this phenomenon occurs is known

as pKa which represents the threshold value of the molecule to be protonated[130].

Keratin like most proteins shows low or no solubility in many organic or inorganic solvents and even low solubility in water, due to the fact that keratin is a structural protein that acts as a protective hard tissue that is exposed to environmental conditions, making of keratin a slightly soluble protein in water. However, the presence of cysteine residues (7-20%)[27] in keratincontributes the reactivity of the molecule, making it susceptible to pH variations as part of the chemistry behind thiol groups, suggesting that the solubility of Keratin could be attributed to the relatively high abundance of thiol groups in its structure. For this particular example, the original solution obtained after dialysis had a slightly basic value of 6.56 at which the keratin was still soluble presumably due to the thiol groups being deprotonated (-S$^-$), meaning that keratin is negatively charged as an anionic macromolecule (Scheme 3.1). Upon addition of HCl 10% the pH decreases by neutralising free hydroxyl anions (OH$^-$) until reaching protonation of thiol groups (-SH) in keratin, causing loss in solubility allowing precipitation to take place (Scheme 3.1). Precipitation was reached at pH 4.8 suggesting this could be a threshold value that can be related to the pKa value of the thiol groups in hair keratins, however further characterisation should be conducted in order to prove this result right, since keratin is a protein that has many amino acids in its structure and they all contribute to isoelectric point, which is another important physical constant in proteins that also accounts for their solubility in a solvent[131].

It was observed a significant solubility of H5 in Phosphate Buffer Solution pH 7.4 as similar as observed in the previous freeze-dried hair keratins (H1-H5). Sample H6 on the other hand displayed very low solubility in Phosphate Buffer Solution pH 7.4, possibly attributed to a denser degree of aggregation caused by precipitation. Further

characterisation will be necessary to prove this assumption to be accurate. Yields for first and second batch of Shindai isolation method produced 16% (H5) and 39% (H6) respectively (Table 3.1).

Table 3.1. Yields for very batch of isolation of keratin from hair by Na_2S and Shindai Method. All these keratins were obtained from raw material No. 1.

Sample	Batch	Isol. Method	purification	Yield (%)
H1	1	Na_2S	Dialysis+freeze-drying	
H2	1	Na_2S	Dialysis+freeze-drying	10
H3	1	Na_2S	Dialysis+freeze-drying	
H4	2	Na_2S	Dialysis+freeze-drying	14
H5	3	Shindai	Dialysis+freeze-drying	16
H6	4	Shindai	pH precipitation	39

Samples H5 and H6 along with samples H1-H4 conformed the first six samples of keratins obtained from the same natural source used during the first stage of this work that aimed to compare the properties of keratins of identical origin extracted in two different conditions. Yields reported in this section along with results obtained after characterisation of the first six keratins were conclusive in the decision-making process which led to choose Shindai conditions as the exclusive isolation method of keratin for the subsequent natural sources used. Wool fibres as well as hair from different origin (ethnic group) were used as keratin sources in successive extraction batches.

Reaction of thiols with NaOH

pH 6.56

HCl 10%

precipitation

pH 4.8
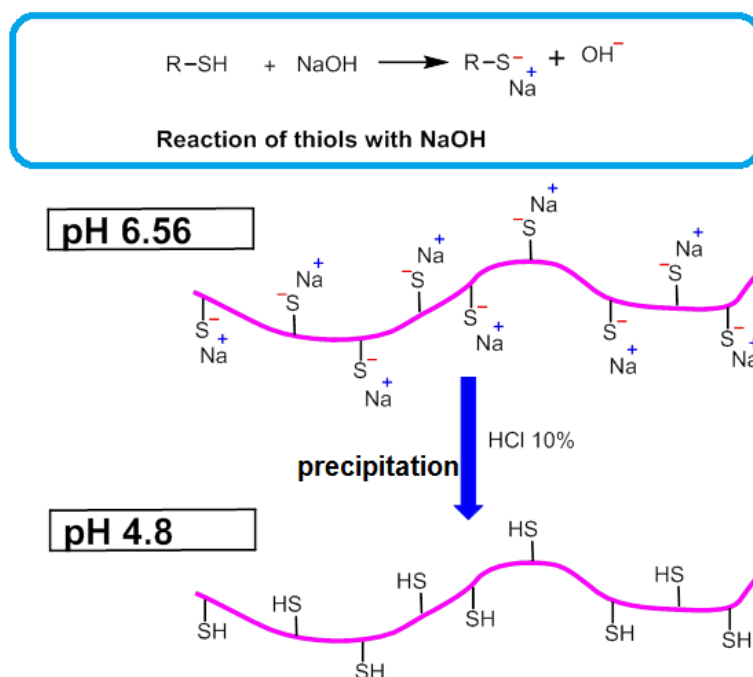
Scheme 3.1. *pH precipitation of keratin and chemistry of thiol groups in basic media (blue-rounded rectangle).*

Wool Keratin was extracted from wool fibres (Raw material 4) obtained from Welsh sheep (*Badger Face Welsh Mountain sheep*) at a local farm (North Wales, United Kingdom). The fifth isolation batch using wool fibres was carried out under Shindai method conditions with no variations to the original method reported in section 2.3.3. Another isolation batch was carried out (6th batch) on the same raw material splitting the dialysed solution in two identical portions in order to perform freeze drying on one of them and replacing freeze drying for precipitation in cold acetone on the other half. The precipitation in cold acetone has proven to be successful in separating keratin in solution by precipitation in a cold organic solvent like acetone, as it happens for this case making the drying and separation process quicker in comparison to freeze-drying[132]. Precipitated wool keratin was dried under vacuum in Buchner funnel initially and finally freeze-dried analogically as the rest of the keratin samples.

Wool keratin unlike hair keratin was pale in colour and similar to non-tinted wool textiles in colour. Physical aspects observed in wool keratin in terms of texture and consistency, resembles the fluffy and soft texture already seen in hair keratin. The observations mentioned above are applicable to the wool keratin obtained from the first batch as well as the portion freeze dried from the second batch named as W1 and W2 respectively (Figure 3.3).

Wool keratin obtained by precipitation in cold acetone (6th batch) named as W2-pp (Figure 3.3) displayed the compact consistency and flaky appearance already observed in H6 (hair keratin obtained by pH precipitation). On the other hand, keratin sample W2-pp was finer than H6, exhibiting thinner flakes which is presumably due to the freeze-drying step which was absent in H6. Two important factors beyond the nature of the starting material made a big difference between the keratins obtained by precipitation and they include the media used and the additional step conducted on one that was absent on the other. Keratin sample H6 was precipitated in aqueous media without freeze-drying, producing a robust material which on account of the low volatility of the solvent might suggest some water molecules were entrapped into the keratin aggregates as keratin solidified and sank at the bottom of the beaker. Moreover, the vacuum conditions on a Buchner funnel might not be enough to remove the water content entrapped in keratin particles and possibly it only removed external water closer to the particle surface, making the final product looked dried on the surface but also heavy due to remnant water inside.

Keratin sample W2-pp on the other hand, was precipitated in cold acetone, dried initially on Buchner funnel but also subsequently freeze-dried. Keratin like most proteins in general has poor solubility in organic solvents and their solubility in water is still limited depending on the type on tertiary structure they are arrange in. For globular proteins solubility in water is fairly good while for fibrous proteins like

Keratin their solubility is quite low and this is often related to the structural function those proteins perform in the body in which the integrity of the macromolecule must be preserved[133]. Keratin sample W2-pp was successfully purified in cold acetone thanks to the inherent low solubility of the protein, increased by the fact that keratin is a fibrous protein and the low temperature in which the precipitation was conducted, taking into account that the cold acetone used for this purification was kept in the fridge overnight, suggesting that the precipitation took place at temperature range of 5-10° C. The aprotic nature of acetone as a solvent, results in poor interactions with keratin in which the amino acids residues are mainly pH responsive. As a result of dropwise addition of dialysed keratin solution in cold acetone, auto entanglement of keratin chains occurred causing instantaneous precipitation proving the solute-solvent low interactions previously described for this system (Scheme 3.2).
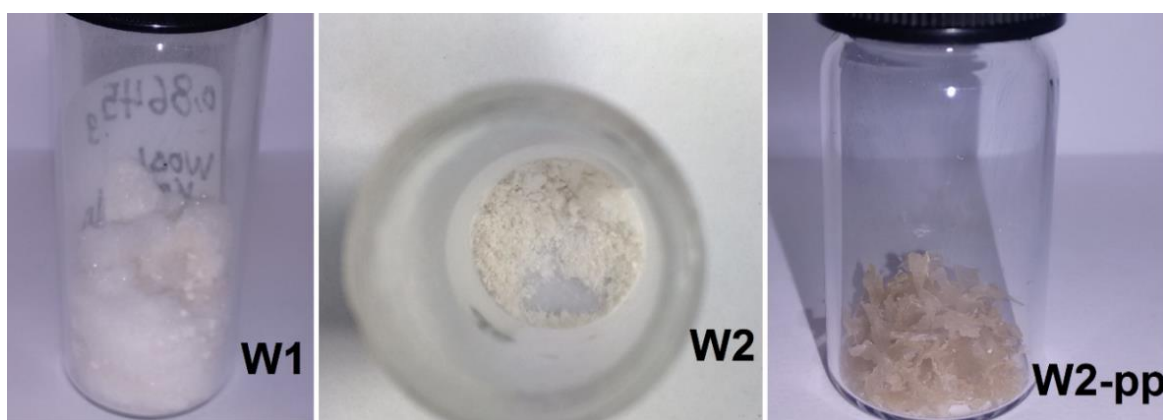
Figure 3.3. *Wool keratins: W1 (1st batch), W2 (2nd batch with no variations to the method) and W2-pp (2nd batch obtained by precipitation in cold acetone).*
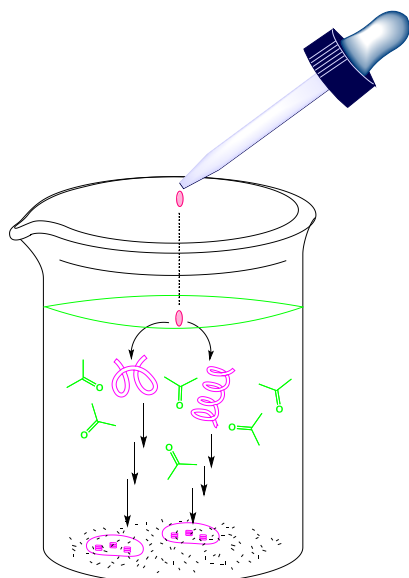
Scheme 3.2. *Schematic representation of precipitation of wool keratin (W2-pp) in cold acetone. Keratin coils (pink) and self-assembles into micro particles (pink granules at the bottom) due to their low interactions with cold acetone (green), causing precipitation by gravity.*

Wool keratins extractions produced 28% and 21.8% yields for the first and second batch, respectively (table 3.2). Partial yields were also obtained for the second batch with respect to each sample included within (W2 & W2-pp. Table 3.2). The selection of the purification procedure for Shindai Method of successive batches was made on the basis of yields obtained and the solubility of the keratins from the second batch in which the purification comparison provided evidence of a greater yield value of 23.1% and solubility of 4.1 mg/mL in Phosphate Buffer Solution pH 7.4 for the unaltered purification method (sample W2) against a lower yield of 21.8% and solubility in Phosphate Buffer Solution pH 7.4 of 4.0 mg/mL for the purification by precipitation in cold acetone (sample W2-pp). In addition, the characterisation data supports the decision made on the purification method chosen because of the milder conditions Shindai offer along with significant yields.

Table 3.2. *Yields obtained from wool keratin isolation following Shindai method under pre-set conditions and modificated purification process.*

Batch	Sample	Purification	Partial yield (%)	Total yield (%)
5	W1	Dialysis+ freeze drying	N/A	28
6	W2	Dialysis+ freeze drying	23.1	21.8
	W2-pp	Dialysis+ precipitation+ freeze drying	20.4	
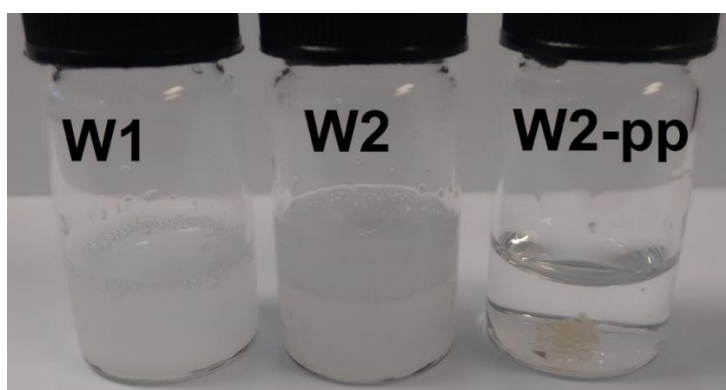
Figure 3.4. *Wool Keratins in Phosphate Buffer Solution pH 7.4: W1 (4.0 mg/mL), W2 (4.1 mg/mL), W2-pp (4.0 mg/mL). Solubility test for all the samples was conducted at room temperature.*

Further isolation of keratin was extracted from hair using two new hair samples of different ethnical origin. Black hair of South American origin and light-brown hair of British origin, both male hair samples. Shindai method under standard conditions previously reported (original reaction followed by dialysis and freeze-drying) was carried out on both samples obtaining keratins named as HK-2 (South American origin) and HK-3 (British origin). Samples HK-2 and HK-3 displayed the same physical appearance already observed in previous keratins with fluffy texture, however different colour. HK-2 likewise H1-H6 keratins were obtained from dark hair samples, producing a brown final product (Figure 3.5) as a consequence of residual melanin (eumelanin) still present in the sample after dialysis. HK-3 on the other hand, was pale in colour (Figure 3.5) as expected for a light-brown hair in which the dark pigment eumelanin content is not significant[134]. Solubility test in

phosphate buffer solution of samples HK-2 and HK-3 revealed partial solubility for both samples, displaying particles in suspension with a subtle brown colour in solution for HK-2 (4.1 mg/mL) and swollen fibres of low density in a perfectly clear solution (4.0 mg/mL) for HK-3 (Figure 3.6). Isolation percentage yields for hair keratins HK-2 and HK-were obtained in 37.8% and 41.7% respectively.
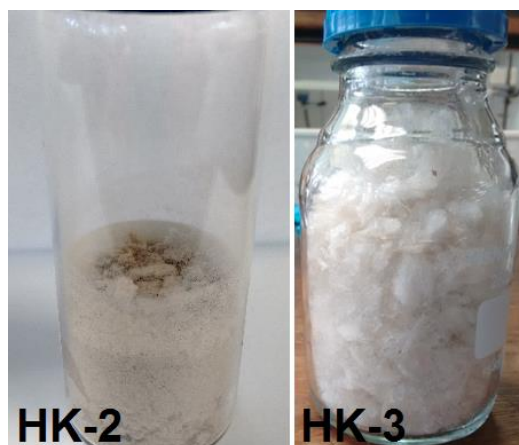
Figure 3.5. *Freeze dried samples (both) hair keratins HK-2 and HK-3.*
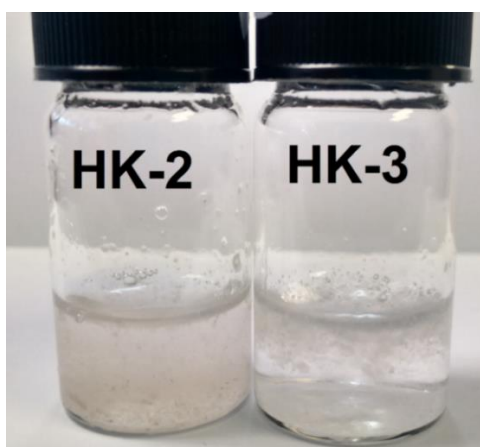
Figure 3.6. *Wool Keratins in Phosphate Buffer Solution pH 7.4: HK-2 (4.1 mg/mL), HK-3 (4.0 mg/mL). Solubility test for all the samples was carried out at room temperature.*

Throughout previous sections keratins H1-H6, W1, W2, W2-pp, HK-2, HK-3 were described from a qualitative point of view contrasting and linking the observations with the methods of obtention, given the variations to which some of the methods were subjected. Partial conclusions were withdrawn but no conclusive information was taken from this section regarding the properties of the keratins obtained. The

following section will deal with the characterisation performed on the keratin samples obtained and the relationship with the respective isolation method.

3.3. Spectroscopic characterisation of keratins

3.3.1. Intro

Moving from qualitative observations of the isolation process gathered in previous sections to more advance analysis, in this section the observations suggesting potential properties in the extracted keratins will be now assessed by spectroscopic methods in order to confirm these properties. Qualitative and quantitative spectroscopic characterisation techniques for identification and quantification of functional groups such as Fourier-Transform Infrared (FTIR), UV-vis spectroscopy and Proton Nuclear Magnetic Resonance ^{1}H-NMR were selected for this purpose. Relevant information regarding the structural composition of the extracted keratins was initially obtained by the spectra, suggesting the prevalence and domain of some functional groups which was eventually quantified by UV-vis light by performing Ellman's assay. Furthermore, the evidence collectively collected from these spectroscopic techniques served as solid basis to explain the observations made on the solubility of the keratins in previous sections.

3.3.2. FTIR, UV-vis and ^{1}H-NMR Spectra of keratins

Fourier-Transform Infrared instrument featuring ATR accessory allowed the obtention of spectra from the keratin samples in solid state without pre-manipulation or pre-treatment of the samples, reducing

potential damage to the sample or background signal coming from solvents or solid chemicals used in conjunction with other techniques. The FTIR spectra of hair and wool keratins are presented in Figure 3.7 and 3.8 revealing the typical bands of the peptide linkage reported for each keratin in table 3.3. The absorption band Amide A represents the NH stretching that is observed in the keratins in the range of 32570-3280 cm^{-1}. The second absortion band observed is the Amide I, which is mainly attributed to C=O stretching (80%) plus a minor contribution of NH bending (20%) observed in the range of 1625-1649 cm^{-1}. Similarly, Absorption band Amide II is the result of two vibrations occurring approximately at the same ratio, displaying CN stretching and NH bending in the range of 1511-1536 cm^{-1}.

 Additonally, absorption band Amide III is also represented by the same vibrations in Amide II, however they have exhibit lower wavenumbers in Amide III ranging from 1224 to 1294 cm^{-1}. Concluding with the Amide family, absorptions bands Amide IV (625-767 cm^{-1}), Amide V (640-800 cm^{-1}) and Amide VI (537-606 cm^{-1}) are expected to be present at wavenumbers below 1000 cm-1, where every band is overlapping and bordering on each other making difficult differenciation in the spectra. It is only possible to assign these vibrations to OCN bending in Amide IV, Out-of-plane NH bending in Amide V and Out-of-plane C=O bending in Amide VI[135,136].

Amide I is a segment in the spectral region that is especially sensitive to fluctuations found between 1600-1700 cm-1, these vibrations are mainly due to the C=O and the changes in the vibrations of this band can tell some information about the secondary structure of the protein. It is observed that the data in Table 3.3 for this band is found within the expected fluctuations (1625-1649 cm^{-1}), however further characterisation should be conducted in order to assumed specific conformations in the keratin, since FTIR because the individual components of absorption bands attributed to certain conformational

substructures, such as α-helix and β-sheet, cannot be satisfactorily resolved by this technique [135,136].

In addition to the Amide family absorptions, some other functional groups such methyl ν(CH$_3$) asymmetric and symmetric modes are observed at 2941 cm^{-1} and 2922 cm^{-1}, respectively. Methylene ν(CH$_2$) asymmetric and symmetric modes are observed at 2856 cm^{-1} and 2834 cm^{-1}, respectively and carbon-sulphur C-S stretching modes bonds are recognised as alkyl thiols in the range 872–546 cm^{-1}. The spectra on the other hand shows no peaks related to the cysteine ν(S-H) in the region 2550-2600 cm^{-1}, suggesting thiol groups could have been oxidised due to the dialysis process or environmental conditions. This doesn not suggest thiols are absolutely absent in these keratins but this technique does not suffice to clarify the presence of these groups and successive sections will address this question by using a more selective approach.
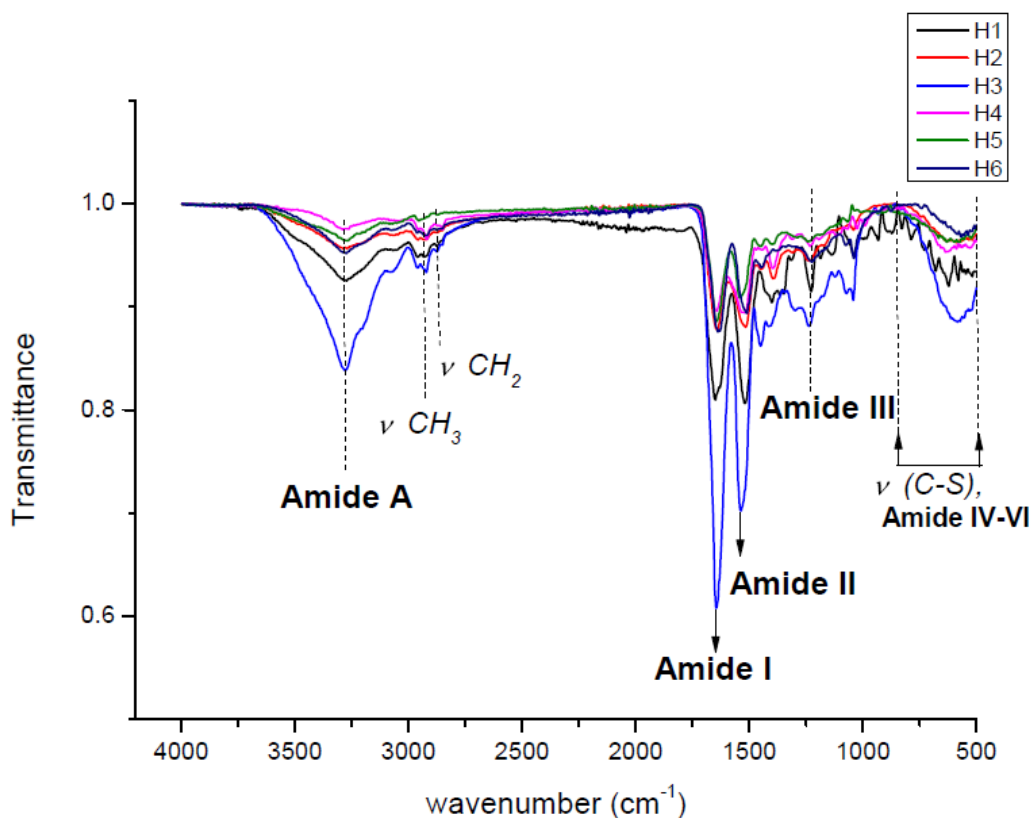
Figure 3.7. *FTIR Spectra of hair keratins H1-H6.*
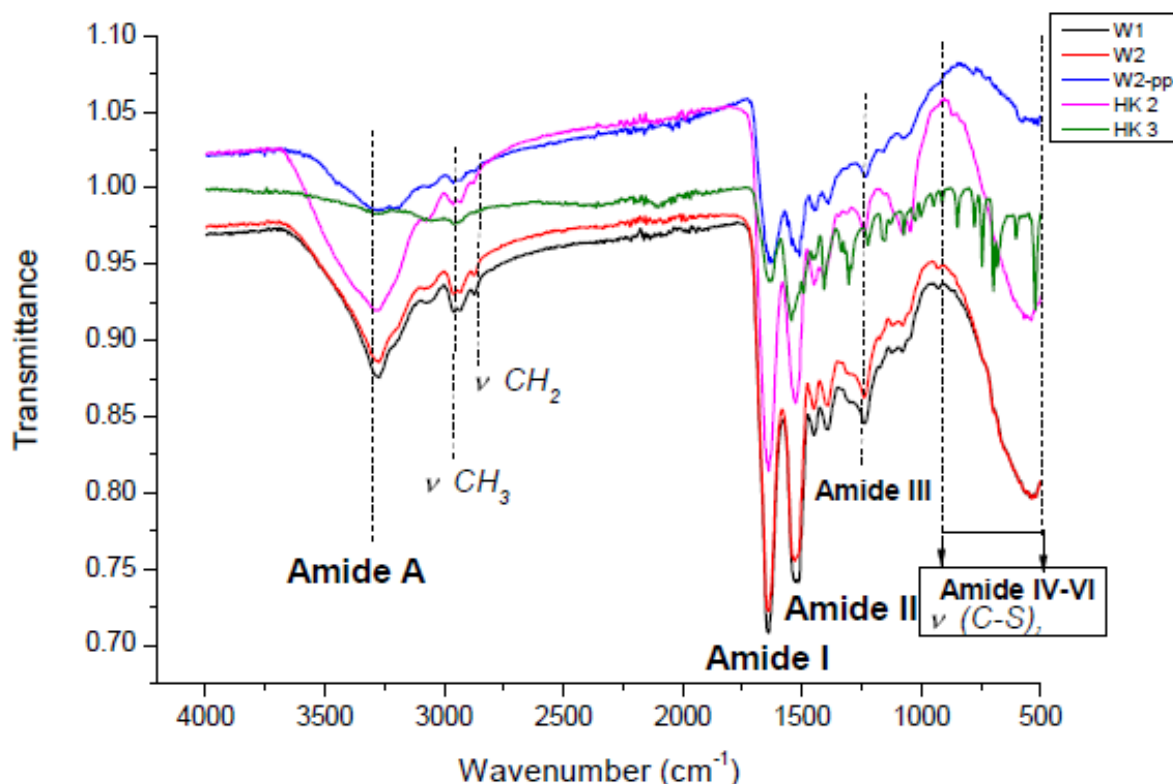
Figure 3.8. FTIR Spectra of hair keratins HK-2,HK-3 and wool keratins W1, W2 and W2-pp.

Table 3.3. Characteristic FTIR absortions of the peptide linkage in hair and wool keratins.

Sample	FTIR Bands (cm⁻¹)			
	Amide A	Amide I	Amide II	Amide III
H1	3272	1645	1521	1224
H2	3278	1641	1518	1234
H3	3280	1645	1532	1238
H4	3281	1645	1521	1233
H5	3270	1649	1536	1238
H6	3270	1639	1515	1227
W1	3280	1639	1515	1238
W2	3276	1645	1532	1234
W2-PP	3270	1625	1511	1233
HK-2	3280	1639	1525	1242
HK-3	3274	1632	1540	1293

In the same way, ^{1}H-NMR spectra for hair keratin (Figure 3.9) and wool keratin (Figure 3.10) exhibit remarkable signals from the amino acids conforming the protein backbone such ash at the-CH_3 methyl protons at 0.84 ppm (Isoleucine, leucine, valine), –CH_2 methylene protons at 1.12 and 1.30 ppm for hair keratin and 1.14 and 1.33 ppm for wool keratin acknowledging this signals to the presence of this amino acids: Isoleucine, leucine, phenylalanine, tyrosine, lysine,

arginine, ornithine, hisitidine, citruline, aspartic acid, glutamic acid, serine, cysteine, cysteic acid, tryptophan. Signals of -CH proton at 1.55 ppm, 1.98 ppm are observe for hair keratin and 1.54 and 1.92 ppm for wool keratin presumably resulting from amino acids: Alanine, valine, Isoleucine, leucine, phenylalanine, tyrosine, lysine, arginine, ornithine, hisitidine, citruline, aspartic acid, glutamic acid, threonine, serine, cysteine, cysteic acid, tryptophan) and some aromatic protons at 6.72-7.22 ppm for hair keratin and 6.71-7.25 ppm for wool keratin presumably due to tyrosine residues[137].

Given the substantial sulphur content in keratin due to Cysteine residues, it seems plausible to acknowledge the presence of the thiol proton –SH by the signals 2.21 ppm and 4.24 ppm (however, this statement must be confirmed by other methods). The first signal at 2.21 indicates the usual chemical shift observed on alkane thiols assuming the thiol group in the cysteine to behave as such, to a certain level. On the other hand the signal at 4.24 ppm shows a different aspect also associate with thiols that accounts for the relative acidic nature of this group, allowing proton interchange with the deuterated solvent D_2O which can be also helped by facilitated by the basic media (buffer solution: PBS pH 7.4 prepared in D_2O) which enhances the anionic structure of the thiol groups making proton interchange between solvent and the substrate more effective. As a result of this interchange, the mono deuterated species "HOD" is formed and it has been often identified in the literature around 4.80 ppm chemical shift for thiolated molecules [137], however the chemical shift associated to this species for the spectra in figure 9 seems to be located between 4.18 and 4.24 ppm. Given the presence of phosphates anions in solution acting as a basic species, proton withdrawal can occur leading to the anionic structure –SH^- that interacts with D_2O as shown in the dash box in Scheme 3.3. In absence of external basic species the equilibrium between thiols and D_2O normally happens as displayed in

the solid box at the bottom of Scheme 3.3, in which the undetectable, deuterated thiol species –S-D appears. However, the existence of an equilibrium for this process suggest some thiols -SH remain unaltered and therefore their signals can be observed as an alkane thiol at 2.21 ppm.
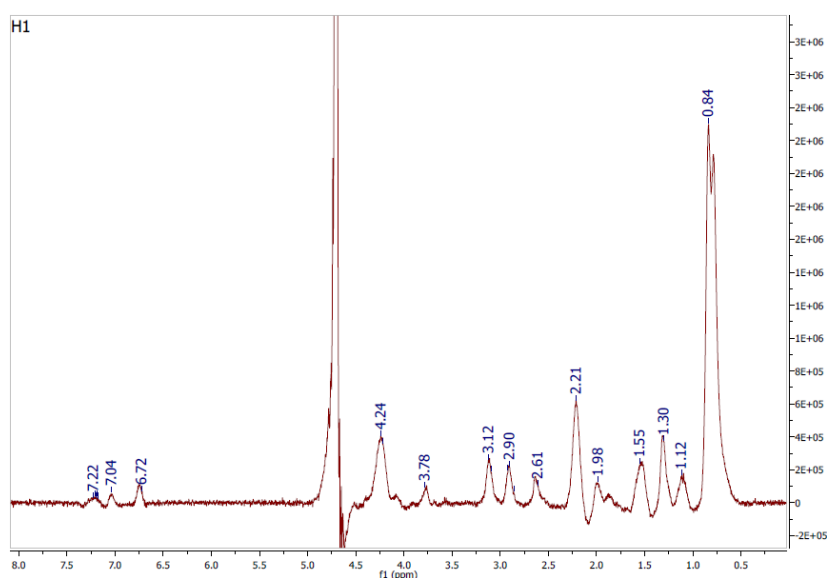
Figure 3.9. *H-NMR Spectrum of representative Hair keratin in solution of D_2O with Phosphate buffer (sample H1)*
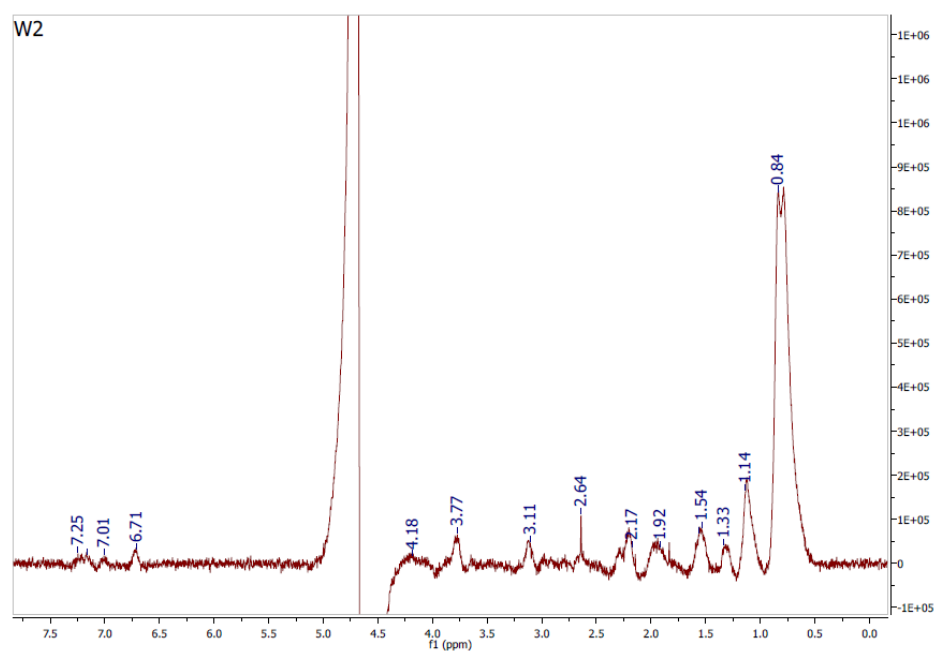
Figure 3.10. *H-NMR Spectrum of representative Wool keratin in solution of D_2O with Phosphate buffer (sample W2)*

62
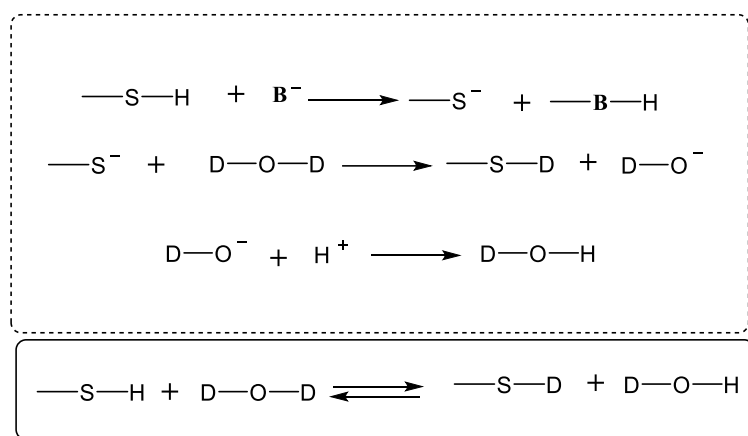
Scheme 3.3. *Thiol Proton interchange process, where base B represents the phosphates in solution used to dissolved the NMR samples that could possibly deprotonate thiols leading to more interchanges as it is shown in the dashed box. The solid lined box at the bottom illustrates the equilibrium between thiols and D2O in absence of external basic species.*

UV-VIS spectra on the other hand, confirms the presence of Chromophores in amino acids residues such as tyrosine displaying the absorbance of the aromatic ring that is reported in literature around 276 nm, however observed at 268 nm in the spectra in Figure 3.11 . Tyrosine is one of the few amino acids present in keratin that is UV active and despite of its moderate abundance in the amino acid sequence, it is possible to observe the absorption band significantly above the almost flat base line for larger wavelengths [138].
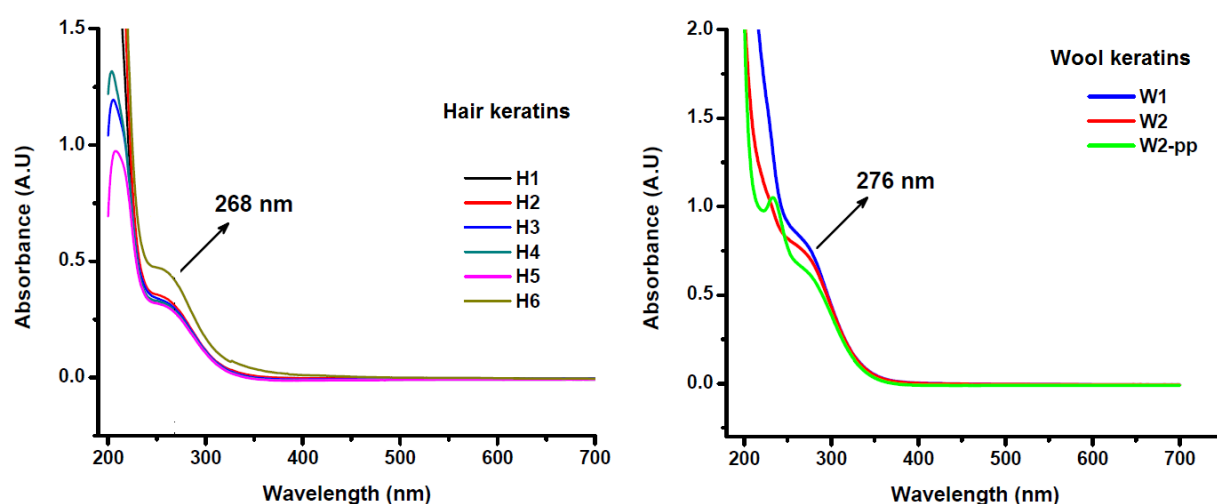
Figure 3.11. *UV-vis spectra of hair and wool keratins*

3.3.3. Thiol content quantification by Ellman's assay

Keratin's UV-vis spectra proved the presence of functional groups active in the UV region as observed in the absorptions at 268 nm from the aromatic ring in tyrosine residues. These residues are fairly abundant as to be seen in the spectrum as a qualitative characterisation, however the quantification of these groups should result somewhat complicated and not fully accurate as these signals can be also attributed to the tryptophan residues. Thiols groups on the other hand, in spite of being unresponsive to UV light, can be accurately quantified by this spectroscopic technique by means of a disulphide interchange reaction that produces a UV active by-product. Ellman developed such reaction in which reagent DTNB also known as Ellman's reagent symmetrically splits at its disulphide bond generating two identical anions one of remains as anion TNB^{2-} and the other half reacts instantaneously with a surrounding sulfhydryl molecule forming a new disulphide bond with this (Scheme 1.2). As a result of the disulphide interchange reaction and its simple stoichiometry, it is possible to quantify the free thiol groups in solution on account of the TNB^{2-} anions produced that can be easily identified at 412 nm. This methodology was proposed by Ellman and has been widely used since with a certain degree of confidence. Given the reliability and selectiveness towards identification of thiol groups only, Ellman's assay has been selected as the quantification method to determine the thiol content of the keratins extracted in this work.

Thiol content reported as the density of thiols per mass unit of keratin in µmol/g are listed in table 3.4. The table also provides information about every batch indicating, the raw material used, the extraction method, post reaction treatment and batch number in the general ranking. As a general observation, Shindai and reduction with Na_2S

methods have both reached the highest thiol content in the table (180 µmole thiol/ g keratin), the former obtained from a wool keratin and the latter from a hair keratin.

Table 3.4. *Thiol content determined by Ellman's assay detailing the sample name,batch number, Raw material (R.M) number and the post-reaction treatment for every keratin extracted. Entries displaying D+F-d in the post-reaction treatment refer to diialysis followed by Freeze-drying is displayed as, whereas the precipitation methods only included dialysis for the entry referred as D+pp+F-d (dialysis followed by precipitation in cold acetone and finally freeze-drying).*

Sample	Batch	R.M	Method	Post-reaction	µmole thiol per g keratin
H1	1	1	Na_2S	D+ F-d	137
H2	1	1	Na_2S	D+ F-d	180
H3	1	1	Na_2S	D+ F-d	170
H4	2	1	Na_2S	D+ F-d	140
H5	3	1	Shindai	D+ F-d	110
H6	4	1	Shindai	pH precipitation	85.4
W1	5	4	Shindai	D+ F-d	138
W2	6	4	Shindai	D+ F-d	180
W2pp	6	4	Shindai	D+pp in acetone+Fd	114
HK-2	7	2	Shindai	D+ F-d	0.4
HK-3	8	3	Shindai	D+ F-d	1.39

The results in the table beyond making a comparison of the effectiveness in obtaining free thiol groups between the methods seems also to converge into the fact that the value obtained for the wool keratin reflects the usage of 2-mercaptoethanol a mild reducing agent over a slightly richer source of thiol groups as wool is. On the other hand, the thiol value for the hair keratin seems to be the outcome obtained from using a strong reducing agent over a slightly poorer source of thiols groups as hair is. Therefore, the facts exposed from each side of the extraction methods seems to equilibrate themselves

resulting in exact same values observed in this work for samples H2 and W2. Following a more comparative analysis of thiol results based on identical raw material used in both methods, raw material 1 is the only raw material that has undergone both extractions methods that has produced samples H1-H6 which thiol values can be compared with each other. However sample H6 could be excluded from the comparison list due to have undergone a different post-reaction treatment from the other fellow hair keratins. Reduction with Na_2S has identically obtained samples H1, H2, H3 and H4 displaying thiols contents 137, 180, 170, 140 µmol thiol/g keratin respectively. Shindai method has only obtained sample H5 under identical conditions as the counterpart method with a thiol content of 110 µmol thiol/g keratin, which clearly reveals a significantly lower thiol content even below the lowest value in Na_2S method observed in H1(137 µmol thiol/g keratin). The difference in thiol content between these samples can be now be explained by the effectiveness of the extraction method and the reducing agents used confirming that 2-mercaptoethanol is a milder reducing agent that produced the lowest value (110 µmol thiol/g keratin) than Na_2S that generated a wider and superior range of thiol content values of 137-180 µmol thiol/g keratin.

Keratin sample H6 in contrast to the series H1-H5 has reported the lowest thiol content in the series fully obtained from raw material 1. This seems to have relation with the post-reaction treatment which was totally different from the rest of the keratins in the same series. Precipitation by pH adjustment have brought the keratin H6 to a higher level of oxidation possibly due to the acidic media, hence altering the thiol content that could have possibly be achieved straight after Shindai reaction and this prospective value could be not so different from that of H5 taking into account both keratins were initially extracted under identical conditions.

The thiol content of wool keratins was found between 114-180 µmol thiol/g keratin corresponding to a relevant value that matches the solubility in PBS observed in samples W1 and W2 which were almost entirely soluble in this solvent system, proving the connection between the thiol content and the solubility in PBS of this samples. Wool keratin samples W2pp was rather insoluble in the solvent system despite of having a thiol within the range of the fairly soluble keratins H1-H5. This can be easily noticed by recalling the observations made on Keratin sample H6 and its low thiol content in comparison to their fellow hair keratins H1-H5 which also pointed out this value (85.4 µmol thiol/g keratin) as a prospective threshold thiol content value for judging the solubility and by following this principle, the thiol content and the solubility found in keratin sample H6 stands up as a counter example that provides the evidence that suggest that solubility of keratins in PBS or any aqueous systems might not depend exclusively on the thiol content, taking into account that if it does then the keratin sample H6 should be at least partially soluble in PBS but the observations proved it otherwise.

Precipitation processes seems to bring molecules together into a denser arrangement with respect to the state of aggregation than those other processes not involving precipitation such as freeze-drying. This densely packed arrangement might have some implications on the solubility of the compound in solid state obtained by precipitation as it is observed in the keratins H6 and W2pp which showed almost no solubility in PBS. Some other freeze-dried keratins like H5 have partial solubility in PBS in spite of having a lower thiol content than precipitated keratin W2pp which shows poor solubility. This seems to be ought to the densely-packed solid formed during precipitation that makes the precipitated keratins less permeable and responsive to the surrounding media event it is chemically compatible.

Last batches of isolation of keratin in the list brings us back to hair type keratins, this time including two new and different kinds. Raw materials 3 and 4 produced keratins HK-2 and HK-3 respectively, each sample is from different ethnical origin and both keratins were extracted under the standard conditions for the Shindai method. As a result, the thiol content determined for HK-2 and HK-3 were 0.4 and 1.39 µmol thiol/g keratin respectively, supporting the low solubility in PBS observed for this samples which seems to have a direct correlation with the lower values of thiol content. Furthermore, these values might not be definitive and conclusive as to decide the overall solubility of the keratins, however they provide a rough estimation of what the solubility threshold in terms of thiol content should be around and by this acknowledging the degree of importance thiol content contributes to the solubility of keratin in PBS.

The observations and assumptions confined in this section reflect the data collected from Ellman's assay that accounts only for free thiol or sulfhydryl groups found in the keratins extracted. However, the assay does not account for the total content of sulphur in the keratins, yet the thiol content remained relevant as reference value of what the total sulphur content should be and this is because thiol groups once generated after reduction are susceptible to oxidation by a numbers of factors [35-40] including the air as source of oxygen. Following this reasoning, it is plausible to infer that most of the keratin reported in this section with low thiol content might possibly have a high sulphur content in the form of cysteic acid among and also forming disulphide bonds that were originally free thiol groups right after the isolation process and that could have been oxidised to disulphide bonds throughout the time the samples were stored by atmospheric oxygen or any other agents, meaning that the real thiol could have been slightly higher. On the other, the previous assumption can have no great or no significant implications with regards to the thiol content as

much as the isolation conditions could have had on the samples, given the fact that the raw materials were from different ethnical origin and the reduction conditions remained unaltered for the all the isolation batches suggesting that stronger conditions could have possibly released more free thiol groups in those keratins with low Ellman's thiol content.

3.3.4. Molecular weight determination by GPC

A Biosep SEC-S2000 protein column usually used in GPC instruments was adapted to a GPC system in order to run the keratins and determine their molecular based on their retention time. The procedure and the fundamental theory and concepts that apply to standard GPC systems used purely to detect the presence of molecules in a mixture, also applies to the system used in this work. In this work, the combination of a GPC column with a GPC system was not only to accurately record the retention times of the keratins but also to determine their molecular weight based on the retention times and this was achieved by means of the column which provides information about the retention times obtained based on the hydrodynamic volume of the molecules in the sample solution which are segregated by the pores inside the column leading to a certain retention time resulting from the degree of interaction with the stationary phase. These pores in the column have specific molecular weight cut-offs that can only hold molecules within their cut-off values discarding the bigger molecular weights that don't fit in the pore meaning that these big molecules show early departures from the outlet of the column resulting in shorter retention times. Following this principle, it is possible to infer that the shorter the retention time is the bigger the molecular weight is due to the poor or no interactions these molecules have with the pores inside

in the column and when the opposite applies to smaller molecules which due to the small size their retention time is increased by the interaction they may have with the pores in the column which can trapped them for short times until they are flushed out by the mobile phase and eventually taken out of the column displaying longer retention times than those with bigger sizes and lower interactions with the pores. In addition, the UV-detector attached to the GPC instrument provides accurate detection for keratins as it was observed previously in the UV-vis spectra of keratins showing a distinctive peak near 270 nm, proving that keratin can be easily identified by a GPC system featuring a UV-light detector that makes the retention times reliable and accurate for this particular protein or any other UV active molecule.

Chromatograms of keratins obtained from this system are shown in Figures 3.12-3.14 as well as their respective molecular weights in Table 3.5. The molecular weight of samples W1, W2 and HK-2 were extrapolated from the range obtained in the calibration curve, assuming a Log10 behaviour. It can be noticed as a general observation that the biggest values in the list are not particular to one species alone and the evidence is found in the both hair keratins (HK-2, 80 kDa) and wool keratins (W2, 82 kDa) whose molecular weights are above 80 kDa which is considered a high molecule on average for most keratins in general. In a similar way, the smallest values in the list can be observed in both hair (H5:15 kDa and H3: 16 kDa) and wool (W2-pp, 16 kDa) keratins and unlike the top values in the list, the smallest entries seem to be within the values found and reported for some types of keratins in the literature [35-40].

Table 3.5. *Molecular weight of keratins determined by a GPC instrument featuring a GPC column for molecular weight of proteins*

Sample	Batch	RT (min)	MW (kDa)
H1	1	7.927	41
H2	1	7.493	46
H3	1	11.69	16
	1	5.481	76
H4	2	8.163	39
H5	3	11.735	15
	3	5.473	77
H6	4	11.058	18
W1	5	5.353	79
W2	6	5.209	82
W2-pp	6	11.496	16
HK-2	7	5.303	80
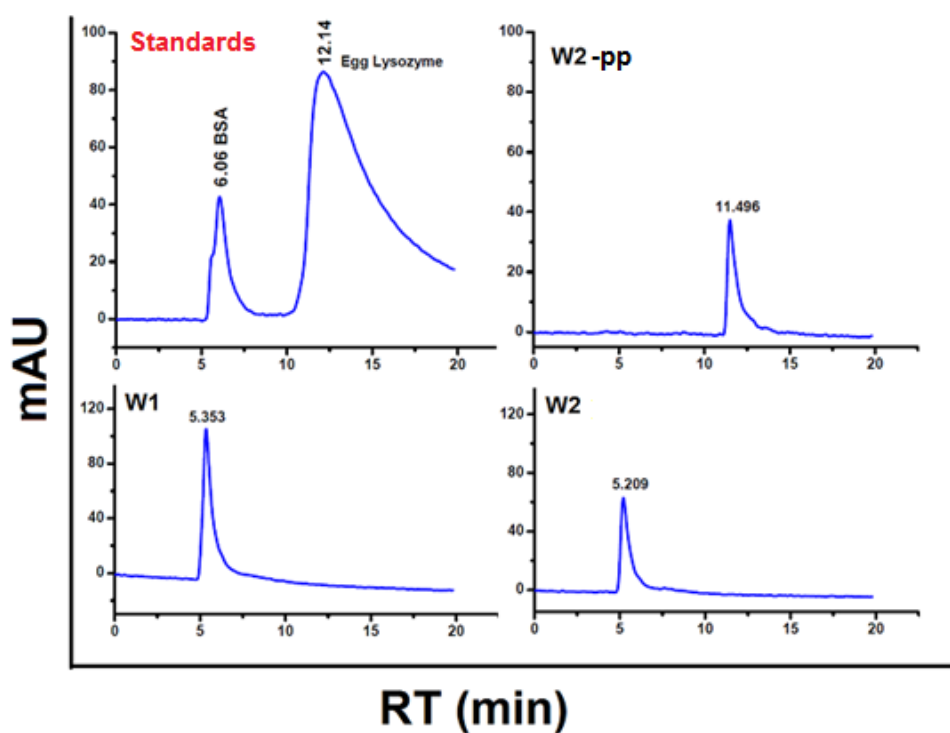
Figure 3.12. *GPC chromatograms of keratin samples W1, W2, W2-pp and Calibration Standards.*
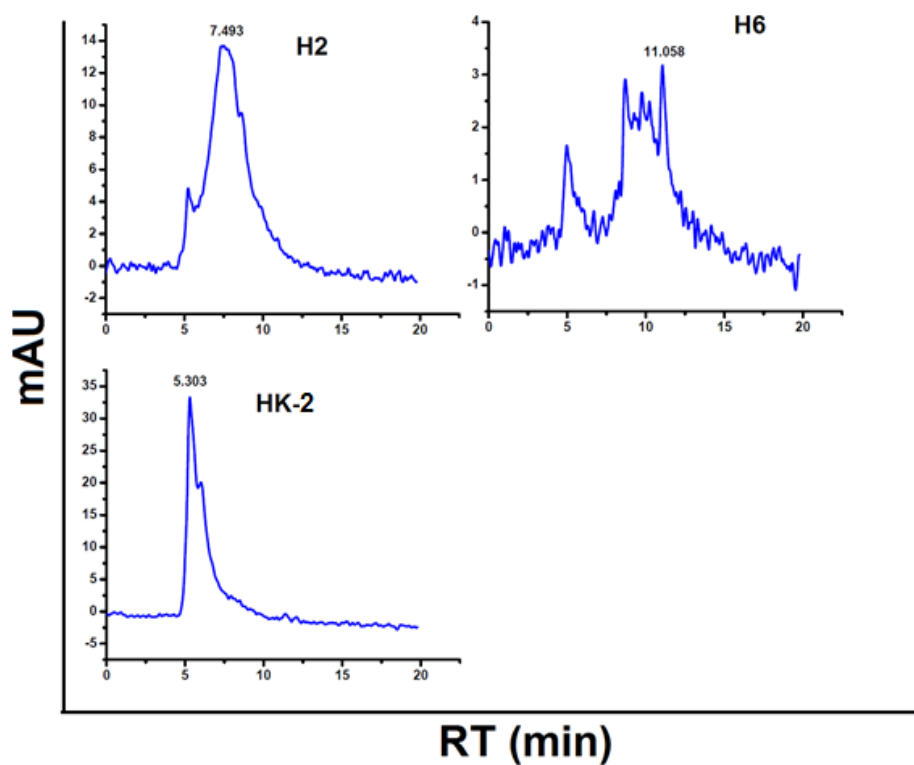
Figure 3.13. GPC chromatograms of keratin samples H2, H6 and HK-2.
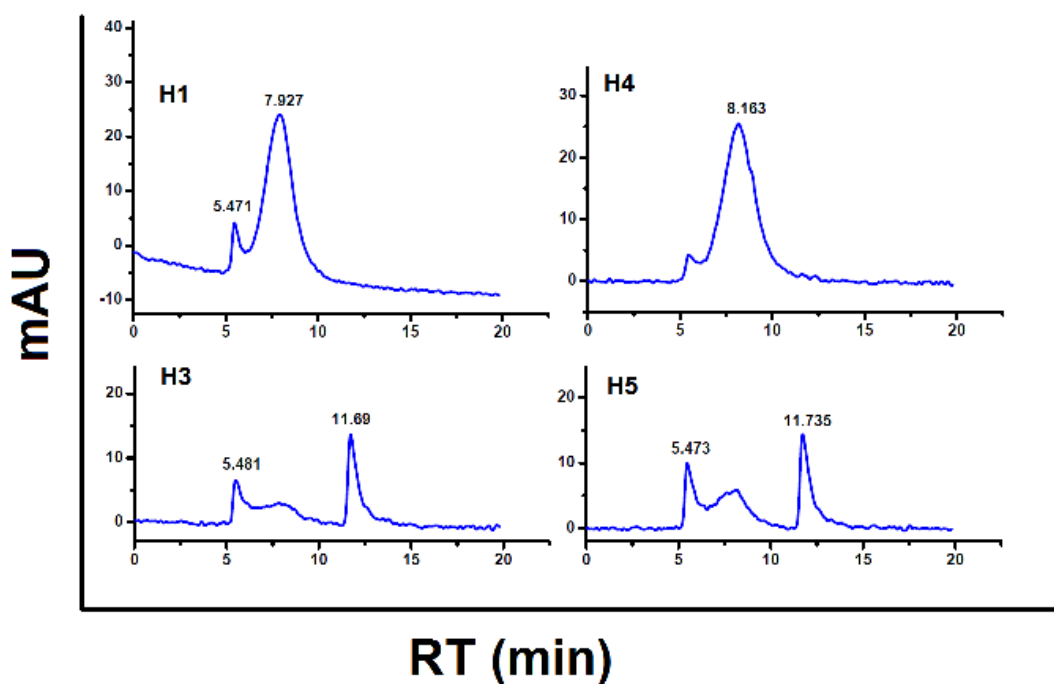
Figure 3.14. GPC chromatograms of keratin samples H1, H3, H4 and H5.

From a systematic point of view, the molecular weights determined provided relevant information regarding the impact of the reduction

conditions over one type of sample, as it happens to raw material 1 which is the only raw material that underwent two reduction conditions exemplified in Shindai method and reduction with Na_2S. The latter method produced the highest molecular weight in sample H2 (46.2 kDa) amongst the series H1-H6 exclusively isolated from raw material 1. Fellow keratins H1 and H3 from batch 1 displayed molecular weights values of 41.4 kDa and 16 kDa respectively proving that a range of molecular weights can be found within one isolation batch, presumably due to two different types of conformations in the keratin coexisting within a common matrix. This finding has been previously observed in many types of keratins where the domain of a certain conformation is associated to some species and for the particular case of the keratin isolated under Na_2S method from the raw material 1, the situation seems to clarify by looking at the molecular weight of H4 (39 kDa), where no fractioning was carried out and the whole batch was equally purified and freeze dried resulting in a single value of molecular weight that points out at an α-conformation by the magnitude of the molecular weight. This result might serve as supportive information to the evidence found in literature that claims the domain of α-helices over β-sheets in hair keratins [39-43].

Shindai method in contrast with reduction with Na_2S has shown two populations of molecular weight in keratin H5 (15.8 kDa and 77 kDa) where the magnitudes suggest β-sheet conformations prevailing over α-helices by looking at the intensities of the Absorbance signals. However, the domain of this β-sheet conformation seems suspicious for this particular case due to the fact that it is a hair keratin where the α-helices are more abundant and yet the β-sheet conformation seems to be the most abundant in this keratin and fully dominant on H6 with a low magnitude of molecular weights that suggest the exclusive presence of β-sheet conformation for this keratin. Nonetheless, it is important to remember that the previously assumption is merely based

by judging the magnitudes of the molecular weight that are usually attributed to certain conformations in keratin but further characterisation should be conducted in order to prove the identity of these conformations and the presence of two populations of molecular weight is not something new and exclusive to this isolation method, since keratin H3 was obtained under different conditions and it shows a similar pattern that could serve as evidence of the co-dominance of the two conformations in hair keratins, taking into account the similitude of the peaks of the shortest retention times in both chromatograms and as a result the molecular weights were not significantly different (H3: 76 kD; H5: 77 kD).

Conversely, a higher molecular weight was found in a subsequent batch under Shindai conditions as occurred in the seventh batch where keratin HK-2 obtained a molecular weight of 80.4 kDa which is regarded as a high molecular weight for a keratin [36-39], demonstrating that Shindai reduction conditions can be more drastic over some substrates than on others and the evidence is found in this keratin HK-2 which unlike the series H1-H6 exclusively extracted from raw material 1 was isolated from raw material 2. Raw materials 1 and 2 despite of both being hair samples that share common properties in terms of amino acid composition and protein conformation, were collected from individuals of different ethnical groups with distinctive features on their own which presumably might explain the difference in molecular weights found despite of being isolated under the same conditions and method and to do justice to the Shindai reduction conditions which remained unaltered for the keratins discussed, it is possible to say that the reduction conditions have greater impact on raw material 1 where the molecular weight has reached low values in keratins H5 and H6 presumably due to the thickness (Figure 3.15) of the hair strands that makes them susceptible to be lowered in size by the external conditions as to reach fragmentations of the protein chain,

producing low-molecular-weight keratins. By comparison, raw material 2 has thicker hair strands that are less susceptible to be fragmented meaning that the influence of the external media are not strong enough to cope with the toughness of the hair matrix in raw material 2.
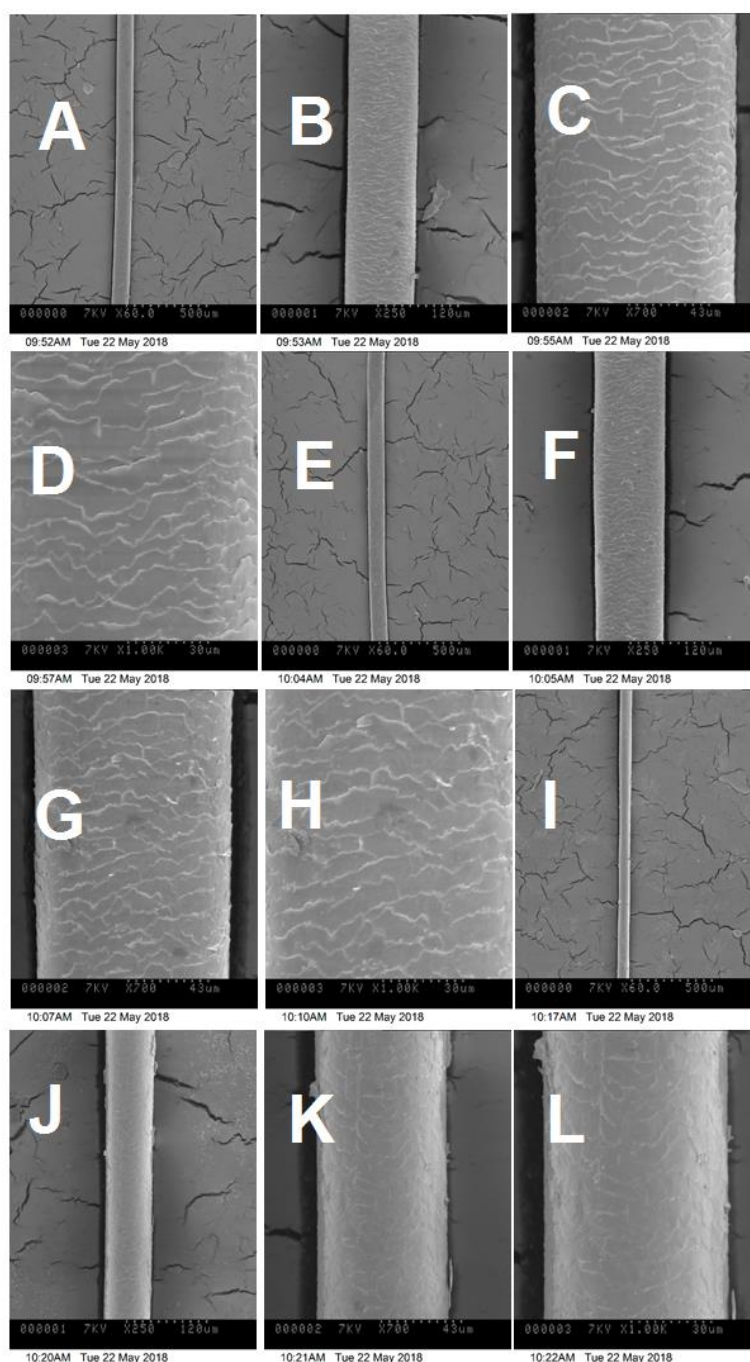
Figure 3.15. SEM micrographs of Raw materials 1, 2 and 3 in 4 different zoom ins: x60; x250; x700; x1000. : Raw material 1 (A-D), Raw material 2 (E-H) and Raw material 3 (I-L).

With regards to the Wool keratins the molecular weights are not drastically different in magnitude being 79.4 and 82.3 kDa for W1 and W2 respectively. Similarly explained, as observed in hair keratins the outcome obtained in terms of molecular weight is a combination of the influence the external reducing media has over the matrix of wool fibers, producing the high molecular for these products of the Shindai method with no modifications to the original procedure. By comparison, wool keratin W2-pp has a rather low molecular weight in magnitude (16.8 kDa), drastically below the values from their fellow wool keratins, especially from wool keratin W2 that belongs to the same isolation batch, meaning that these two keratins were reduced under identical conditions but their post-reaction treatment were different, and hence they both have their own identities. The post-reaction treatment has had significant implications on wool keratin W2-pp reducing it to a low molecular weight (16.8 kDa) that drastically differs from the value observed in wool keratin W2. This situation has been observed previously in Hair keratins H5 and H6 that were despite on not belonging to the same batch were reduced under identical conditions but a precipitation step was conducted on H6 instead of the usual freeze-drying and dialysis as occurred to keratin H5, and by this analogy seems plausible to infer that the precipitation step is responsible for the low molecular weights observed in H6 and W2-pp regardless of the nature of the precipitation technique. It is important to clarify that those lower values of molecular weight for H6 and W2-pp only correspond to the soluble phase of each sample and possibly there is a greater fraction of keratins with higher molecular weight values remaining in the insoluble phase as a result of the densely packed arrange the sample assembled as part of the process of precipitation.

3.4. Gelation studies with keratin by Michael addition reactions

Throughout the characterisation section the presence of functional groups in the keratins were confirmed by spectroscopic methods and the relevance of some of these was evident in aspects like the solubility in basic aqueous media where thiol groups seem to play a role. These thiol groups were also quantified and the results were contrasted with the observations in the solubility test in order to estimate more accurately the importance of the thiol groups as responsible for the solubility of the protein in aqueous media. In addition, chromatographic techniques were performed on the keratins in order to determine the molecular weight and classified each value according to the species the keratin was isolated from. Collectively, thiol content and molecular represent two major properties in keratins regarded as the key factors that undermine the relative inert nature of keratin as a structural protein, where in the native state the majority of the thiol gropus are in the form of disulphide bonds. These properties play a role in gelation processes where the thiol groups and the molecular contribute with reactivity and size to the process facilitating the transition into a higher state of aggregation. Thiol groups confer the necessary reactivity towards double bonds for a Michael addition reaction where double bonds in acrylates or methacrylates can react with the free thiol groups in keratin forming a new covalent bond. This reactivity in conjunction with the appropriate molecular weight provides the size necessary to produce macro structures that form a network capable of retaining water in the structure and this is aided by the hydrophilic behaviour of acrylates and methacrylates, resulting in the structures known as hydrogels. In this section, a series of hydrogels were synthesised by combining keratin with a methacrylated molecule and two acrylated compounds under similar conditions and by means of SEM the morphology of the gels was revealed.

Keratin-PEGDA, Keratin-SoyBoil and Keratin-Mth.Alginate gels were moulded in 1.5-mL Eppendorf tubes to allow incubation in a water bath at 38.5 °C, obtaining gels with conical shape that remained unaltered after freeze drying (Figure 3.16). In order to discard possible self-crosslinking between the acrylates or methacrylates that could possibly result in a significant degree of gelation, every gel was casted along with a blank reaction containing only the respective acrylate or methacrylate under identical conditions for the synthesis of the gels and the results were negative for all the blank reaction discarding any possible contribution coming from self-crosslinking proving that each gel gained consistency ass a consequence of the Michael addition reaction.
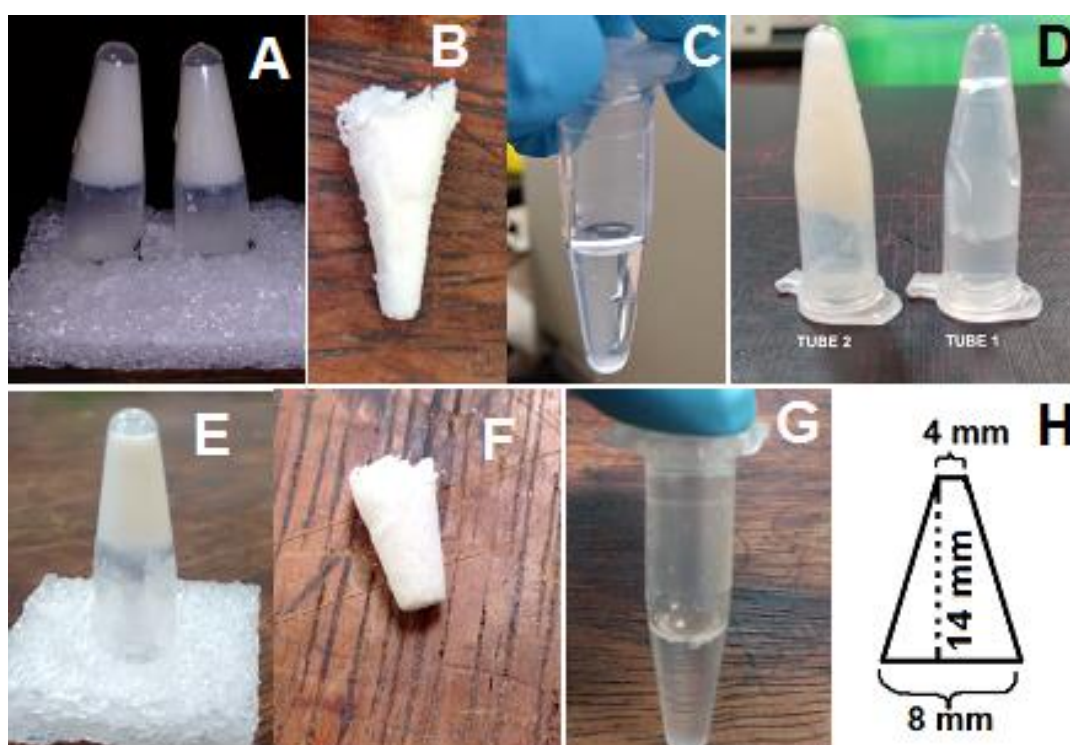
Figure 3.16. *Keratin-PEGDA gel (A:wet gel; B:dry gel, C: Blank reaction), Keratin-Ma.Alginate gel (D: wet gelin tube 2 and Blank reaction in tube 1)Keratin-SBoil gel (E:wet gel; F: dry gel, G: Blank reaction) And Average dimensions of the conical dry gels (H).*

SEM micrographs revealed the surface morphology of the dry gels, observing a flaky pattern in Keratin-PEGDA gels (Figure 3.17: G,H.I)

and a smoother pattern in the Keratin-SBoil (Figure 3.17: A,B,C) and Keratin-Ma.Alginate gels (Figure 3.17: D,E,F).
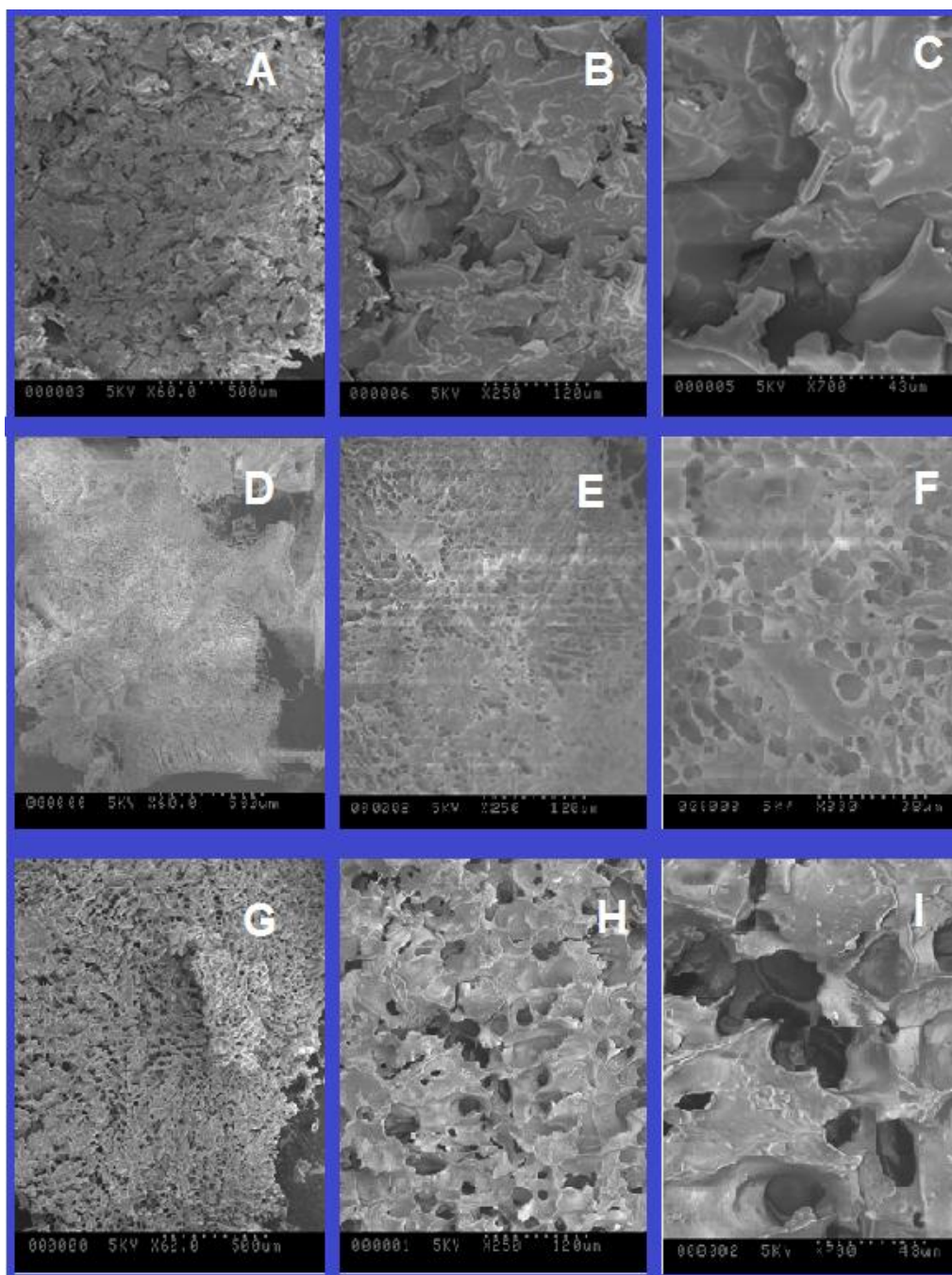
Figure 3.17. *SEM micrographs of Keratin-SBoil gel (A,B,C), Keratin-Ma.Alginate gel (D,E,F) and Keratin-PEGDA gel (G,H,I).*

Keratin-PEGDA gel displays the simplest crosslinking in the series in which a bifunctional ester PEG-DA (575 Dalton) acts as the cross linker

of Keratin (79391.8 Dalton) that joints two different protein chains together or it can also join two thiol groups along the same protein chain (scheme 3.4) and therefore building up a random crosslinked network that results in a hydrogel structure. In the same way, but also due to its size soybean oil epoxidised acrylated acts a crosslinker in Keratin-SBoil gels in which a higher branched pattern has been achieved in comparison to Keratin-PEGDA gels due to the multifunctional nature of soybean oil epoxidised acrylate, that has four acrylate groups in its (Scheme 3.5 molecular structure inside yellow frame) that reinforces the interconnection between keratin chains consequently making the gel network mechanically stronger (Scheme 3.5). On the other hand, Keratin-Mth.Alginate gel includes in its composition Methacrylated alginate a large polysaccharide with a molecular weight around 300 kDa that makes it comparable with keratin (60 kDa) in terms of size both being macromolecules. This fact makes difficult to establish a crosslinker behaviour for the keratin-Ma.Alginate gel and a co-crosslinking relationship seem more suitable for this gel in which each type of molecule bridge one to another in a rather aligned arrange. The sodium alginate backbone in methacrylated alginate confers hydrogen-bonding properties that enhances the gelation process. This was primarily observed gel consistency superior to the other two gels possibly resulting not only from the thio-ene click reaction but by the viscosity resulting from the hydrogen-bonding between hydroxyl groups in Methacrylated alginate interacting with each other and with those in keratin. This property is native to the precursor Sodium alginate which forms viscous solutions in water and can be even ionically crosslinked by divalent cations such as Ca^{2+} forming gels in relatively low concentrations of the cation (2-5% w/v) due to the assistance of the hydrogen-bonding in the gelation process.

SEM micrographs of the dry gels revealed the surface morphology of each type of gel by showing a marked flaky pattern in Keratin-PEGDA gels (Fig 3.17 G,H,I) presumably due to the small size of PEGDA which leaves keratin as the predominant component and possible responsible for the texture. Soy bean oil epoxidised acrylate in spite of being a small molecule in comparison with keratin has modified the morphology of the keratin-SBoil gel in a different way by making the flaky pattern more compact (Fig 3.17 A,B,C) than Keratin-PEGDA gels owing to the fact of the multiple acrylate groups in SBoil that provides a higher number of linking points per molecule making the network structure more compact. In the same way, SEM micrographs of Keratin-Ma.Alginate (Figure 3.17 D,E,F) exhibit a very compact pattern on the surface with the smallest cavities of the gel series and a more homogeneous pattern that could be explained by the similarity in size and results in a better alignment that constrains the network structure tighter producing smaller cavities or cells.
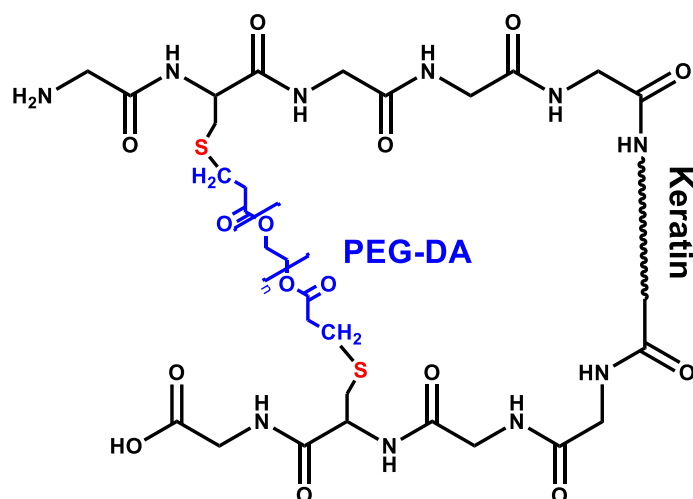
Scheme 3.4. *Keratin-PEGDA crosslinking scheme (segment).*
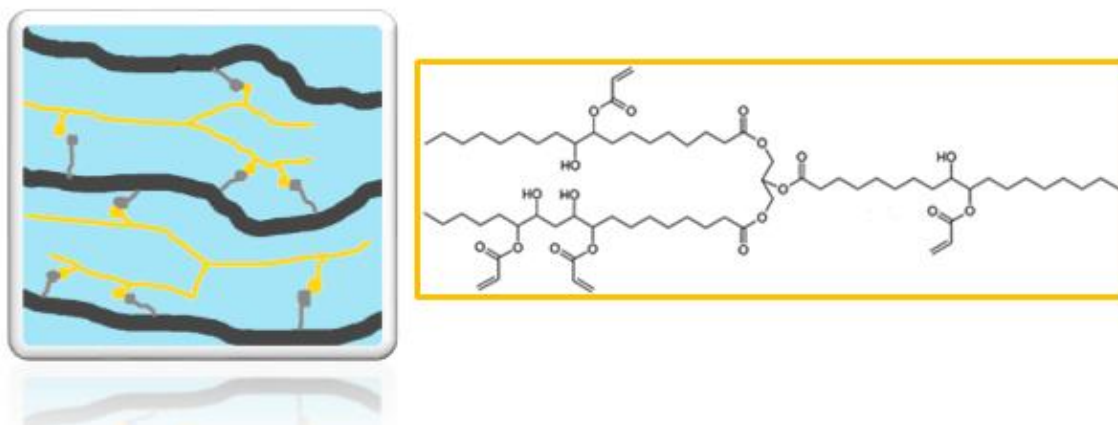
Scheme 3.5. *Keratin-SBoil gel scheme: Soy bean oil epoxidised acrylate is represented in yellow branched lines and its molecular structure displayed inside the rectangular yellow frame. Grey thick lines represent keratin chains.*

3.5. Methacrylation of Sodium alginate and Chitosan

Upon vacuum drying in Buchner funnel, the flaky texture of Methacrylated alginate was revealed and remained unaltered after freeze drying, resulting in small white scales as final product, yielding 3.74 g of Methacrylated alginate (Figure 3.18 A). On the other hand, Methacrylated Chitosan exhibited a spongy and soft appearance after drying, producing big pieces of cottony material (Figure 3.18 B) that accounted for 1.1435 g of final product.

Figure 3.18. *Methacrylated alginate (A) and methacrylated chitosan (B).*

Figure 3.19 displays the ^{1}H-NMR Spectrum of the synthesised Methacrylated alginate in D_2O, observing the typical signals of Methyl

protons at 2.39 ppm (red square), anomeric protons at 4.94, 5.11, 5.51 ppm and double bond protons at 6.18 ppm (yellow square) and 6.62 ppm (purple square). The presence of these signals confirms qualitatively the funcitonalisation in the precursor has occurred and the final product exhibits methacrylation in its structure.
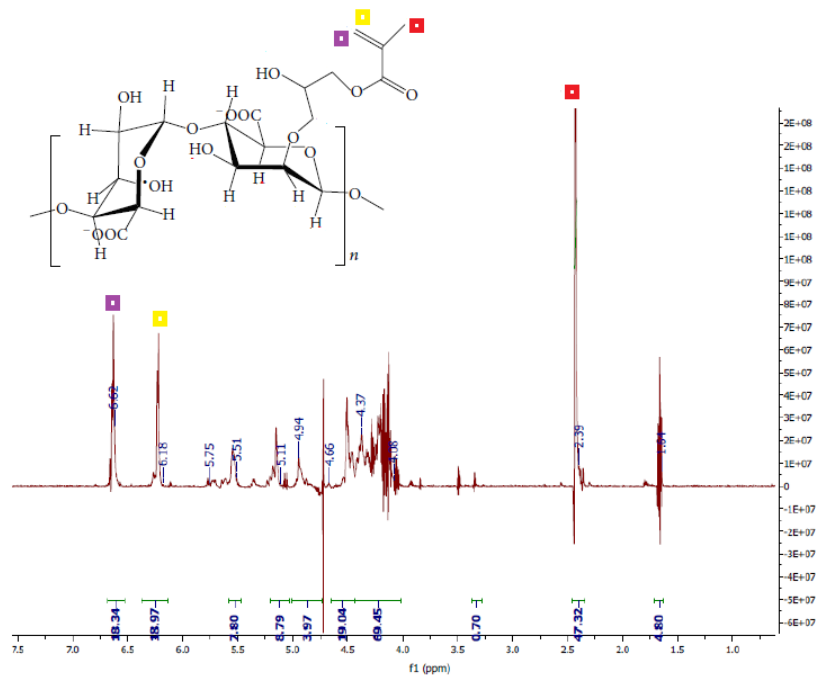
Figure 3.19. *1H-NMR spectra of M-Alginate in D2O*

3.6. Photo crosslinking reactions

Conventional Plastic syringes were converted into sample moulds by removing the tip (Needle-inlet surface) leaving the barrel totally open and expose to UV-light prevenient from the curing lamp (Figure 3.20 A). Methacrylated Alginate and Methacrylated Chitosan gels adopted the shape of the mould, maintaining the inner diameter of the syringe and the height given by the volume used for the synthesis leading to a final disc-like geometry .In the same way, the final transparent colour of the gels was due to the original colour of the starting liquid material.
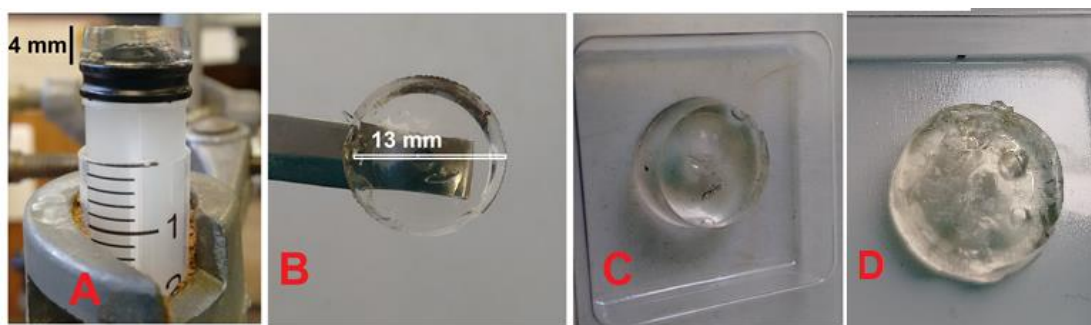
Figure 3.20. *Photo-crosskinked gels dimensions (A,B), methactylated alginate gel (C) and methacrylated chitosan gel (D)*

Photo-crosslinking of Methacrylated alginate/chitosan was conducted via free radical reactions between double bonds in methacrylate groups using Irgacure 2959 as photo initiator and methacyrlated alginate/chitosan as monomers. Although the Photo crosslinking reactions followed the kinetics of a free-radical polimerisation displayed in Scheme 3.6, the reactions is limited to the crosslinking of the functionalised sugar chains and the process starts by the cleavage of the Irgacure D-2959 molecule (scheme 3.6, box) that releases two radicals that promoted the reaction on to a propagation stage until all radicals have reacted and the last two remaining radical species join together in the termination step.
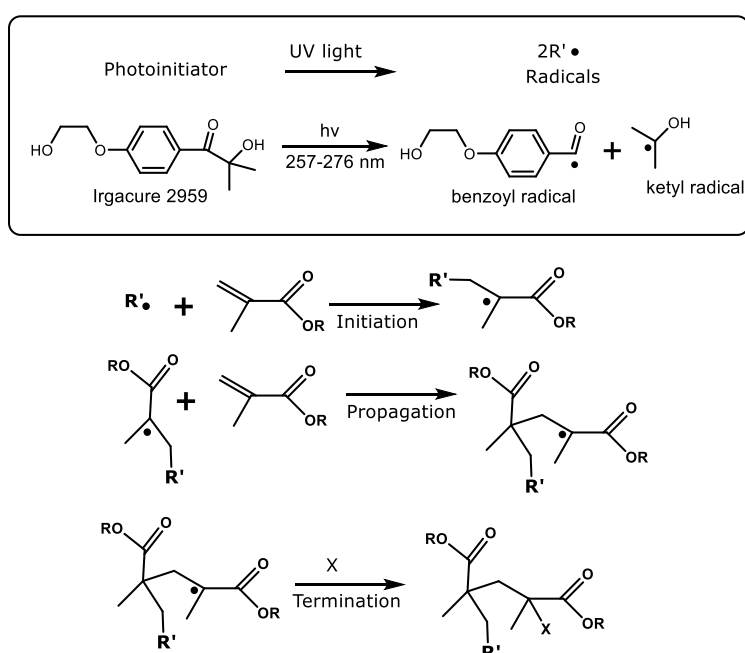
Scheme 3.6. *Free-radical polymerisation process for methacrylates and cleavage of photo-initiator Irgacure D-2959 (box).*

The free-radical reaction was assisted by UV light provided by the bluewave®200 spot lamp working at the maximum intensity of 40 W/cm^2, located at a distance d (d=4.5 cm, see Figure 2.4) away from the sample delivering a wavelength range of 280-450 nm. Every gel was moulded in modified plastic syringes in order to obtain a disc-like geometry gel, which reached total gelation after 6 minutes of curing under the conditions reported section 2.7. The gel consistency obtained in both materials suggest the mechanical properties might be explained by the hydrogen-bonding characteristic of alginate and chitosan which is initially observed in their viscous solutions in water and eventually evident upon gelation. SEM micrographs of Methacrylated Alginate gels (Figure 3.21) revealed a smooth surface pattern with interconnected rounded cavities, presumably due to the water originally entrapped in the hydrogel.
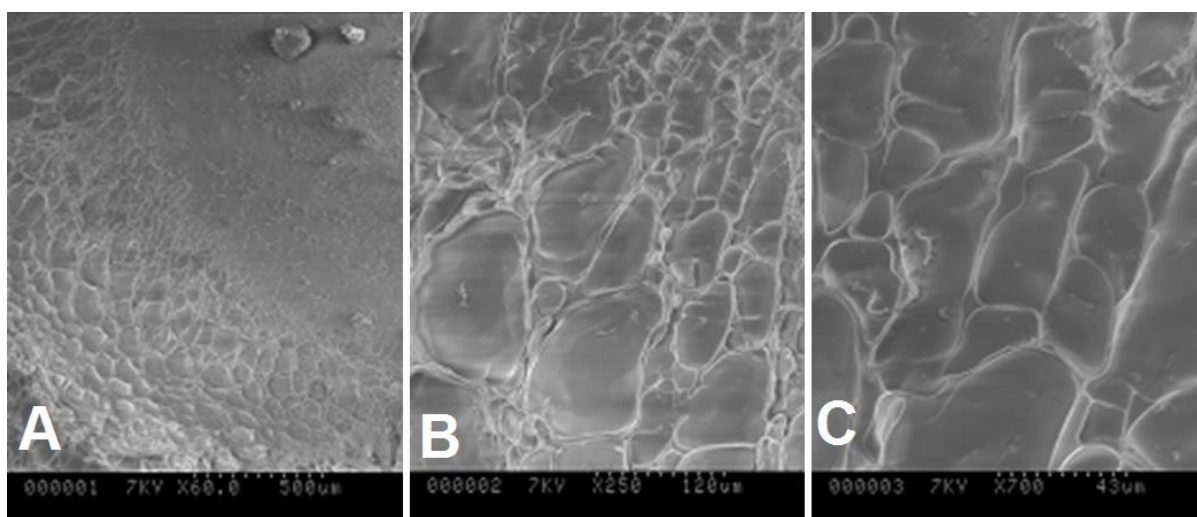
Figure 3.21. *SEM micrographs of Ma. Alginate gels in different zoom-in: x60 (A), x250(B), x700(C).*

3.7. Two-step casting method

Keratin-Methacrylated Alginate gel synthesised by this method combines two different crosslinking reaction that complement each other in attempt to reinforce the network structure. The two-step method takes advantage of the reactivity of the methacrylate groups in methacrylated alginate towards photo-crosslinking and the thiol groups in keratin towards the Michael addition reaction. The gel obtained from this two-step method showed remarkable gel consistency and visually improved mechanical properties, being easily moulded and removed from the Eppendorf tube where it was casted (Figure 3.22).
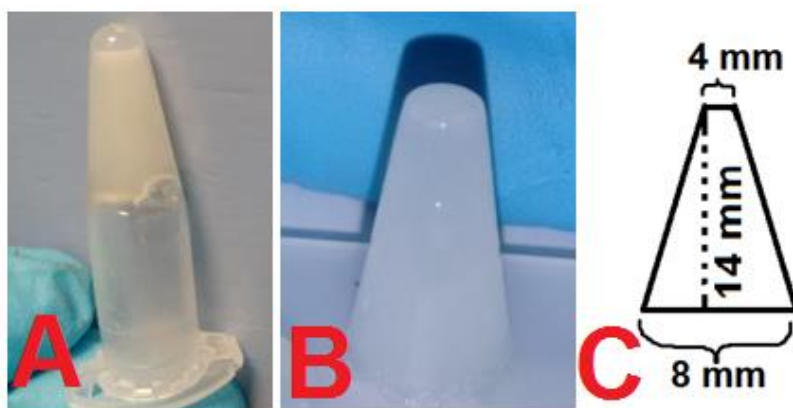
Figure 3.22. *Ma.Alginate gel by two-step method inside (A) and out (B) of the mould. Gel dimensions (C)*

Combining the two casting methods previously discussed in sections 3.5 and 3.7, a two-step method was developed initially driven by a Michael addition click reaction and followed by a photo-crosslinking reaction (Scheme 3.7). The process was intended to reinforce and enhance the mechanical properties of the original Keratin-Ma.Alginate gel by using an excess of Ma.Alginate to perform photo-crosslinking of the unreacted methacrylate groups from the Michael addition reaction. During the first step a hydrogel was produced by Michael addition reaction, but gelation was complete after the second step when a free-radical reaction was conducted, making evident the improved gel

properties in the obtained material which was easily and immediately removed from the Eppendorf tube after casting (wet gel), unlike the Michael addition gel that show more resistance to be taken out if the eppendorf tube immediately after casting. This combined reaction proved the feasibility of combining the reactivity of keratin and functionalised alginate in the fabrication of bio degradable and bio compatible hydrogels with potential applications in the design of hydrogel-based wound dressings.
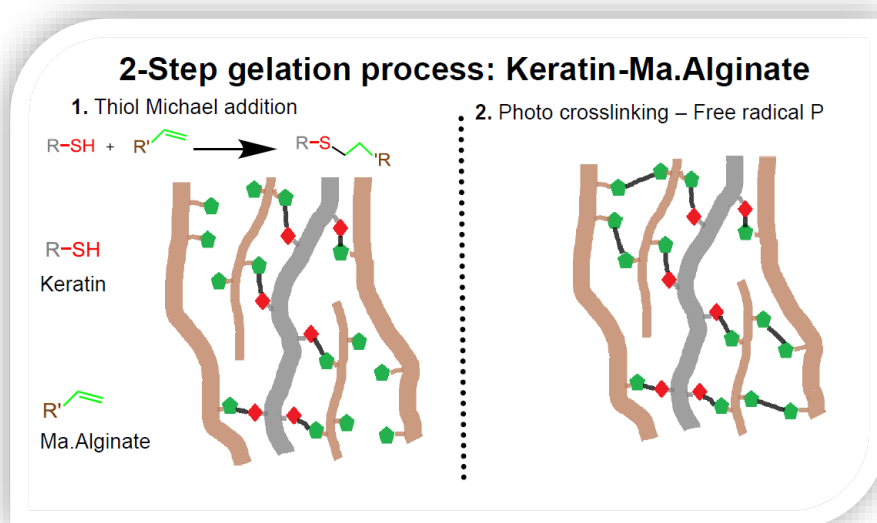
Scheme 3.7. *Scheme of the Two-step casting method*

3.8. Swelling studies in water for methacrylated alginate and methacrylated chitosan gels

Swelling in water was monitored over time for all the synthesised gels to evaluate their water retention properties and their integrity upon prolonged immersion in water for the gel synthesised by photo-crosslinking reaction. Figure 3.23 displays the results of data obtained for the swelling studies for methacrylated alginate and methacrylated chitosan, calculated according to the equation in scheme 3.8.
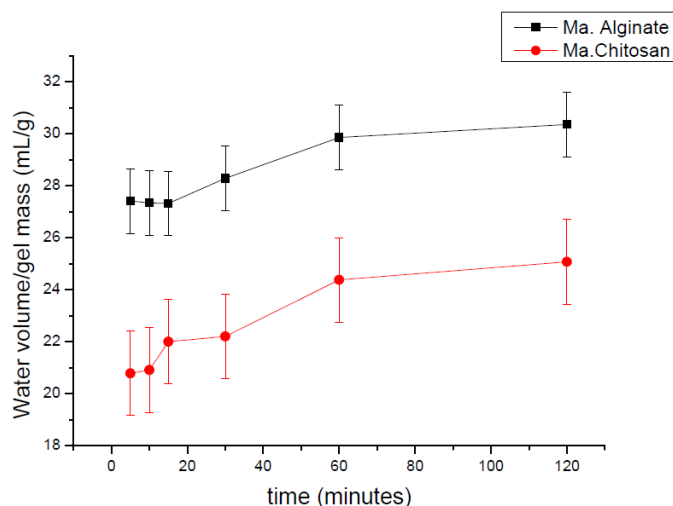
Figure 3.23. Swollen volume diagrams for Methacrylated alginate and Methacrylated chitosan

Methacrylated Alginate/chitosan gels remained unaltered upon long periods of immersion in water, demonstrating the integrity of the gels is not affected for periods of time up to two hours. As a general trend, both gels increased their swelling capacity over longer immersions, especially during the first hour after 15 (Figure 3.23, 30-minute entry) and 30 minutes (Figure 3.23, 60-minute entry) of immersion in the media, where the swelling capacities reached 28.3 and 29.9 mL/g for Methacrylated alginate and 22.2 and 22.4 mL/g for Methacrylated chitosan. These values account for 93.1% and 98.4% of the total swelling capacity in Methacrylated Alginate gels and 88.4% and 97.2% of the total swelling capacity in Methacrylated Chitosan gels. During the second hour the swelling capacity increased only 1.6% in methacrylated alginate and 2.7% methacrylated chitosan, suggesting that the swelling process is achieved to a greater extent during the first and to a lower extent during the second hour.

$$\frac{swollen\ volume\ in\ mL}{gel\ mass\ in\ g} = \frac{\dfrac{wet\ mass_{Hydrogel} - dry\ mass_{dry\ gel}}{density_{water}}}{mass\ of\ dry\ gel}$$

Scheme 3.8. Equation for the swollen volume/gel mass for the swelling studies.

The swelling properties determined in this test might explain the observations made on the morphology displayed in SEM micrographs of Methacrylated alginate gels (Figure 3.21), where the rounded geometry of the cavities seems to have the purpose of optimising the storage of water in the network structure.

3.9. 3D Printing experiments

3.9.1. Introduction

The findings reported in this section include a qualitative description and some visual observations made on these 3D printing experiments, clarifying the fact that they only constitute an early stage of rapid prototyping with this system and further research should be conducted on this experiments to successfully print out objects with the polymer systems reported in this thesis. The experiments used Sodium alginate as a paste material for its easy manual-handling and low toxicity to the environment. In addition, the inclusion of this polysaccharide is encouraged by the positive findings observed in the functionalised polysaccharide in the photo-crosslinking experiments (section 3.5). Potential combination of sodium alginate with keratin either by physical blending or by a combined chemical reaction as it was observed in the two-step method reported in section 3.6 is another advantage in favour of the inclusion of sodium alginate as the initial material for early testing.

3.9.2. 3D printing experiments with sodium alginate: Syringe test

These experiments were fundamentally based on the ionic gelation that sodium alginate undergoes when combined with $CaCl_2$ so that Sodium alginate in aqueous solution was loaded in the syringe as the paste material (Figure 2.5) and once extruded on the print bed, $CaCl_2$ aqueous solution was added to allow solidification of the printed material by ionic cross-linking. Three different syringes were implemented for the extrusion of Sodium alginate 6% w/v (Figure 2.5 A, B,C). The first experiment was carried out by using the 10-mL glass syringe (Figure 2.5 A) attached to the 1-mL needle nozzle (Fig 2.5 B) since the former provides the best fit for the syringe holder and the latter produces finer filaments. The first layer obtained (Figure 3.24 A) flattened in spite of its high viscosity, losing the desired definition which is visible in the preview screen from the software (Figure 3.24 B). Once the first layer was obtained, the process was paused to add $CaCl_2$ 5 % and the resulting solid (Figure 3.24 C) shrank in comparison to the liquid original layer in Figure 3.24 A. After a couple layers, the shrinking effect affected the morphology of the cube since some areas of the printing were not extruded due to the nozzle being flying over spaces where the layer was under levelled so no deposition occurred, while it occurred over those areas within the reach of the nozzle as can be observed for the fifth layer immediately after extrusion (Figure 3.24 D), Subsequently, it was notorious a more drastic change in the overall morphology of the layer by the swelling that took place upon addition of $CaCl_2$ 5 % (Figure 3.24 E). The observations point at a non-homogeneous swelling process which causes loss of definition of the extruded filaments, which seem to be merging together as one amorphous gel rather than maintaining the original shape.
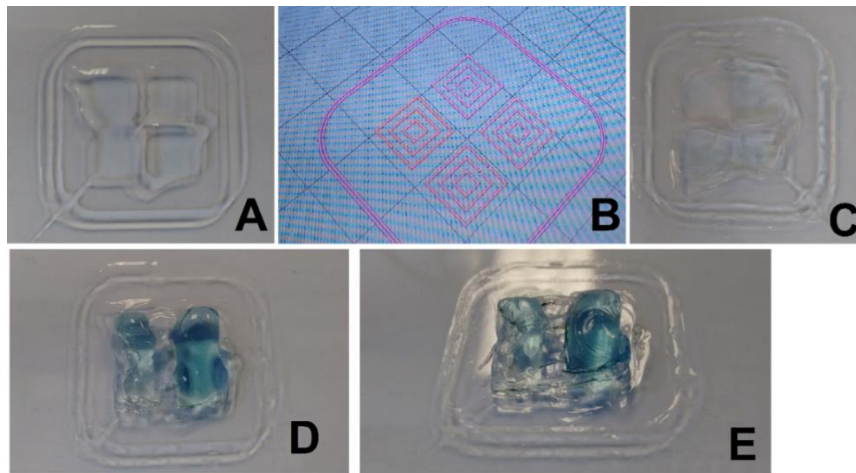
Figure 3.24. *Partial printing of a cube (glass syringe 10 mL). First layer after extrusion (A), preview in software Repetier-Host V2.0.5 (B) and after crosslinking with CaCl2 (C). Fifth layer after extrusion (D) and after crosslinking (E).*

In the same way, a 12-mL-plastic syringe (Figure 1.5 C) attached to the 1-mm needle (Figure 1.5 B) was tested under the identical conditions as the first experiment, however extruding only one layer (Figure 3.25). Results were not visually different in terms of performance and definition. However, the main difference found in using this plastic syringe is the rubber less plunger which produces more friction so the printer needed to impart a bigger extrusion force to make the liquid come out of the nozzle in comparison to the previous glass syringe.
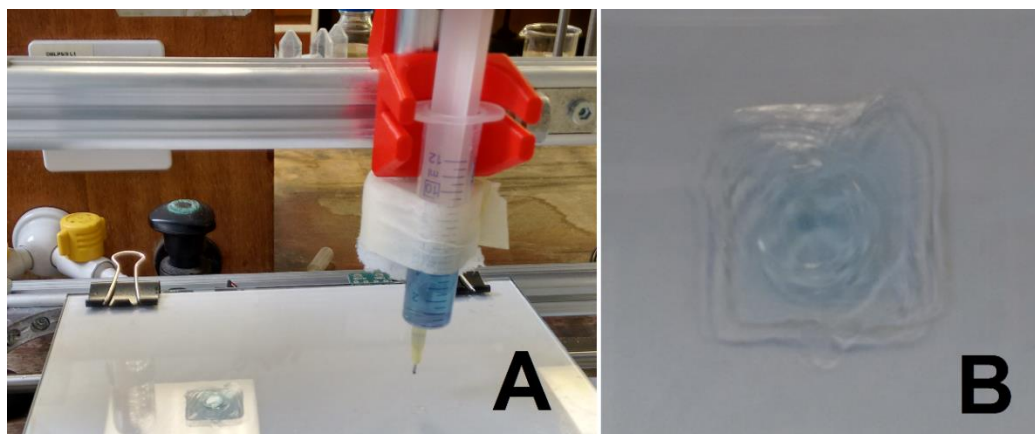
Figure 3.25. *Partial printing of a cube (A-plastic syringe 12 mL). First later after crosslinking with CaCl$_2$ (B).*

Analogically to the previous tests, a 5-mL plastic syringe was used for testing the printing of first layer of the cube. This syringe showed the lowest extrusion resistance since it has a plunger with a rubber head and the smallest size of the three syringes, so the obtained layer was not well-define due to overflowing of the sodium alginate solution from the nozzle, that extruder thick filaments that swollen with no define shape (Figure 3.26).

The observations made on the printing of the layers provided valuable information with regards to the syringe type that should be implemented for the extrusion of Sodium alginate 6% w/v using the equipment reported. It is evident the suitability of the 10-mL glass syringe, however its effectiveness would have not been as pronounced as observed without the inclusion of the 1-mm needle nozzle. Similarly, the 12-mL plastic syringe was satisfactorily effective for the printing of the first layer but subsequent layer the extrusion of subsequent layer could be significantly affected by the resistance its plunger produces towards the release of the liquid material from the nozzle. The 5-mL plastic syringe in contrast with the other syringes show the lowest resistance in its plunger and it distorted the shape of the printed layer, therefore making this syringe unsuitable for this purpose.
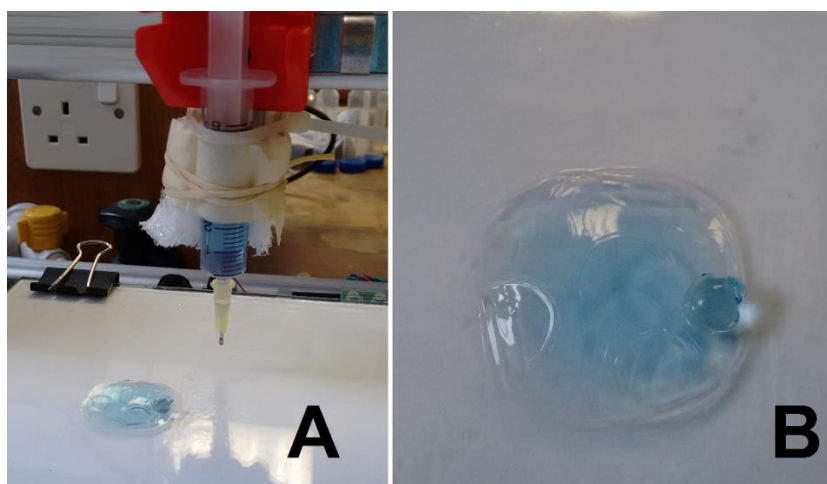
Figure 3.26. *Partial printing of a cube (A-plastic syringe 5 mL). First later after crosslinking with CaCl2 (B).*

3.9.3. Direct deposition of sodium alginate in CaCl$_2$ solution

This section presents the results obtained from the deposition of Sodium alginate (2% w/v) over a platform covered by CaCl$_2$ solution (5% w/v), in order to evaluate the ability to form a filament on a wet surface. It was observed the formation of a bulky filament that was dragged along the liquid media by the syringe nozzle (Figure 3.27). This could be due to the easiness of the solution to flow down the nozzle on account of the low viscosity of the dilute concentration (2%), suggesting that a more concentrated solution would probably provide better results in terms of forming a more solid and defined filament in solution.

Figure 3.27. *Printing of the first of a cube in CaCl$_2$-liquid-phase platform using alginate 2% w/v.*

Following the results from the previous experiments, Sodium alginate was also tested using a more concentrated solution (3%) which was extruded over the same platform covered by CaCl$_2$ solution (5%). It was observed the formation of a thinner filament than the filament formed when using less concentrated (2%) solutions (Figure 3.28). This result proved that a more concentrated solution helps to form a more defined filament, however, as occurred in the previous experiment, the printing of the layers had a limitation with regards to the nozzle which was incapable of depositing material beyond the 7th layer, due to non-homogenous swelling in the filament and the deformation of the layers caused by the nozzle, which dragged the

filament from its original position, since the wet surface didn't allow the filament to adhere tightly over the glass print bed.
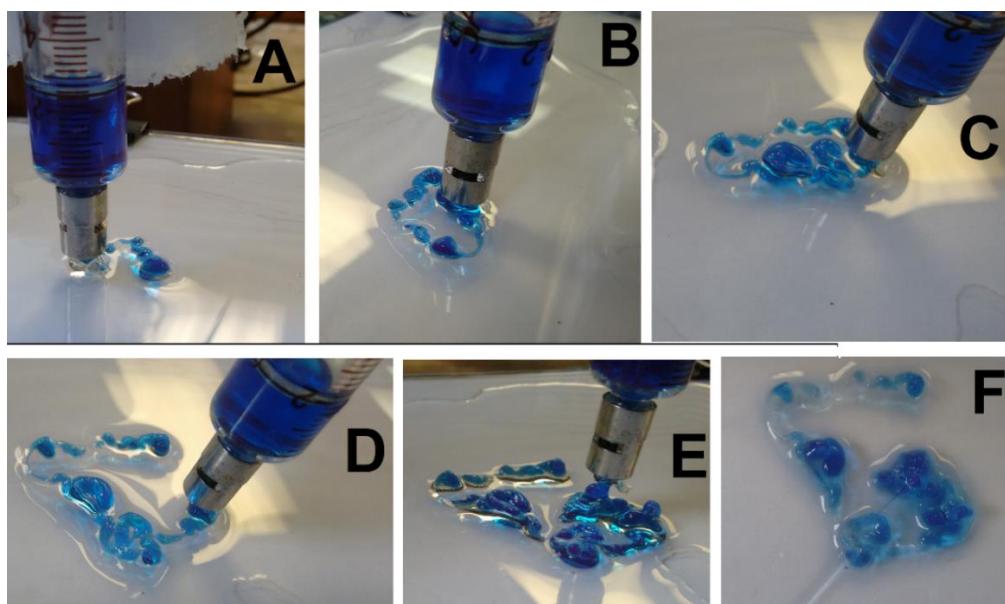
Figure 3.28. *Printing of a cube in CaCl2-liquid-phase platform using alginate 3% w/v: 1st layer (A). 2nd layer (B), 3rd layer (C), 4th layer (D), 7th layer (E), 7th layer (no nozzle).*

Finally, Sodium alginate was tested in concentrations 4% w/v & 5% w/v over the platform covered by $CaCl_2$ solution (5%). Sodium alginate 4% solution displayed a similar performance during extrusion as the solution 3% w/v solution in terms of the ability to form a filament. They both form a bulky-beaded filament. Five layers were extruded using 4% (Figure 3.29) solution before the extruder stopped depositing due to non-uniform level of the printed object. In contrast, no layer were extrude using Sodium alginate 5% since the concentration of the polysaccharide high enough to cause the extruder nozzle to clog with solidified product soon after contact with the $CaCl_2$ solution (Figure 3.30).
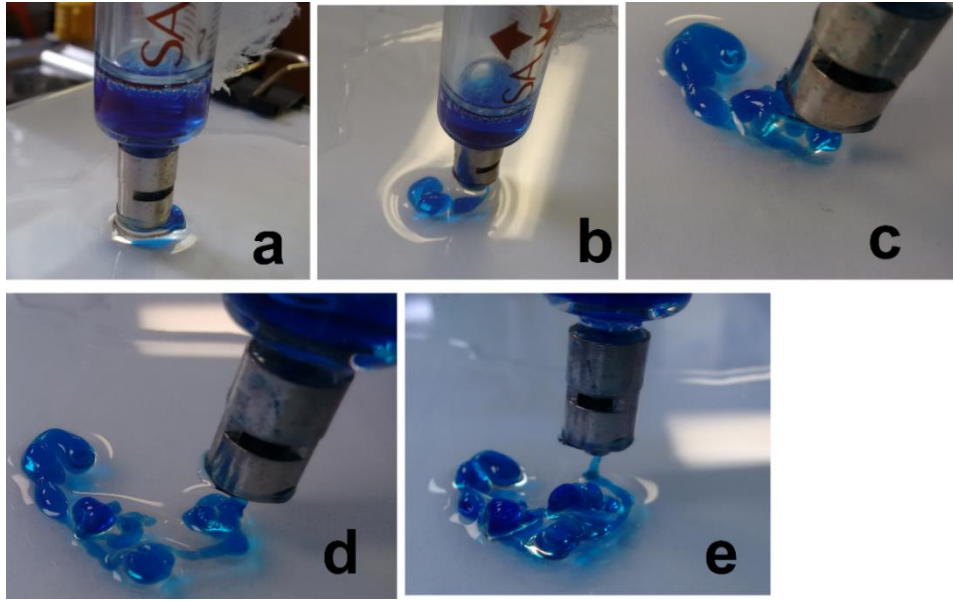
Figure 3.29. *Printing of a cube in CaCl$_2$-liquid-phase platform using alginate 4% w/v: 1st layer (a). 2nd layer (b), 3rd layer (c), 4th layer (d), 5th layer (e).*
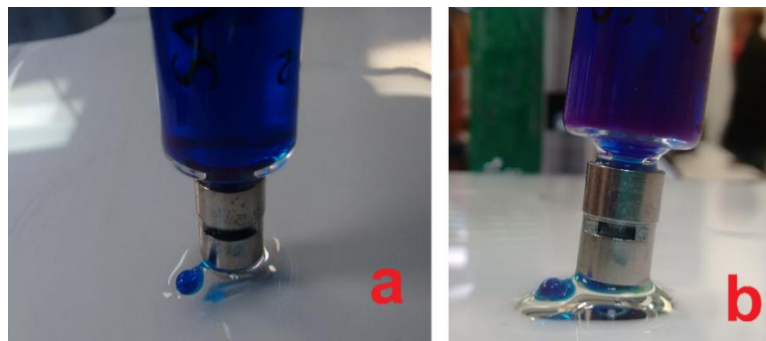
Figure 3.30. *Printing of a cube in CaCl2-liquid-phase platform using alginate 5% w/v: 1st layer front view (a) and sided view (b).*

The experiments using sodium alginate as paste material for the printing of layers allowed to understand two important facts with respect to this system. Firstly, the uniformity and the definition of the filament extruded must be ensured regardless of the concentrations of paste material used, so that the level of the layers is within reach of the nozzle. Secondly, Concentration becomes an important parameter for the present system using a wet print bed, where the gelation can interfere the deposit of material from the nozzle as evidenced in the direct extrusion over CaCl$_2$ surface where the 5% w/v solution did not allowed the extrusion because the concentration was high enough to allow gelation to take place as the extrusion occurred leading to blockage of the nozzle hole.

4.0. Conclusions

4.1. Isolation of keratin from sheep wool and human hair

Keratin was successfully extracted from sheep wool and human hair, carrying out two different methods referred to as Na_2S and Shindai method. Purification of the keratins was performed mainly by dialysis, however some precipitations methods by pH and organic solvents were also included. Results from characterisation suggest Shindai method provides the milder conditions of extraction as well as higher yields when compared to Na_2S method which provided more drastic conditions for extraction that could compromise the quality of the final product. As an alternative purification procedure, precipitation of keratins from hair and wool were tested as part of the post-reaction treatment: pH precipitation for hair keratins and precipitation in acetone for wool keratins producing keratins significantly different from the freeze dried ones. This was evident by the solubility of the keratins in PBS pH 7.4, observing lower solubility in keratins purified by precipitation than the ones treated by dialysis/freeze-drying. This trending was also confirmed by the results of the thiol content estimated by Ellman's assay, where precipitated keratins showed the lowest quantification values, suggesting a relevant contribution by the free thiol groups in keratin towards the solubility in basic phosphate buffer solutions.

4.2. Fabrication of keratin-based hydrogels by Michael addition

The fabrication of these gels allowed to confirm the functionality and reactivity of the thiol groups in the extracted keratins by the obtention of the gels following the Michael addition reactions approach. The results obtained from these experiments as well as the characterisation served as supporting information to justify the feasibility of the extraction of keratin from its natural sources following Shindai methodology, trusting the properties of the final product will be applicable for the fabrication of

hydrogel following Michael addition chemistry. SEM images of the surface morphology were obtained for every gel, revealing the influence of size and functionality in the hydrogel structure, showing a well-defined crosslinking role for the small molecules PEGDA and soybean oil epoxidised acrylate when combined with Keratin. In addition, the multi functionality of soybean oil epoxidised acrylate resulted in a more compacted structure than the bi-functional PEGDA which shows greater cavities in the structure. Methacrylated alginate on the other hand, displays a co-dominance of to have a shared crosslinking role with keratin due to the similarity in size of both molecules. This similarity was observed in the SEM images that displayed a uniform and smooth pattern that can be explained by a better alignment between Methacrylated alginate and keratin chains, presumably facing each other. Further characterisation will be required to reassure the observations drawn from the SEM analysis of the gels.

4.3. Photo-crosslinking of Methacrylated alginate and 2-step gel casting method

The UV-light-assisted gel casting method carried out in this work was designed as a preliminary test for the development of a casting method for 3D-printing. The results obtained in the present work are in favour of the inclusion of this bio-polymer system in the prototyping of objects with smart morphologies by 3D- printing and further studies will be conducted by using velleman K8200 3D-printing equipment. Methacrylated alginate/chitosan were successfully synthesised and included in the gel casting process by photo-crosslinking reactions using the reported equipment, demonstrating the viability of the obtention of hydrogels in short time without needing drastic conditions or hazardous chemicals. The reactivity of the functionalised polysaccharides methacrylated alginate and methacrylated chitosan proved to be satisficatory under the conditions reported and it shows potential towards the combination with keratin by

the results observed in the 2-step method, where gelation was a contribution of both photo-crosslinking and Michael addition reactions, suggesting that each reactions reinforces the other in the production of a hydrogel. Moreover, the combination of keratin with functionalised alginate in the two-step casting method is also endorsed by the biological properties such as biocompatibility and biodegradability that keratin and derived alginate compounds add to the system, which could be useful in the treatment of chronical wounds.

In the same way, the swelling studies carried out in this work are intended to provide relevant information about the swelling capacity of the hydrogels in aqueous over time for potential usage as a wound dressing. The evidence presented in this work is far from conclusion and further studies (drug delivery, swelling studies, 3D-printing) should be conducted in order to come to support the findings in this work.

4.4. 3D printing experiments with sodium alginate

The sodium alginate polymer system was tested as paste material for the printing of layers using the reported equipment. The experiments revealed important aspects to ensure successful extrusion layer by layer. It is essential that the uniformity and the definition of the filament extruded remains constant regardless of the concentrations of the paste material used, so the level of the layers is within reach of the nozzle. For the reported experiments with sodium alginate, extrusion on dry print bed and wet print bed were both tested and it was observed better definition of the filament for the wet system, however the adhesion of the filament over the dry surface was better than the wet surface, since the wet print bed allowed the free movement of the filament and its position was easily altered by the nozzle while deposition new layers. This free-movement affects the printing of the layer since the system operates following specific coordinates on the print bed and any location shifts could result in

overlapping of layers instead of the perfectly stacked arrangement that should be observed.

Concentration is important to maintain the good consistency of the filament and sometimes this is achieved by increasing concentration of paste material, however this could interfere the extrusion as it observed in the sodium alginate/CaCl$_2$ (wet print bed) system where the most concentrated solution 5% experienced gelation too quickly resulting in the blockage of the nozzle, which stops the extrusion of filament. It was also observed in both extrusions (dry or wet) that sodium alginate/ CaCl$_2$ system forms a beaded filament that causes poor uniformity of the filament so the deposition of upcoming layers was affected by this fact and therefore a full printing of the object was not achieved due to the nozzle being physically far apart from the printed layers.

4.5. Future work

The research conducted in this MPhil proved the successful isolation of keratin from sheep wool and human hair. Similarly, the fabrication of hydrogels using this isolated keratins as well as the inclusion of a partner reaction as evidenced in the photo-crosslinking reactions with methacrylated alginate which led to the development of a 2-step method. The last stage of the project showed the 3D experiments with sodium alginate intended to present an early stage of a gel casting system, in which sodium alginate was included due to be the precursor of methacrylated alginate which is capable to work in partnership with keratin as it was proved by the 2-step method. Additionally, the resemblance of sodium alginate in solution with its equivalent methacrylated compound, serves as a relevant point of comparison which should encourage the inclusion of methacylated alginate in the 3D printing system reported in this work, providing the pertinent adjustments on the equipment are applied. The

current 3D printing equipment is designed for liquids that upon printing could solidify by the action of a physical or chemical stimuli, therefore a UV-light curing system should be incorporated for the methacrylated alginate system and it should synchronise with the 3D printing instrument so that the light beam is effectively delivered into the liquid and the photo-crosslinking occurs. Further functionalisation of keratin and sodium alginate could also improve the gelation process and the mechanical properties of the gels and this could lead to the development of a novel formulation for the gel casting of this polymer system.

References

1. Tadmor, Z; Gogos, C.G.; *Principles of polymer processing*; John Wiley & Sons: New York, 2006; pp 984.

2. W, D.F.; *The Williams Dictionary of Biomaterials*, Liverpool University Press: United Kingdom, 1999; pp 23-25.

3. L.S, N; C.T, L. Biodegradable polymers as biomaterials. Prog. Polym. Sci, **2007**, *32*, 762–798 pp.

4. Y, Hu; W, Dan; S, Xiong; Y, Kang; A, Dhinakar; J, Wu; Z, Gu. Development of collagen/polydopamine complexed matrix as mechanically enhanced and highly biocompatible semi-natural tissue engineering scaffold. *Acta Biomater*, **2007**, *47*, 135–148 pp.

5. Weixian, Xi; Timothy, F.S; Christopher, J.K; Christophe, N.B. Click chemistry in materials science. *Adv. Funct*. *Mater*, **2014**, *24*, 2572–2590 pp.

6. Yoon, D.M.; Fisher, J.P.; *Natural and synthetic polymeric scaffolds*; Biomed. Mater.,Springer US: United States, 2009; pp 415–442.

7. Malafaya, P.B; Silva, G.A; Reis, R.L. Natural–origin polymers as carriers and scaffolds for biomolecules and cell delivery in tissue engineering applications. *Adv. Drug Deliv. Rev*, **2007**, *59*, 207–233 pp.

8. Hacker, M; Krieghoff, J; Mikos, A.G.; *Principles of Regenerative Medicine*, 3rd Edition; Academic Press, 2019; pp 559-590.

9. Shaygan, N; Binde, W.H. Graphene as initiator/catalyst in polymerization chemistry. *Progress in Polymer Science*, **2017**, *67*, 48–76 pp

10. Guilherme, M.R; Reis, A.V; Takahashi, S.H; Rubira, A.F; Feitosa, J; Muniz, E.D. Synthesis of a novel superabsorbent hydrogel by copolymerization of acrylamide and cashew gum modified with glycidyl methacrylate. *Carbohydrate Polymers*, **2005**, *61*, 464–471 pp.

11. Bajpai, A. K., & Giri, A. Water sorption behaviour of highly swelling (carboxy methylcellulose-g-polyacrylamide) hydrogels and release of potassium nitrate as agrochemical. *Carbohydrate Polymers*, **2003**, *53*(3), 271–279 pp.

12. Kabiri, K., Omidian, H., Hashemi, S. A., Zohuriaan-Mehr, M. J. Synthesis of fast-swelling superabsorbent hydrogels: Effect of

crosslinker type and concentration on porosity and absorption rate. *European Polymer Journal*, **2003**, *39*, 1341–1348 pp.

13. Muniz, E. C., & Geuskens, G. Compressive elastic modulus of polyacrylamide hydrogels and semi-IPNs with poly(N-isopropylacrylamide). *Macromolecules*, **2001**, *34*, 4480–4484 pp.

14. Sitterli, A; Heinze, T.H. Studies about reactive ene-functionalized dextran derivatives for Thiol-ene click reactions, *Reactive and Functional Polymers*, **2019**, *136*, 66–74 pp.

15. Wang, B; Yang, W; McKittrick, J; Meyers, M.A. Keratin: Structure, mechanical properties, occurrence in biological organisms, and efforts at bioinspiration. *Progress in Materials Science*, **2016**, *76*, 229–318 pp.

16. Coulombe, P.A; Omary, M.B. 'Hard' and 'soft' principles defining the structure, function and regulation of keratin intermediate filaments. *Curr Opin Cell Biol*, **2002**, *14*(1), 110–22 pp.

17. McKittrick, J. Chen, P.Y; Bodde, S.G; Yang, W; Novitskaya, E.E; Meyers, M.A. The structure, functions, and mechanical properties of keratin. *JOM*, **2012**, *64*(4), 449–68 pp.

18. Kadir, M; Wang, X; Zhu, B; Liu, J; Harland , D; Popescu, C. The structure of the "amorphous" matrix of keratins. *Journal of Structural Biology*, **2017**, *198*, 116-123 pp

19. Rebman, R.C; *Turles and Tortoises*, 1st Edition; Perrota M, Eds; Marshall Cavendish Benchmark: New York, 2007; pp 13-18.

20. Sherbrook, W.C; *Introduction to horned Lizards*, 2nd Edition; University of California Press: Berkeley and Los Angeles, 2003; pp 9-11.

21. King, S.A; *ANIMAL DREAMING the spiritual and symbolic language of AustralAsian animals*, 1st Edition; Blue Angel Gallery: Australia, 2003; pp 130.

22. Wu, P; Dai, X; Chen, K; Li, R; Xing, Y. Fabrication of regenerated wool keratin/polycaprolactone nanofiber membranes for cell culture. *International Journal of Biological Macromolecules*, **2018**, *114*, 1168-1173 pp.

23. M. Zoccola, A. Aluigi, C. Tonin. Characterisation of keratin biomass from butchery and wool industry wastes. *J. Mol. Struct*, **2009**, *938* , 35–40 pp.

24. Jiang, Z; Yuan, J; Wang, P; Fan, X; Xu, J; Wang, Q; Zhang, L. Dissolution and regeneration of wool keratin in the deep eutectic solvent of choline chloride-urea. *International Journal of Biological Macromolecules*, **2018**, *119*, 423-430 pp.

25. Basit, A; asghar, F; Sadaf, S; Akhtar, MW. Health improvement of human hair and their reshaping using recombinant keratin K31. *Biotechnology Reports*, **2018**, https://doi.org/10.1016/j.btre.2018.e00288.

26. Leichner, C; Steinbring, C; Angela Baus, R; Baecker, D; Gust, R; Bernkop-Schnürch, A. Reactive keratin derivatives: A promising strategy for covalent binding to hair. *Journal of Colloid and Interface Science*, **2018**, *534*, 533-541 pp.

27. Vasconcelos, A; Freddi, G; Cavaco-Paulo, A. Biodegradable materials based on silk fibroin and keratin. *Biomacromolecules*, **2008**, *9*(4), 1299–1305 pp.

28. Wilson, R.H; Lewis, H.B. The cystine content of hair and other epidermal tissues. *Journal of Biological Chemistry*, **1927**, *73*(2), 543-553 pp.

29. Ziegler, K; *Crosslinking and self-crosslinking in keratin fibers*. In Chemistry of Natural Protein Fibers, Springer: 1977; pp 267-300.

30. Esparza, Y; Bandara, N; Ullah, A; Wu, J. Hydrogels from feather keratin show higher viscoelastic properties and cell proliferation than those from hair and wool keratins. *Materials Science & Engineering C*, **2018**, *90*, 446-453 pp.

31. Robbins, C.R.; chemical composition of different hair types. In: *Chemical and physical behaviour of human hair*; Springer: USA, 2012; pp 112.

32. Ward, W.H.; Lundgren H.P.; The formation composition and properties of the keratins, In: *Advances in protein chemistry*; Academic Press, New York, 1955.

33. Clay, R.C; Cook, K; Routh, J.I. Studies in the composition of human hair. *J Am Chem Soc*, **1940**, *62*, 2709–2710 pp.

34. Bradbury, J.H; et al. Separation of chemically unmodified histological components of keratin fibers and analyses of cuticle. *Nature*, **1966**, *210*, 1333–1334 pp.

35. Lang, J; Lucas, C. Analysis of hair keratin. I: application of microbiological techniques to hydrolyzates of human hair. *Biochem J*, **1952**, *52*, 84–87 pp.

36. Horvath, A.L. Solubility of structurally complicated materials: 3 Hair. *Sci. World J*, **2009**, *9*, 255–271 pp.

37. Ashish, G.; Sankar, K.P.; *Soft computing approach to pattern recognition and image processing*; World scientific: Singapore, 2002; pp 314.

38. Posatia, T; Giuria, D; Nocchettib, M; Sagnellac, A; Gariboldid, M; Ferronia, C; Sotgiua, G; Varchia, G; Zambonia, R; Aluigia, A. Keratin-hydrotalcites hybrid films for drug delivery applications. *European Polymer Journal*, **2018**, *105*, 177-185 pp.

39. Fraser, R.B.D.; Mac Rae, T.P.; Rogers, G.E.; *Keratins, their Composition, Structure and Biosynthesis*; CC Thomas Publishing: Springfield, IL, USA, 1972.

40. Holkara, C.R; Jainb, S.S; Jadhava, A.J; Pinjari, D.V. Valorization of keratin based waste. *Process Safety and Environmental Protection*, **2018**, *115*, 85-98 pp.

41. Rouse, J.G; Van Dyke, M.E. A review of keratin-based biomaterials for biomedical applications. *Materials (Basel)*, **2010**, *3*, 999–1014, http://dx.doi.org/10.3390/ma3020999.

42. Shanmugasundarama, O.L; Syed Zameer Ahmedb, K; Sujathac, K; Ponnmurugand, P; Srivastavaa, A; Ramesha, R; Sukumara, R; Elanithia, K. Fabrication and characterization of chicken feather keratin/polysaccharides blended polymer coated nonwoven dressing materials for wound healing applications. *Materials Science & Engineering C*, **2018**, *92*, 26-33 pp.

43. Molloy, P.L; Powell, B.C; Gregg, K; Barone, E.D; Rogers, G.E. Organisation of feather keratin genes in the chick genome. *Nucleic Acids Res*, **1982**, *10*, 6007–6021 pp.

44. Srinivasan, B; Kumar, R; Shanmugam, K; Sivagnam, U.T; Reddy, N.P; Sehgal, P.K. Porous keratin scaffold−promising biomaterial for tissue engineering and drug delivery. *J. Biomed. Mater. Res*. *Part B Appl. Biomater*, **2010**, *92*(B), 5–12 pp.

45. Tachibana, A; Furuta, Y; Takeshima, H; Tanabe, T; Yamauchi, K. Fabrication of wool keratin sponge scaffolds for long-term cell cultivation. *J. Biotechnol*, **2002**, *93*, 165–170 pp.

46. Vasconcelos, A; Cavaco-Paulo, A. The use of keratin in biomedical applications. *Curr. Drug Targets*, **2013**, *14*, 612–619 pp.

47. Langbein, L; Rogers, M.A; Praetzel-Wunder, S; Böckler, D; Schirmacher, P; Schweizer, J. Novel Type I Hair Keratins K39 and K40 Are the Last to be Expressed in Differentiation of the Hair: Completion of the Human Hair Keratin Catalog. *Journal of Investigative Dermatology*, **2007**, *127*(6), 1532-1535 pp.

48. Tonin, C; Aluigi, A; Vineis, C; Varesano, A; Montarsolo, A; Ferrero, F. Thermal and structural characterization of poly(ethylene-oxide)/keratin blend films. *J. Therm. Anal. Calorim*, **2007**, *89*, 601–608 pp.

49. Yamauchi, K; Yamauchi, A; Kusunoki, T; Kohda, A; Konishi, Y. Preparation of stable aqueous solution of keratins, and physiochemical and biodegradational properties of films. *J. Biomed. Mater. Res*, **1996**, *31,* 439 pp.

50. Zhao, W; Yang, R; Zhang, Y; Wu, L. Sustainable and practical utilization of feather keratin by an innovative physicochemical pretreatment: high density steam flash explosion. *Green Chem*. **2012**, *14*, 3352–3360 pp.

51. Vasileva-Tonkova, E; Gousterova, A; Neshev, G. Ecologically safe method for improved feather wastes biodegradation. *Int. Biodeterior. Biodegrad.* **2009**, *63*, 1008–1012 pp.

52. Xie, H; Li, S; Zhang, S. Ionic liquids as novel solvents for the dissolution and blending of wool keratin fibers. *Green Chem*, **2005**, *7*, 606–608 pp.

53. Idris, A; Vijayaraghavan, R; Rana, U.A; Patti, A.F. Macfarlane D.R. Dissolution and regeneration of wool keratin in ionic liquids. *Green Chem*, **2014**, *16*, 2857–2864 pp.

54. Mori, H; Hara, M. Transparent biocompatible wool keratin film prepared by mechanical compression of porous keratin hydrogel. *Materials Science & Engineering C*, **2018**, *91*, 19-25 pp.

55. De Guzman, R.C; Merrill, M.R; Richter, J.R; Hamzi ,R.I; Greengauz-Roberts, O.K; Van Dyke, M.E. Mechanical and biological properties of keratose biomaterials. *Biomaterials*, **2011**, *32*, 8205–8217 pp.

56. Tomblyn, S; Pettit Kneller, E.L; Walker, S.J; Ellenburg, M.D; Kowalczewski, C.J; Dyke, M.V; Burnett, L; Saul, M. Keratin hydrogel carrier system for simultaneous delivery of exogenous growth factors and muscle progenitor cells. *J Biomed Mater Res B Appl Biomater*, **2016**, *104B*, 864–879 pp.

57. Hill, P; Brantley, H; Van Dyke, M.E. Some properties of keratin biomaterials: keratins. *Biomaterials*, **2010**, *31,* 585–593 pp.

58. Reichl, S; Borrelli, M; Geerling, G. Keratin film for ocular surface reconstruction. *Biomaterials*, **2011**, *32*, 3375–3386 pp.

59. Borrelli, M; Joepen, N; Reichl, S; Finis, D; Schoppe, M; Geering, G; Schrader, S. Keratin films for ocular surface reconstruction: evaluation of biocompatibility in an in-vivo model. *Biomaterials*, **2015**, *42*, 112–120 pp.

60. Aluigi, A; Tonetti, C; Vineis, C; Tonin, C; Mazzuchetti, G. Adsorption of copper(II) ions by keratin/PA6 blend nanofibers. *Eur. Polym. J*, **2011**, *47* 1756–1764 pp.

61. Wang, S; Wang, Z; Foo, S.E; Tan, N.S; Yuan, Y; Lin, W; Zhang, Z; Ng, K.W. Culturing fibroblasts in 3D human hair keratin hydrogels. *ACS Appl. Mater. Interfaces*, **2015**, *7*, 5187–5198 pp.

62. Barba, C; Martí, M; Roddick-Lanzilotta, A; Manich, A.; Carilla, J; Parra, J. L; Coderch, L. Effect of wool keratin proteins and peptides on hair water sorption kinetics. *Journal of Thermal Analysis and Calorimetry*, **2010**, *102*(1), 43-48 pp.

63. Roddick-Lanzilotta, A; Kelly, R; Scott, S; Chahal, S. New keratin isolates: actives for natural hair protection. *Journal of cosmetic science*, **2007**, *58*, (4), 405-411 pp.

64. Barba, C; Scott, S; Roddick-Lanzilotta, A; Kelly, R; Manich, A. M; Parra, J. L; Coderch, L. Restoring important hair properties with wool keratin proteins and peptides. *Fibers and Polymers*, **2010**, *11*(7), 1055-1061 pp.

65. Fernandes, M. M; Lima, C. F; Loureiro, A; Gomes, A; Cavaco-Paulo, A. Keratin-based peptide: biological evaluation and strengthening

properties on relaxed hair. *International journal of cosmetic science*, **2012**, *34*(4), 338-346 pp.

66. Deutscher, J. The mechanisms of carbon catabolite repression in bacteria. *Current Opinion in Microbiology*, **2008**, *11* (2), 87-93 pp.

67. Studier, F. W. Protein production by auto-induction in high-density shaking cultures. *Protein expression and purification*, **2005**, 41(1), 207-234 pp.

68. Fischer, B; Perry, B; Sumner, I; Goodenough, P. A novel sequential procedure to enhance the renaturation of recombinant protein from Escherichia coli inclusion bodies. *Protein engineering*, **1992**, *5*(6), 593-596 pp.

69. Ishii, D; Abe, R; Watanabe, S; Tsuchiya, M; Nöcker, B; Tsumoto, K. Stepwise characterization of the thermodynamics of trichocyte intermediate filament protein supramolecular assembly. *Journal of molecular biology*, **2011**, *408*(5), 832-838 pp.

70. Gray, J. Hair care and hair care products. *Clinics in Dermatology*, **2001**, *19*(2), 227-236 pp.

71. Bolduc, C; Shapiro, J. Hair care products: waving, straightening, conditioning, and coloring. *Clinics in Dermatology*, **2001**, *19*(4), 431-436 pp.

72. Schweizer, J; Bowden, P. E; Coulombe, P. A; Langbein, L; Lane, E. B; Magin, T. M; Maltais, L; Omary, M. B; Parry, D. A. D; Rogers, M. A; Wright, M. W. New consensus nomenclature for mammalian keratins. *The Journal of cell biology*, **2006**, *174*(2), 169-174 pp.

73. Schweizer, J; Langbein, L; Rogers, M. A; Winter, H. Hair follicle-specific keratins and their diseases. *Experimental Cell Research*, **2007**, *313*(10), 2010-2020 pp.

74. Posati, T; Sotgiu, G; Varchi, G; Ferroni, C; Zamboni, R; Corticelli, F; Puglia, D; Torre, L; Terenzi, A; Aluigi, A. Developing keratin sponges with tunable morphologies and controlled antioxidant properties induced by doping with polydopamine (PDA) nanoparticles. *Mater. Des,* **2016**, *110*, 475–484 pp.

75. Nayak, K.K, Gupta, P. Study of the keratin-based therapeutic dermal patches for the delivery of bioactive molecules for wound treatment. *Mater. Sci. Eng*, **2017**, *C 77*, 1088–1097 pp.

76. Roy D.C, Tomblyn, S, Isaac, K.M, Kowalczewski, C.J, Burmeister, D.M, Burnett, L.R, Christy, R.J. Ciprofloxacin-loaded keratin hydrogels reduce infection and support healing in a porcine partial-thickness thermal burn. *Wound Repair Regen*, **2016**, *24*, 657–668 pp.

77. Aluigi, A; Rombaldoni, F; Tonetti, C; Jannoke, L. Study of Methylene Blue adsorption on keratin nanofibrous membranes. *J. Hazard. Mater*, **2014**, *268*, 156 pp.

78. Li J., Li Y., Li L., Mak A.F., Ko F., Qin L. Preparation and biodegradation of electrospun PLLA/keratin nonwoven fibrous membrane. *Polym. Degrad*. *Stab*, **2009**, *94*, 1800–1807 pp.

79. Li, J.-S; Li, Y; Liu, X; Zhang, J; Zhang, Y. Strategy to introduce an hydroxyapatite–keratin nanocomposite into a fibrous membrane for bone tissue engineering. *J. Mater. Chem*. **2013**, *B 1*, 432–437 pp.

80. Gupta, P; Nayak, K.K. Optimization of keratin/alginate scaffold using RSM and its characterization for tissue engineering. *Int. J. Biol. Macromol*, **2016**, *85*, 141–149 pp.

81. Saravanan, D; Sameera, A; Moorthi, A; Selvamurugan, N. Chitosan scaffolds containing chicken feather keratin nanoparticles for bone tissue engineering. *Int. J. Biol. Macromol*, **2013**, *62*, 481–486 pp.

82. Xu, H; Cai, S; Xu, L; Yang, Y. Water-stable three-dimensional ultrafine fibrous scaffolds from keratin for cartilage tissue engineering. *Langmuir*, **2014**, *30*, 8461–8470 pp.

83. Nayak, K.K; Gupta, P. In vitro biocompatibility study of keratin/agar scaffold for tissue engineering. *Int. J. Biol. Macromol*, **2015**, *81*, 1–10 pp.

84. Hoeksema, H; Vandekerckhove, D; Verbelen, J; Heyneman, A; Monstrey, S; Deitch, E.A. A comparative study of 1% silver sulphadiazine (Flammazine®) versus an enzyme alginogel (Flaminal®) in the treatment of partial thickness burns. *Burns*, **2013**, *39*, 1234–1241 pp.

85. Gupta, P; Nayak, K.K. Compatibility study of alginate/keratin blend for biopolymer development. *J. Appl. Biomater. Funct. Mater*, **2015**, *13*, e332–e339 pp.

86. Balaji, S; Kumar, R; Sripriya, R; Kakkar, P; Ramesh, D.V; Reddy, P.N.K. Preparation and comparative characterization of keratin–chitosan and keratin–gelatin composite scaffolds for tissue engineering applications. *Mater. Sci. Eng*, **2012**, *C 32*, 975–982 pp.

87. Jayakumar, R; Prabaharan, M; Sudheesh, P.T; Nair, S.V; Tamura, H. Biomaterials based on chitin and chitosan in wound dressing. *Biotechnol. Adv*, **2011**, *29*(3), 322–337 pp.

88. Ong, S-Y, et al. Development of a chitosan-based wound dressing with improved hemostatic and antimicrobial properties. *Biomaterials*, **2008**, *29*(32), 4323–43332 pp.

89. Shanmugasundaram, O.L; Mahendra-Gowda, R.V. Development and characterization of bamboo gauze fabric coated with polymer and drug for wound healing. *Fibres Polym*, **2011**, *12*(1), 15–20 pp.

90. Mi, F-L; Shyu, S.S; Wu, Y.B; Lee, S.T; Shyong, J.Y. Fabrication and characterization of a sponge-like asymmetric chitosan membrane as a wound dressing. *Biomaterials*, **2011**, *22*(2), 65–173 pp.

91. Attwood, A.I. Calcium alginate dressings accelerate split graft donor site healing. *Br. J. Plast. Surg*, **1989**, *42*(4), 373–379 pp.

92. Sayag, J; Meaume, S; Bohbot, S. Healing properties of calcium alginate. *J. Wound Care*, **1996**, *5*(8), 357–362 pp.

93. Yimin, Q. Absorption characteristics of alginate wound dressings. *J. Appl. Polym. Sci*, **2004**, *91*(2), 953–957 pp.

94. Shanmugasundaram, O.L. Antimicrobial finish in textiles. *Indian Text. J*, **2007**, *117*, 53–56 pp.

95. Lakshminarayanan, R; Sridhar, R; Jun, X. Interaction of gelatine with polyenes modulatesantifungal activity and biocompatibility of electrospun fibre mats. Int. *J. Nanomedicine*, **2014**, *9*, 2439–2458 pp.

96. Navarro, J; Swayambunathan, J; Lerman, M; Santoro, M; Fisher, J.P. Development of keratin-based membranes for potential use in skin repair. *Acta Biomaterialia*, **2018**.

97. Loan, F; Cassidy, S; Marsh, C; Simcock, J. Keratin-based products for effective wound care management in superficial and partial thickness burns injuries. *Burns*, **2016**, *42*(3), 541–547 pp.

98. Sierpinski, P; Garrett, J; Ma, J; Apel, P; Klorig, D; Smith, T; Koman, L.A; Atala, A; Van Dyke, M. The use of keratin biomaterials derived from human hair for the promotion of rapid regeneration of peripheral nerves. *Biomaterials*, **2008**, *29*(1), 118–128 pp.

99. Verma, V; Verma, P; Ray, P; Ray, A.R. Preparation of scaffolds from human hair proteins for tissue-engineering applications. *Biomed. Mater*, **2008**, *3*(2).

100. Pace, L.A; Plate, J.F; Smith, T.L; Van Dyke, M.E. The effect of human hair keratin hydrogel on early cellular response tosciatic nerve injury in a rat model. *Biomaterials*, **2013**, *34*(24), 5907–5914 pp.

101. Saul, J.M; Ellenburg, M.D; De Guzman, R.C; Van Dyke, M. Keratin hydrogels support the sustained release of bioactive ciprofloxacin. *J. Biomed. Mater. Res.- Part A*, **2011**, *98 A*(4), 544–553 pp.

102. Nakata, R; Tachibana, A; Tanabe, T. Preparation of keratin hydrogel/hydroxyapatite composite and its evaluation as a controlled drug release carrier. *Mater. Sci. Eng*, **2014**, *C 41*, 59–64 pp.

103. Xu, S; Sang, L; Zhang, Y; Wang, X; Li, X. Biological evaluation of human hair keratin scaffolds for skin wound repair and regeneration. *Mater. Sci. Eng*, **2013**, *C 33*(2), 648–655 pp.

104. Poranki, D; Whitener, W; Howse, S; Mesen, T; Howse, E; Burnell, J; Greengauz-Roberts, O; Molnar, J; Van Dyke, M. Evaluation of skin regeneration after burns in vivo and rescue of cells after thermal stress in vitro following treatment with a keratin biomaterial. *J. Biomater. Appl*, **2014**, *29*(1), 26–35 pp.

105. S. Khalil, J; Nam, W. Sun. Multi-nozzle deposition for construction of 3D biopolymer tissue scaffolds. *Rapid Protyp J*, **2005**, *11(*1), 9-17 pp.

106. Li, Q; Zhu, L; Liu, R; Huang, D; Jin, X; Che, N; Li, Z; Qu, X; Kang, H; Huang, Y. Biological stimuli responsive drug carriers based on keratin for triggerable drug delivery. *J. of Mat. Chem*, **2012**, *22*, 19964–19973 pp.

107. Hollister, S.J; Maddox, R.D; Taboas, J.M. Optimal design and fabrication of scaffolds to mimic tissue properties and satisfy biological constraints. *Biomaterials*, **2002**, *23*(20), 4095-4103 pp.

108. Kemppainen, J.M; Hollister, S.J. Tailoring the mechanical properties of 3D designed poly(glycerol sebacate) scaffolds for cartilage applications. *J. Biomed. Mater. Res*, **2010**, *A 94A(1)*, 9-18 pp.

109.   Zhang, P.B; Hong, Z.K; Yu, T; Chen, X.S; Jing, X.B. In vivo mineralization and osteogenesis of nanocomposite scaffold of poly (lactide-co-glycolide) and hydroxyapatite surface-grafted with poly(L-lactide). *Biomaterials*, **2009**, *30*(1), 58-70 pp.

110.   Ji, C.D; Annabi, N; Khademhosseini, A; Dehghani, F. Fabrication of porous chitosan scaffolds for soft tissue engineering using dense gas CO_2. *Acta Biomater*, **2011**, *7*(4), 1653-1664 pp.

111.   Pham, Q.P; Sharma, U; Mikos, A.G. Electrospinning of polymeric nanofibers for tissue engineering applications: a review, *Tissue Eng*. **2006**, *12*(5), 1197-1211 pp.

112.   Mondschein, R J; Kanitkar, A; Williams, C. B; Verbridge, S.S; Long, T.E. Polymer structure-property requirements for stereolithographic 3D printing of soft tissue engineering scaffolds. *Biomaterials*, **2017**, *140*, 170-188 pp.

113.   Sanatgara, R; Campagneb, C; Nierstrasz, V. Investigation of the adhesion properties of direct 3D printing of polymers and nanocomposites on textiles: Effect of FDM printing process parameters. *App. Surf. Sci*, **2017**, *403*, 551-563 pp.

114.   Chua, C.K; Leong, K.F; Lim, C.S. Rapid Prototyping, WORLD SCIENTIFIC, 2010.

115.   Liu, T; Guessasma, S; Zhua, J; Zhanga, W; Nouri, H; Belhabib, S. Microstructural defects induced by stereolithography and related compressive behaviour of polymers. *J Mat Proc Tech*. **2018**, *251*, 37-46 pp.

116.   Bourell, D.L; Beaman, J.J; Marcus, H.L; Barlow, J.W. Solid Freeform Fabrication an advanced Manufacturing Approach. *The University of Texas at Austin*. **1992**, 1-7 pp.

117.   Chartiera,T; Dupasa, C; Geffroy, P; Pateloup, V; Colas, M; Cornette, J; Guillemet-Fritsch, S. Influence of irradiation parameters on the polymerization of ceramic reactive suspensions for stereolithography. *J. EU. Cer. Soc*. **2017**, *37*, 4431-4436 pp.

118.   Snyder, J.E; Hunger, P.M; Wang, C; Hamid, Q; Wegst, U.G.K; Sun, W. Combined multi-nozzle deposition and freeze casting process

to superimpose two porous networks for hierarchical three-dimensional microenvironment. *Int. Soc. BioFab*. **2014**, *6*, 1-10 pp.

119. http://apm-designs.com/fdm-vs-sla-3d-printer-tech-comparison/ (consulted on 21 Dec 2019)

120. Agarwal, V; Gopi Panicker, A; Indrakumar, S; Chatterjee, K. Comparative study of keratin extraction from human hair. *Int. J. Bio. MacroMol*, **2019**, *133*, 382-390 pp.

121. Wang, S; Taraballi, F; Poh Tan, L; Woei Ng, K. Human keratin hydrogels support fibroblast attachment and proliferation in vitro. *Cell. Tissue. Res*, **2012**, *347*, 795–802 pp.

122. Nakamura, A; Arimoto, M; Takeuchi, K; Fujii, T. A Rapid Extraction Procedure of Human Hair Proteins and Identification of Phosphorylated Species. *Biol. Pharm. Bull*, **2002**, *25*(5), 569-572 pp.

123. Ellman, G. L. Tissue sulfhydryl groups. *Arch. Biochem. Biophys*, **1959**, *82*, 70–77 pp.

124. Zahler, W. L. and Cleland, W. W. A specific and sensitive assay for disulfides. *J. Biol. Chem*, **1968**, *243*, 716–719 pp.

125. Anderson, W. L. and Wetlaufer, D. B. A new method for disulfide analysis of peptides. *Analyt. Biochem*, **1975**, *67*, 493–502 pp.

126. Wang, X; Hao, T; Qu, J; Wang, Ch, Chen, H. Synthesis of Thermal Polymerizable Alginate-GMA Hydrogel for Cell Encapsulation. *J of Nanomats*, **2015**, *2015*, 1-8 pp

127. Tiwari, A; Grailer , J.J; Pilla, S; Steeber, D.A; Gong, S. Biodegradable hydrogels based on novel photopolymerizable guar gum–methacrylate macromonomers for in situ fabrication of tissue engineering scaffolds. *Act Biomat*, **2009**, *5*, 3441–3452 pp.

128. Elizalde-Peña, E.A.; Flores-Ramirez, N; Luna-Barcenas, G; Vasquez-Garcia, S.R; Arambula-Villa, G; Garcia-Gaitan, B; Rutiaga-Quiñones, J.G; Gonzalez-Hernandez, J. Synthesis and characterization of chitosan-g-glycidyl methacrylate with methyl methacrylate. *Eu Pol J*, **2007**, *43*, 3963–3969 pp.

129.   Flores-Ramírez, N; Elizalde-Peña, E.A; Vásquez-García, S.R; González-Hernández, J; Martinez-Ruvalcaba, A; Sanchez, I.C; Luna-Bárcenas, G; Gupta, R.B. Characterization and degradation of functionalized chitosan with glycidyl methacrylate. *J of Biomat Sci*, **2013**, *16*(4), 473-488 pp.

130.   Cussler, E. L.; *Difussion mass transfer in fluid systems*, 2nd Edition; Cambridge University Press: United Kingdom, 1997; pp 406

131.   Vaclavik, V.A; Christian, E.W.; *Essentials of food science*, 3rd Edition; Heldman D.R, Eds; Springer: New York, 2008; pp 152.

132.   Wong, S.Y; Lee, C.C; Ashrafzadeh, A; Junit, S.M; Abrahim, N; Hashim, O.H. A High-Yield Two-Hour Protocol for Extraction of Human Hair Shaft Proteins. *PLoS ONE*, **2016**, *11*(10), 1-15 pp.

133.   Roberts, M; Reiss, M; Monger, G. Advanced biology; Nelson: United Kingdom, 2000; pp 30.

134.   Birngruber, C; Ramsthaler, F; Verhoff, M.A. The color(s) of human hair Forensic hair analysis with SpectraCube. *Forensic Science International*, **2009**, *185*, e19-e23 pp

135.   Estévez-martínez, Y., Velasco-santos, C., Delgado, G., Cuevas-yáñez, E., Alaníz-lumbreras, D., Duron-torres, S., & Castaño, V. M. Grafting of Multiwalled Carbon Nanotubes with Chicken Feather Keratin. *J of Nano Mat*, **2013**, *2013*, 8–10 pp.

136.   Kong, J., & Yu, S. Fourier Transform Infrared Spectroscopic Analysis of Protein Secondary Structures Protein FTIR Data Analysis and Band Assign-, *Acta Biochimica et Biophysica Sinica*, **2007**, *39*(20745001), 549–559 pp.

137.   Clayden, J; Greeves, N; Warren, S; *Organic Chemistry*, 2nd Edition; Oxford University Press: United Kingdom, 2012; pp 276-285.

138.   Kozłowska, J., Płanecka, A., Kurzawa, M., & Sionkowska, A. Photochemical behaviour of hydrolysed keratin, *Int J of Cosm Sci*, **2011**, *33*, 503–508 pp.